

Doctoral Dissertation(Censored)

博士論文（要約）

Molecular mechanisms underlying metamorphosis and color formation
in dragonflies.

（トンボの変態と体色形成を制御する分子基盤）

A Dissertation Submitted for the Degree of Doctor of Philosophy

December 2020

令和2年12月博士（理学）申請

Department of Biological Sciences, Graduate School of Science,
The University of Tokyo

東京大学大学院理学系研究科

生物科学専攻

Genta Okude

奥出 絃太

Abstract

The order Odonata (dragonflies and damselflies) is one of the most ancestral insects with wings and metamorphosis and exhibits diverse colors in adult wings and bodies. Odonata has attracted attention in the study of the evolution of metamorphosis and the diversity of insect coloration from ecological and evolutionary points of view. However, the molecular mechanisms involved in metamorphosis and adult coloration in Odonata have remained totally unknown, mainly because of the lack of model Odonata species and the absence of molecular genetic tools applicable to Odonata. In this study, first, I established the framework of developmental staging for describing the process of metamorphosis using 49 Odonata species. Next, I improved the electroporation-mediated RNAi method, which I previously developed for a specific dragonfly species, to make it generally applicable to diverse Odonata species. Then, using the blue-tailed damselfly *Ischnura senegalensis* (Coenagrionidae) and the pied skimmer dragonfly *Pseudothemis zonata* (Libellulidae) as model species, I performed comprehensive surveys of functional genes underpinning the metamorphosis and body coloration of Odonata, which were achieved by RNA sequencing of more than 200 samples and electroporation-mediated RNAi targeting more than 200 genes. As a result, I successfully identified many genes involved in the metamorphosis and body coloration of Odonata. These findings provide important insights into the molecular mechanisms underlying the colors, patterns, development, ecology and evolution of the most ancestral winged insect group with metamorphosis, Odonata.

Abbreviations (in alphabetical order)

20E: 20-hydroxyecdysone

bla: *beta-lactamase*

dsRNA: double-stranded RNA

EGFP: *enhanced green fluorescent protein*

F-0: Final larval instar (=Final minus 0)

F-1: Penultimate larval instar (=Final minus 1)

ITS: internal transcribed spacer

JH: juvenile hormone

MCO2: *multicopper oxidase 2*

RFLP: restriction fragment length polymorphism

RNAi: RNA interference

siRNA: small interfering RNA

TPM: transcripts per million

(第3章～第7章に関わる略号は、5年以内に雑誌等で刊行予定のため、非公開。)

Table of contents

Abstract	2
Abbreviations	3
General Introduction	5
Chapter 1: Comprehensive comparative morphology and developmental staging of final instar larvae toward metamorphosis in the insect order Odonata.	11
Chapter 2: Improvement of electroporation-mediated RNA interference method in Odonata.	37
Chapter 3: Molecular mechanisms underlying metamorphosis in Odonata.	63
Chapter 4: Functional analyses of ecdysone-related transcription factors in Odonata.	64
Chapter 5: Molecular mechanisms underlying yellow color pattern formation in Odonata.	65
Chapter 6: Molecular mechanisms underlying light blue coloration in <i>Ischnura</i> damselflies.	66
Chapter 7: Interspecific crossing between blue-tailed damselflies and functional analysis of sex-differentiation genes.	67
General Conclusion and Discussion	89
Acknowledgements	92
Supplemental Data	93

General Introduction

Insects account for more than half of the described species and are regarded as the most prosperous organismal group on the earth (Grimaldi and Engel 2005). Over 98% of the insect species exhibit “metamorphosis”, a dramatic morphological transformation from larvae (nymphs) to adults that usually entails development of wings. Drastic metamorphosis and wing acquisition must have contributed to the amazing diversity of insects, by which they can utilize different habitats and resources according in their life cycle (Truman and Riddiford 1999, Nicholson et al. 2014, Rainford et al. 2014).

The order Odonata (dragonflies and damselflies) is one of the most ancestral insects with wings and metamorphosis (Misof et al. 2014, Wipfler et al. 2019, Belles 2020) (Fig. 0-1). Odonata species drastically change their morphology from brownish dull-colored aquatic larvae to colorful terrestrial adults without pupal stage (Fig. 0-2). Because Odonata species are diurnal with well-developed vision, their body color is essential for mutual recognition in their mating and territorial behaviors, often showing remarkable sexual dimorphism, color transition, and color polymorphism (Corbet 1999, Futahashi 2016) (Fig. 0-3). While metamorphosis and color patterns of Odonata have been mainly investigated from ecological and evolutionary points of view (Corbet 1999), molecular mechanisms underlying metamorphosis and coloration remain totally unknown due to the following three obstacles: (i) the lack of model Odonata species that are experimentally tractable and maintainable in the laboratory – because dragonflies and damselflies are avid predators, feeding them is laborious and larval mass-rearing is particularly difficult due to cannibalism; (ii) the lack of basic information on metamorphosis of Odonata – for example, larval morphological changes during the progression of metamorphosis have

been poorly described for Odonata; and (iii) the lack of molecular genetic tools applicable to Odonata.

To overcome these difficulties, during my master course, I have established a mass-rearing procedure for isolated larvae of the blue-tailed damselfly *Ischnura senegalensis*, by which its larval development and morphogenesis were described in detail (Fig. 0-2, Okude et al. 2017b). I also reported a gene knockdown method by electroporation-mediated RNAi in the tiny dragonfly *Nannophya pygmaea* (Libellulidae) (Okude et al. 2017a). During my doctoral course, first, I described morphological changes during the process of metamorphosis using 49 Odonata species representing 14 families (Fig. 0-3) and established a staging method generally applicable to diverse Odonata species (Chapter 1). Next, I improved the RNAi method using *I. senegalensis* (Coenagrionidae) and *Pseudothemis zonata* (Libellulidae) as model species to efficiently analyze gene functions in diverse Odonata species (Chapter 2). Using these information and techniques, I analyzed the molecular mechanisms underlying metamorphosis of Odonata controlled by juvenile hormone (JH) (Chapter 3) and also the molecular mechanisms underpinning adult body coloration regulated by ecdysteroid (20E) (Chapter 4). Moreover, I investigated the molecular mechanisms underlying yellow coloration observed in many Odonata species using *P. zonata* as a model (Fig. 0-3) (Chapter 5), and the molecular mechanisms underlying light blue coloration widely found in diverse Odonata species using *I. senegalensis* as a model (Fig. 0-3) (Chapter 6). Finally, I produced hybrids between *I. senegalensis* and *Ischnura elegans*, two congeneric damselfly species with different sex-specific light blue markings, and analyzed genes involved in sex differentiation in *I. senegalensis* (Chapter 7).

References

- Badejo O, Skaldina O, Gilev A, Sorvari J (2020). Benefits of insect colours: a review from social insect studies. *Oecologia* **194**: 27–40.
- Belles X (2020). *Insect metamorphosis: From natural history to regulation of development and evolution*. Academic Press.
- Corbet PS (1999). *Dragonflies, Behavior and Ecology of Odonata*. Cornell University Press.
- Futahashi R (2016). Color vision and color formation in dragonflies. *Curr Opin Insect Sci* **17**: 32–39.
- Futahashi R (2018). Recent topics on higher classification and DNA analyses in dragonflies. *The Nature and Insects* **53**: 5–9.
- Grimaldi D, Engel MS (2005). *Evolution of the insects*. Cambridge University Press.
- Misof B, Liu S, Meusemann K, Peters RS, Donath A, Mayer C, *et al.* (2014). Phylogenomics resolves the timing and pattern of insect evolution. *Science* **346**: 763–767.
- Nicholson DB, Ross AJ, Mayhew PJ (2014). Fossil evidence for key innovations in the evolution of insect diversity. *Proc R Soc B* **281**: 20141823.
- Okude G, Futahashi R, Kawahara-Miki R, Yoshitake K, Yajima S, Fukatsu T (2017a). Electroporation-mediated RNA interference reveals a role of the multicopper oxidase 2 gene in dragonfly cuticular pigmentation. *Appl Entomol Zool* **52**: 379–387.
- Okude G, Futahashi R, Tanahashi M, Fukatsu T (2017b). Laboratory rearing system for *Ischnura senegalensis* (Insecta: Odonata) enables detailed description of larval development and morphogenesis in dragonfly. *Zool Sci* **34**: 386–397.
- Rainford JL, Hofreiter M, Nicholson DB, Mayhew PJ (2014). Phylogenetic distribution of extant richness suggests metamorphosis is a key innovation driving diversification in insects. *PLoS ONE* **9**: e109085.
- Truman JW, Riddiford LM (1999). The origins of insect metamorphosis. *Nature* **401**: 447–452.
- Wipfler B, Letsch H, Frandsen PB, Kapli P, Mayer C, Bartel D, *et al.* (2019). Evolutionary history of Polyneoptera and its implications for our understanding of early winged insects. *Proc Natl Acad Sci USA* **116**: 3024–3029.

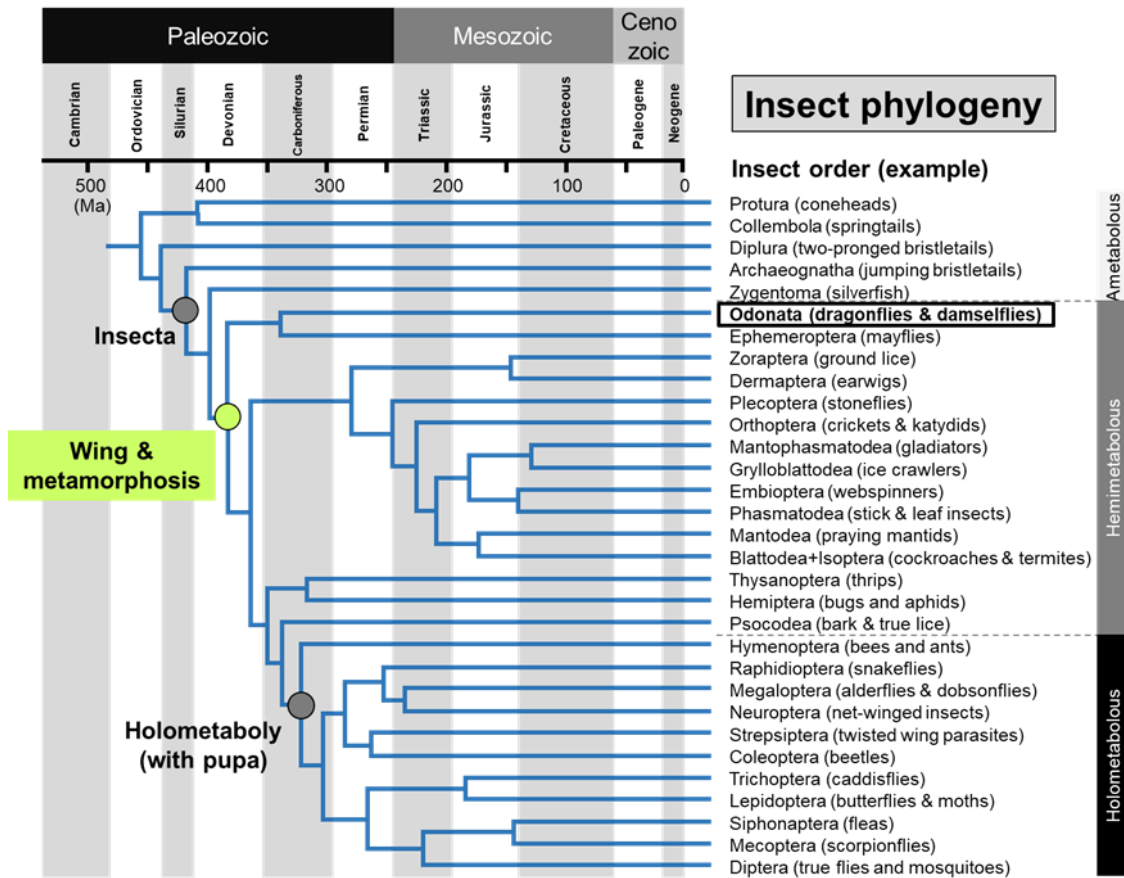


Figure 0-1.

Insect phylogeny. Dragonflies and damselflies (the order Odonata) are among the most ancestral insects with wings and metamorphosis. Figure modified from Misof et al. (2014) and Futahashi (2018).

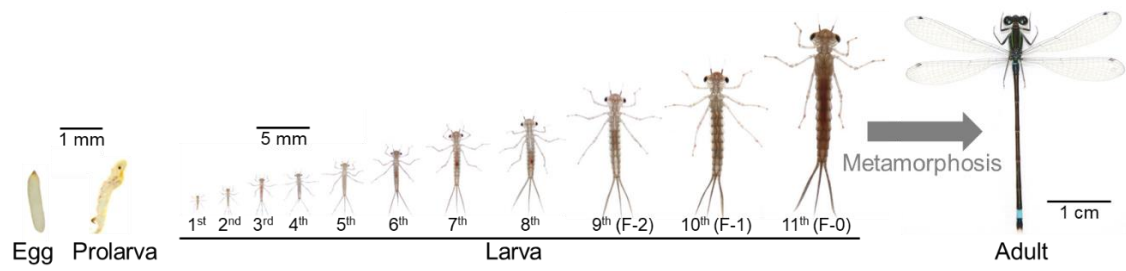


Figure 0-2.

Overview of the developmental process in Odonata. *Ischnura senegalensis* (Coenagrionidae) is shown as a representative example. Figure modified from Okude et al. 2017b. An adult photo courtesy of Ryo Futahashi.

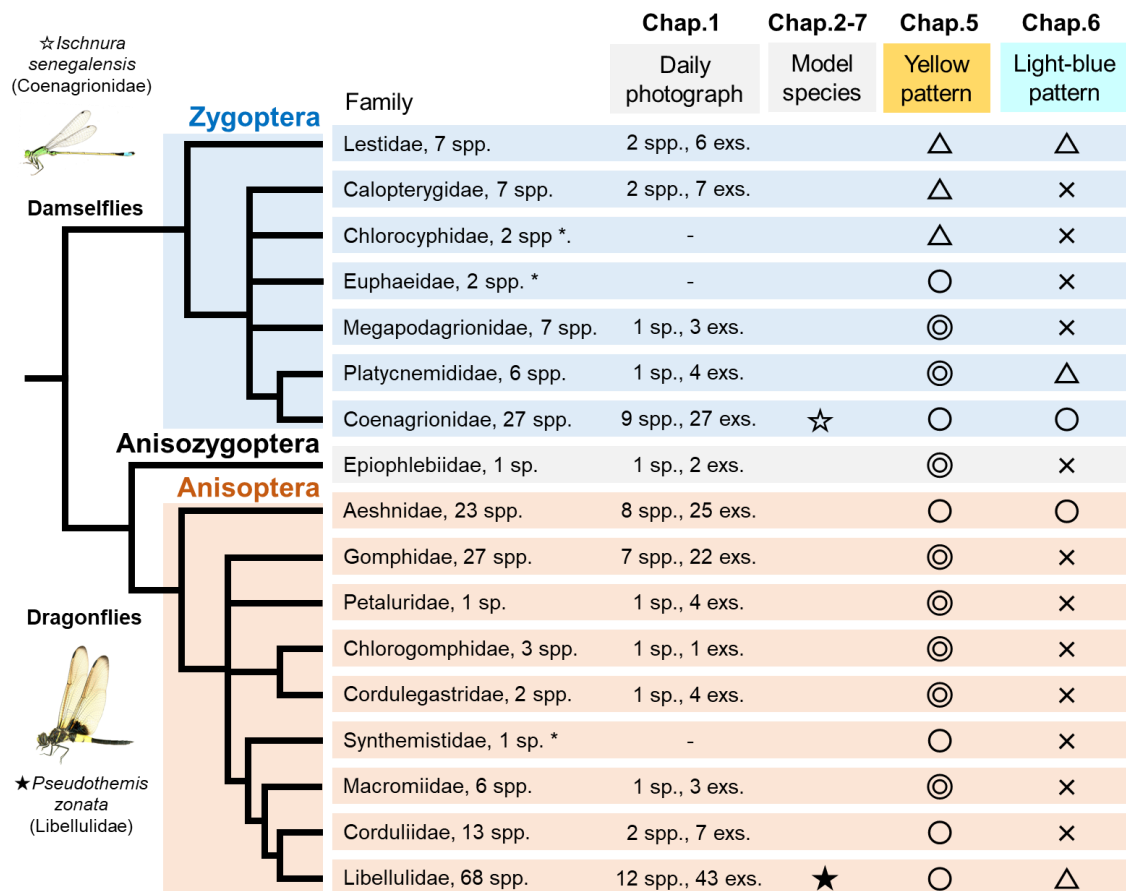


Figure 0-3.

Overview of Japanese Odonata species used in each chapter. The Odonata phylogeny and the numbers of Japanese species in each family are based on Futahashi (2018). *: Only distributed in Yaeyama or Ogasawara Islands. ☆★ Model species mainly used for gene-functional analysis in this study. *Ischnura senegalensis* (Coenagrionidae) was used in Chapter 2, 3, 4, 6, and 7, whereas *Pseudothemis zonata* (Libellulidae) was used in Chapter 2, 3, 4, and 5. The presence of species with yellow and light blue patterns in each family is indicated as follows. ◎: Always found, ○: Frequently found, △: Occasionally found, ×: Not found. Photo courtesy of Ryo Futahashi.

Chapter 1: Comprehensive comparative morphology and developmental staging of final instar larvae toward metamorphosis in the insect order Odonata.

Abstract

The order Odonata (dragonflies and damselflies) is among the most ancestral groups of winged insects with drastic morphological changes upon metamorphosis, and thus important for understanding evo-devo aspects of insects. However, basic developmental descriptions of Odonata have been scarce. In an attempt to establish the foundation of developmental and experimental biology of Odonata, I present an unprecedentedly comprehensive survey of dragonflies and damselflies, in total 158 larvae representing 49 species and 14 families, wherein morphological changes of all the final and/or penultimate instar larvae were photographed and monitored everyday. Although their morphology and development were diverse, I consistently identified two visually recognizable morphogenetic events in the final larval instar, namely start of wing expansion and onset of melanization on the wing sheaths, thereby categorizing the final instar into three stages. While the duration of the first stage ranged from 4 days to 66 days across diverse Odonata species, the second and third stages exhibited relatively small variation ranging from 3 to 22 days and 1 to 8 days respectively, probably reflecting the onset of metamorphosis at the second stage and on. I also described other characteristic morphological changes during the larval development, although they were observed only in some Odonata species and lineages.

Introduction

Dragonflies and damselflies (order Odonata) are among the most ancestral winged insects (Misof et al. 2014, Wipfler et al. 2019) and radically change their morphology, habitat, and behavior from aquatic larvae to terrestrial adults without pupal stage (Corbet 1999, Bybee et al. 2016), which entail drastic changes of gene expression patterns (e.g., opsin genes in compound eyes, Futahashi et al. 2015, Futahashi 2016). In Odonata, while adults show an impressive diversity in their body colors and patterns, larvae exhibit a remarkable diversity in their body shape, which reflect their habitats and ecological niches (e.g., Ozono et al. 2017, Ozono et al. 2019). Because mayflies (order Ephemeroptera), representing the most ancestral winged insects with Odonata, undergo the unique metamorphosis through nymph (larva), subimago, and adult, therefore the progress of the last three stages of Odonata (i.e., penultimate instar larva, final instar larva, and adult) is important in understanding the evolution of insect metamorphosis. Despite the potential biological importance, the basic information on morphological changes of Odonata during larval-adult metamorphosis has been quite fragmentary, mainly because aquatic and carnivorous Odonata larvae are difficult to maintain in the laboratory. The majority of previous studies focused on the morphological changes during the final larval instar of a single species as follows: Coenagrionidae (*Ischnura verticalis*, Grieve 1937; *Coenagrion hastulatum*, Norling 1984; *Pyrrhosoma nymphula*, Corbet and Prosser 1986; *Ischnura senegalensis*, Okude et al. 2017b [my master's thesis]; hybrids of *Ischnura elegans* and *I. senegalensis*, Okude et al. 2020, see Chapter 7), Aeshnidae (*Anax imperator*, Corbet 1957; *Aeshna cyanea*, Schaller 1957; *Aeshna viridis*, Norling 1971), Gomphidae (*Asiagomphus pryeri*, Aoki 1999) and Libellulidae (*Pachydiplax longipennis*, Eller 1963; *Pseudothemis zonata*, Miyakawa 1969; *Urothemis assignata*, Hassan 1977).

In these studies, the final larval instar was categorized into 3 to 8 developmental stages defined by morphological traits. However, since different characteristics were used as indicators of morphological changes among different species and most papers did not describe the precise timing for each stage, it is very difficult to comparatively analyze these morphological and developmental data from different Odonata species in a common framework.

Hence, in an attempt to establish the foundation of developmental and experimental biology of Odonata, I performed an unprecedentedly comprehensive morphological survey of dragonflies and damselflies. I everyday recorded the morphological changes during final and/or penultimate larval instar using 158 individuals of 49 Japanese Odonata species representing 14 families. From the enormous amount of morphological data, notably, the following two morphological changes, namely “the start of wing expansion” and “the onset of melanization on the wing sheaths”, emerged as easily and commonly recognizable developmental indices across the diverse Odonata species. Based on these indicators, the final larval instar of Odonata was generally classified into three developmental stages. Other morphological changes in the compound eyes, heads, larval labia, and wing sheaths were also described in detail, although they were observed in more specific Odonata lineages and species.

Materials and Methods

1. Terminology

Following the convention used in the majority of previous studies on Odonata, I adopt the term “larva” instead of “nymph”, because they drastically change the external

morphology through metamorphosis unlike most other hemimetabolous insects (Tillyard 1917, Corbet 1999). Following the majority of previous publications, I described the final larval instar as F-0 (= Final) and the penultimate larval instar as F-1 (= F minus 1), because the number of larval instars is not fixed in many Odonata species (Corbet 1999, Okude et al. 2017b). I started daily photographing of each larva on the day of ecdysis unless otherwise mentioned (Tables 1-1, 1-2), where the “day 1” denotes the day on which photographing started for each instar.

2. Sample collecting and rearing

All the 158 larvae of 49 Odonata species representing 14 families (Fig. 1-1, listed in Table 1-1) were collected in the field or reared from eggs that were obtained from adult females in Japan (Table 1-2). The larvae were individually kept in petri dishes with water in the laboratory. The damselfly larvae (suborder Zygoptera) were fed with *Artemia* brine shrimps, whereas dragonfly larvae (suborders Anisozygoptera and Anisoptera) were fed with *Chironomus* midge larvae. Soon after feeding cessation of the F-0 instar larvae prior to the melanization on the wing sheaths, I transferred them individually to a plastic cage (10 cm × 15 cm, 3 cm water depth) covered with a disposable non-woven mesh for assisting adult emergence.

3. Species identification

Most Japanese Odonata species were identified by their morphological characters (Ozono et al. 2019), while some species were identified by their nuclear DNA sequences as described below. I extracted DNA from a caudal gill of Zygopteran larvae or a pair of forelegs of newly-emerged Anisopteran adults by using QIAamp DNA Mini Kit (Qiagen).

Nuclear ITS1 region was PCR-amplified from the DNA samples using the primers ITS-F0 (5'- GGA AAG ATG GCC AAA CTT GA-3') and 5.8S-AS1 (5'- GCC GGC CCT CAG CCA G-3') (Futahashi et al. 2018). PCR-amplified products were subjected to DNA sequencing using BigDye Terminator v3.1 Cycle Sequencing Kit (Applied Biosystems) and 3130xl Genetic Analyzer (Applied Biosystems). Nuclear ITS sequences of all the Japanese Odonata species have been previously deposited in the public database (Futahashi 2011).

4. Photographing

F-0 and/or F-1 instar larvae were photographed everyday using a stereoscopic microscope S8APO (Leica Microsystems) with a digital high definition microscope camera MC120HD (Leica), a stereoscopic microscope S9D (Leica Microsystems) with a digital high definition microscope camera MC190HD (Leica), or a stereoscopic microscope SZ-6850T (Relyon) with a digital high definition microscope camera TrueChrome Metrics (Relyon). Most larvae were photographed from the day of ecdysis, whereas some larvae were photographed from the day of collection, when the insects were already F-0 instar (See Table 1-2). The obtained photographs were adjusted by using software GIMP (GNU Image Manipulation Program) 2.10.6.

Results

1. Three developmental stages during F-0 instar commonly observed among diverse Odonata species

I took photos of 158 Odonata larvae (150 F-0 instar and/or 22 F-1 instar) of 49 species

everyday (Fig. 1-1, Tables 1-1, 1-2), and all the photos were aligned for comparison of morphological characters within and between the species (Fig. 1-2, Supplementary Figs. S1, S2, S3). First, I compared daily morphological changes of F-0 instar larvae thoroughly. The indicators used for larval staging were selected on the following criteria: (i) morphological changes can be observed without damaging the larva, (ii) the changes are stepwise rather than continuous so that the specific timing of entry into another stage can be determined, and (iii) the indicator applies to various species and individuals. The most prominent morphological changes commonly observed in almost all the examined species were “the start of wing expansion” and “the onset of melanization on the wing sheaths”. Based on these indicators, the F-0 larval instar could be classified into three developmental stages for most of the examined Odonata species (Fig. 1-3, Table 1-1). In stage 1, the wing sheaths are flat without noticeable structures and pigmentation. The tips of the forewings are hidden under the hindwings (Fig. 1-3B). In stage 2, the wing sheaths begin to expand. I can distinguish stage 2 from stage 1 by the criteria that the tips of the forewings appear from under the hindwings (Fig. 1-3B, white arrowheads). In stage 3, black dots appear around the anterior edges of the wing sheaths, and black pigmentation also appears at the base of the wing sheaths (Fig. 1-3B, black arrowheads). Among the 49 species I examined, stage 3 was difficult to define for only two species (*Epiophlebia superstes* and *Sinogomphus flavolimbatus*), because their entire body is very dark in color (Tables 1-1, 1-2, Supplementary Fig. S1). It should be noted that two species of the genus *Lestes* (Lestidae) did not exhibit black dots on the wings but could be classified as stage 3 by melanization at the base of the wing sheaths (Tables 1-1, 1-2, Supplementary Fig. S1). While a previous study partly mentioned these criteria for developmental staging of *Pyrrhosoma nymphula* (Corbet and Prosser 1986), here I demonstrate that these

developmental criteria are applicable to most of the diverse Odonata species (Table 1-1). Next, I examined morphological changes during F-1 (penultimate) larval instar of Odonata, which a few previous studies described for only three species: *Pachydiplax longipennis* (Eller 1963), *Aeshna viridis* (Norling 1971) and *Ischnura senegalensis* (Okude et al. 2017b). For all the 22 F-1 instar larvae representing 12 species (Tables 1-1, 1-2), the compound eyes gradually tilted during F-1 instar, and the wing sheaths began to expand a few days before ecdysis to F-0 instar (Fig. 1-2C, Supplementary Fig. S2).

2. Variation in the duration of developmental stages during F-0 instar within and between Odonata species

I noticed significant intra-specific variation in the total duration of the F-0 larval instar (Fig. 1-4A, Table 1-2). I compared the durations of these developmental stages and identified large variation in the durations of stage 1 within and between the Odonata species (Fig. 1-4A, 4B). By contrast, the durations of stage 2 and stage 3 were less variable between and within the species (Fig. 1-4). Many river-dwelling Odonata species (e.g., Calopterygidae, Gomphidae, Cordulegastridae, Chlorogomphidae, and Macromiidae) are known to overwinter as F-0 instar larvae (Corbet 1957, Aoki 1999). In these species, notably, while the total durations of F-0 larval instar were generally and conspicuously long (Table 1-2), the durations of stage 2 and stage 3 were relatively short and similar between species, 3-21 days and 1-8 days respectively (Fig. 1-4). It should be noted that the duration of larvae (especially before stage 1) in this study may be different from that in the field, considering that only a limited type of food was supplied in the laboratory. It is also notable that the F-0 larval development generally proceeds without food after stage 2. Overall, the durations after the onset of morphological change (i.e.,

stage 2 and on) exhibited relatively small variation, suggesting that the developmental processes for metamorphosis after stage 2 proceed steadily and irreversibly.

3. Morphological changes in compound eyes of damselfly larvae

To my knowledge, Grieve (1937) first mentioned the expansion of the compound eyes during F-0 larval instar in the damselfly *Ischnura verticalis* (Coenagrionidae). In my master's thesis (published in Okude et al. 2017b), I categorized F-0 larval instar of *I. senegalensis* (Coenagrionidae) into five developmental stages (from stage A to stage E) that entail the following two-step expansions of the compound eyes: the dorsal expansion (Fig. 1-5B, a black arrowhead) in the 2nd stage (stage B) and the posterior expansion (Fig. 1-5C, 5D, white arrowheads) in the 4th stage (stage D) (Fig. 1-5Y). I confirmed that stage A is consistent with stage 1 of this study, whereas stage E is the same as stage 3 of this study (Fig. 1-5Y). My comparative survey of diverse damselfly species (Zygoptera) revealed that the two-step expansions of the compound eyes were recognized only in Coenagrionidae species (Fig. 1-5, Table 1-1), and the two-step expansions are sometimes observed simultaneously during stage 2 in this study (ex. *Enallagma circulatum*; Fig 1-5E-5H).

In Lestidae (Fig. 1-5I-5L) and Calopterygidae species (Fig. 1-5M-5P), the dorsal expansion of the compound eyes was certainly recognizable, but this expansion proceeded gradually from stage 1 to stage 2 and thus was not suitable as an indicator for developmental staging, whereas the posterior expansion of the compound eyes was faintly observed before stage 3 (Fig. 1-5L, 5P, white arrowheads). In Platycnemididae and *Rhipidolestes* (family status is uncertain) species, the expansion of the compound eyes was observed less obviously, which was partly due to the melanization on their body

surface and thus not suitable as an indicator for developmental staging (Fig. 1-5Q-5X). Hence, I concluded that the developmental stages B, C and D defined by my master's thesis (Okude et al. 2017b) (Fig. 1-5Y) are only applicable to some Coenagrionidae species.

4. Morphological changes in compound eyes of dragonfly larvae

Among dragonfly species (Anisozygoptera and Anisoptera), Aeshnidae larvae exhibited the relatively complicated expansion patterns in their compound eyes as previously described (Corbet 1957, Schaller 1957, Norling 1971). During stage 1, the compound eyes expanded gradually toward the midline (Fig. 1-6A-6D). During stage 2, apolysis-like phenomenon was observed from the anterior side to the posterior side of the compound eyes (Fig. 1-6E-6L, black arrowheads; Fig. 1-6Y). This apolysis-like phenomenon was also observed, though faintly, in the compound eyes of some Libellulidae species (e.g., *C. servilia*) (Fig. 1-6O, Supplementary Fig. S1, Table 1-1).

The expansion of the compound eyes was also observed commonly in dragonfly species other than Aeshnidae species (Fig. 1-6M-6X). In some Libellulidae species, newly-formed regions of the compound eyes were clearly distinguishable morphologically (Fig. 1-6N-6P, 6R-6T, white arrowheads, Fig. 1-6Z). These regions gradually expanded from mid-stage 1 to stage 3 (Fig. 1-6M-6T, 6Y, 6Z). Meanwhile, the boundary of the newly formed regions was less obvious in several dragonfly species including Libellulidae (e.g., *Rhyothemis fuliginosa*), and thus cannot be regarded as common developmental indicators (Fig. 1-6U-6X, Table 1-1).

In Gomphidae, Petaluridae, Chlorogomphidae, Cordulegastridae, Macromidae and Corduliidae species, the posterior expansion patterns of the compound eyes were similar

to those in Libellulidae species (Fig. 1-7). It should be noted that the morphological changes of the compound eyes were difficult to observe in species and/or individuals with dark-colored heads (e.g., *Epiophlebia superstes*, Fig. 1-7S-7U), as reported for *Pseudothemis zonata* (Libellulidae) (Miyakawa 1969). On the day before adult emergence, the compound eyes became as bright as those of adult (Fig. 1-7U).

5. Other morphological changes observed in F-0 instar larvae

I also summarized other morphological changes that were constantly observed within some specific Odonata lineages (Fig. 1-8, Table 1). In most damselfly species, specific markings appeared after stage 2 on their heads, prothoraces, around ocelli and mandibles (Fig. 1-8A, 8B, Table 1-1, white arrowheads), and thinning of antennae was observed during stage 2 (Fig. 1-8A, 8B, white arrowhead), as reported in my master's thesis (Okude et al. 2017b).

Previous studies regarded the wrinkles on the wing sheaths (described as “accordion-like” in Schaller 1957) as an indicator of metamorphosis in Odonata (Schaller 1957, Eller 1963, Norling 1984, Corbet and Prosser 1986). In general, the wrinkles appeared a few days after the onset of stage 2 (Fig. 1-8c). While the wrinkles on the wings were clearly visible in many Odonata species (Fig. 1-8D, 8G, white arrowheads, Table 1-1), they were less obvious in some species (e.g., *Orthetrum albistylum*: Fig. 1-8I, 8J). Just before adult emergence at the end of stage 3, the bristles on the body surface were melanized (Fig. 1-8K, 8L), although this change was often masked by dark pigmentation of the body surface.

The degradation of larval labium, or shrinkage of tissues within the larval prementum, has been also used as an indicator of metamorphosis in Odonata (Corbet 1957, Norling 1971, Norling 1984, Corbet and Prosser 1986). I photographed the daily changes in the

larval labium of 18 larvae representing 7 species (Table 1-1, Supplementary Fig. S3). The degradation of larval labium was more prominent in dragonfly species (Anisoptera) (Fig. 1-8Q-8Y) than in damselfly species (Zygoptera) (Fig. 1-8O-8P, 8Z-8b). I confirmed that the degradation of larval labium occurred from late stage 2 to stage 3 (Fig. 1-8Q-8c, white arrowheads). It should be noted that the changes in larval labium were not prominent in some species like *Tanypteryx pryeri* (Petaluridae, Fig. 1-8M-8N) and *I. senegalensis* (Coenagrionidae, Fig. 1-8O-8P).

Discussion

In this study, I described the daily morphological changes of F-0 and/or F-1 instar larvae, using 158 individuals of 49 Odonata species. The comprehensive and detailed information provided by this study enables us to determine precise developmental stages during larval-adult metamorphosis across diverse Odonata species. Based on the morphology of wing sheaths, F-0 larval instar could be classified into three developmental stages for most of the examined Odonata species.

This description of morphological changes during F-0 instar sheds light on the process of drastic metamorphosis without pupal stage. Through metamorphosis, Odonata are known to remarkably change the expression levels and patterns of *opsin* genes in the compound eyes between aquatic larvae and terrestrial adults (Futahashi et al. 2015, Futahashi 2016), while the biological process of metamorphosis in Odonata remain poorly understood. My detailed description will be an indicator for the comparative analysis in morphological, physiological, and molecular biological aspects to reveal the precise process of the Odonata metamorphosis without pupal stage.

Also, Odonata are among the most ancestral insects with metamorphosis and are important in studying the origin of insect metamorphosis. However, even the fluctuance of insect hormones (e.g. ecdysteroids) during F-0 instar, which regulate the drastic changes during metamorphosis in general insects (Andries 1979, Belles 2020), has been only described fragmentarily (Schaller and Hoffmann 1973). Detailed metamorphic process which my description has brought will advance the comparative analysis of the physiological and molecular mechanisms of metamorphosis with other insects toward understanding the evolution of metamorphosis.

Recently I established a gene knockdown method by electroporation-mediated RNAi in Odonata (Okude et al. 2017a, see also Chapter 2). It should be noted the proper larval staging is critical for effective gene knockdown (see Chapter 2). Considering the morphological diversity in Odonata larvae, unified staging across species in this study could be a general indicator to find an appropriate stage for RNAi in the various Odonata species, and consequently facilitates the molecular biological studies on various topics of Odonata.

References

- Andries JC (1979). Effect on exogenous JHI on imaginal determination in *Aeshna cyanea*. *J. Insect Physiol.* **25**: 621–627.
- Aoki T (1999). Larval development, emergence and seasonal regulation in *Asiagomphus pryeri* (Selys) (Odonata: Gomphidae). *Hydrobiologia* **394**: 179–192.
- Belles X (2020). *Insect metamorphosis: from natural history to regulation of development and evolution*. Academic Press.
- Bybee S, Córdoba-Aguilar A, Duryea MC, Futahashi R, Hansson B, Lorenzo-Carballea MO, et al. (2016). Odonata (dragonflies and damselflies) as a bridge between ecology and evolutionary genomics. *Front Zool* **13**: 46.
- Corbet PS (1957). The Life-history of the Emperor dragonfly *Anax imperator* Leach (Odonata:

Aeshnidae). *J Anim Ecol* **26**: 1–69.

Corbet PS (1999). *Dragonflies, Behavior and Ecology of Odonata*. Cornell University Press.

Corbet PS, Prosser RJS (1986). Diagnosis of interecdysial development in final-instar larvae of *Pyrrhosoma nymphula* (Sulzer) (Zygoptera: Coenagrionidae). *Odonatologica* **15**: 23–28.

Dijkstra KD, Kalkman VJ, Dow RA, Stokvis FR, Van Tol J (2014). Redefining the damselfly families: a comprehensive molecular phylogeny of Zygoptera (Odonata). *Syst Entomol* **39**: 68–96.

Eller JG (1963). Seasonal regulation in *Pachydiplax longipennis* (Burmeister) (Odonata: Libellulidae). DrT, Univ. North Carolina, Chapel Hill.

Futahashi R (2011). A revisional study of Japanese dragonflies based on DNA analysis (1). *TOMBO* **53**: 67–74. (in Japanese with English summary)

Futahashi R (2016). Color vision and color formation in dragonflies. *Curr Opin Insect Sci* **17**: 32–39.

Futahashi R, Kawahara-Miki R, Kinoshita M, Yoshitake K, Yajima S, Arikawa K, *et al.* (2015). Extraordinary diversity of visual opsin genes in dragonflies. *Proc Natl Acad Sci USA* **112**: E1247–1256.

Futahashi R, Okude G, Sugimura M, Ugai S (2018). Interspecific hybrids in Japanese Odonata. *TOMBO* **60**: 1–49. (In Japanese with English abstract, figures and tables.)

Grieve E (1937). Studies on the biology of the damselfly, *Ischnura verticalis* (Say), with notes on certain parasites. *Entomol Am* **17**: 121–153.

Hassan AT (1977). The larval stages of *Urothemis assignata* (Selys) (Anisoptera: Libellulidae). *Odonatologica* **6**: 151–161.

Misof B, Liu S, Meusemann K, Peters RS, Donath A, Mayer C, *et al.* (2014). Phylogenomics resolves the timing and pattern of insect evolution. *Science* **346**: 763–767.

Miyakawa K (1969). A study of the life-history of *Pseudothemis zonata* (Burm.) (Odonata, Libellulidae). II. Immature stage. *Kontyû* **37**: 409–422. (in Japanese)

Norling U (1971). The life history and seasonal regulation of *Aeshna viridis* Eversm. in southern Sweden (Odonata). *Insect Syst Evol* **2**: 170–190.

Norling U (1984). The life cycle and larval photoperiodic responses of *Coenagrion hastulatum* (Charpentier) in two climatically different areas (Zygoptera: Coenagrionidae). *Odonatologica* **13**: 429–449.

Okude G, Futahashi R, Kawahara-Miki R, Yoshitake K, Yajima S, Fukatsu T (2017a). Electroporation-mediated RNA interference reveals a role of the multicopper oxidase 2 gene in dragonfly cuticular pigmentation. *Appl Entomol Zool* **52**: 379–387.

Okude G, Futahashi R, Tanahashi M, Fukatsu T (2017b). Laboratory rearing system for *Ischnura senegalensis* (Insecta: Odonata) enables detailed description of larval development and morphogenesis in dragonfly. *Zool Sci* **34**: 386–397.

Okude G, Fukatsu T, Futahashi R (2020). Interspecific crossing between blue-tailed damselflies *Ischnura elegans* and *I. senegalensis* in the laboratory. *Entomol Sci* **23**: 165–172.

Ozono A, Kawashima I, Futahashi R (2017). *Dragonflies of Japan*. (3rd edition) Bunichi-Sogo Syuppan, Co Ltd. (in Japanese)

Ozono A, Kawashima I, Futahashi R (2019). *The handbook of Japanese aquatic insects. Volume 3: dragonfly larvae*. Bunichi-Sogo Syuppan, Co Ltd. (in Japanese)

Schaller F (1957). Préliminaire de la métamorphose chez les Odonates. Observations sur les stades larvaires d'*Aeschna cyanea* Müll. (Odonata). *Act. Soc. linn. Bordeaux* **97**: 121–134. (in French)

Schaller F, Hoffmann JA (1973). Evolution du taux d'ecdysone au cours du dernier stade larvaire d'*Aeshna cyanea* Müll. (Insecte, Odonate). *C. R. Acad. Sc. Paris (D)* **277**: 741–743. (in French)

Wipfler B, Letsch H, Frandsen PB, Kapli P, Mayer C, Bartel D, *et al.* (2019). Evolutionary history of Polyneoptera and its implications for our understanding of early winged insects. *Proc Natl Acad Sci USA* **116**: 3024–3029.

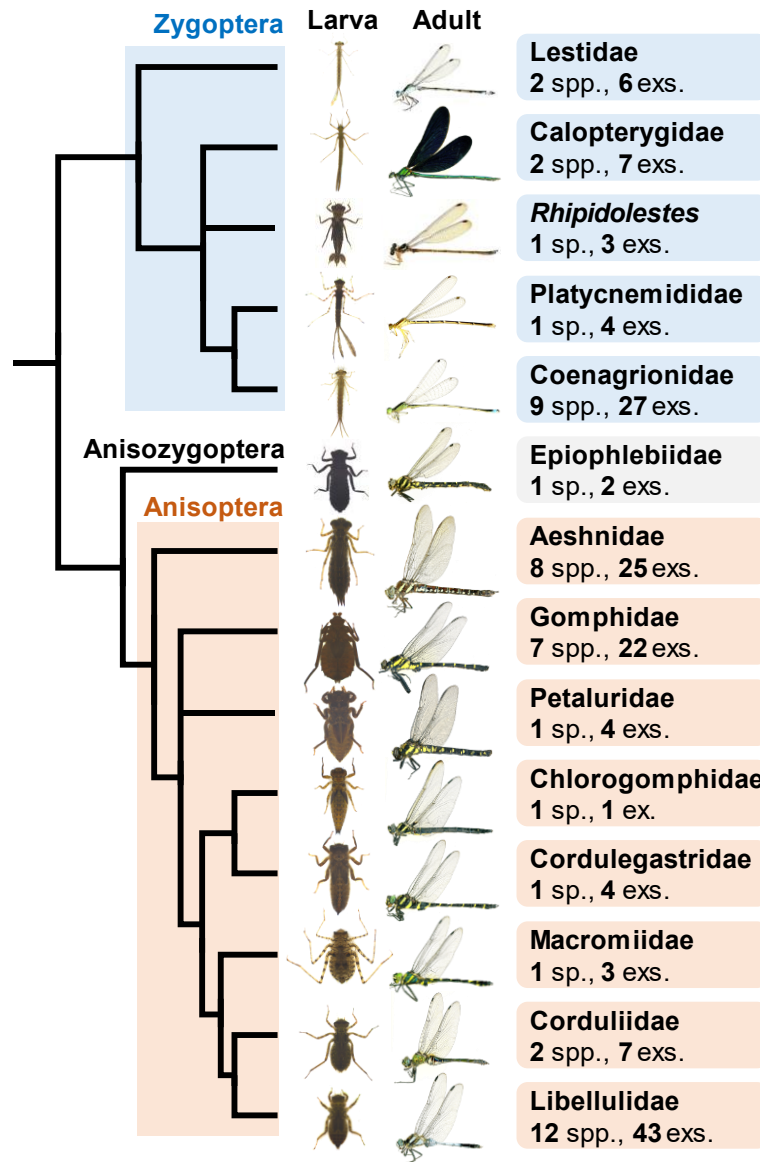


Figure 1-1.

Summary of Odonata species examined in this study. 49 Odonata species (158 individuals) were photographed everyday (see Table 1-1 and Table 1-2 in detail). Phylogenetic tree of Odonata was modified from Bybee et al. (2016). The family status of *Rhipidolestes* is currently uncertain (*Incertae sedis* group 1 in Dijkstra et al. 2014). Larva and adult photos of the following 14 species are shown: *Lestes sponsa* (Lestidae), *Calopteryx japonica* (Calopterygidae), *Rhipidolestes hiraoui* (*incertae sedis*), *Pseudocoperca annulata* (Platycnemididae), *Ischnura asiatica* (Coenagrionidae), *Epiophlebia superstes* (Epiophlebiidae), *Aeshna crenata* (Aeshnidae), *Sieboldius albardae* (Gomphidae), *Tanypteryx pryeri* (Petaluridae), *Chlorogomphus brunneus* (Chlorogomphidae), *Anotogaster sieboldii* (Cordulegastridae), *Macromia daimoji* (Macromiidae), *Somatochlora uchidai* (Corduliidae), and *Orthetrum albistylum* (Libellulidae).

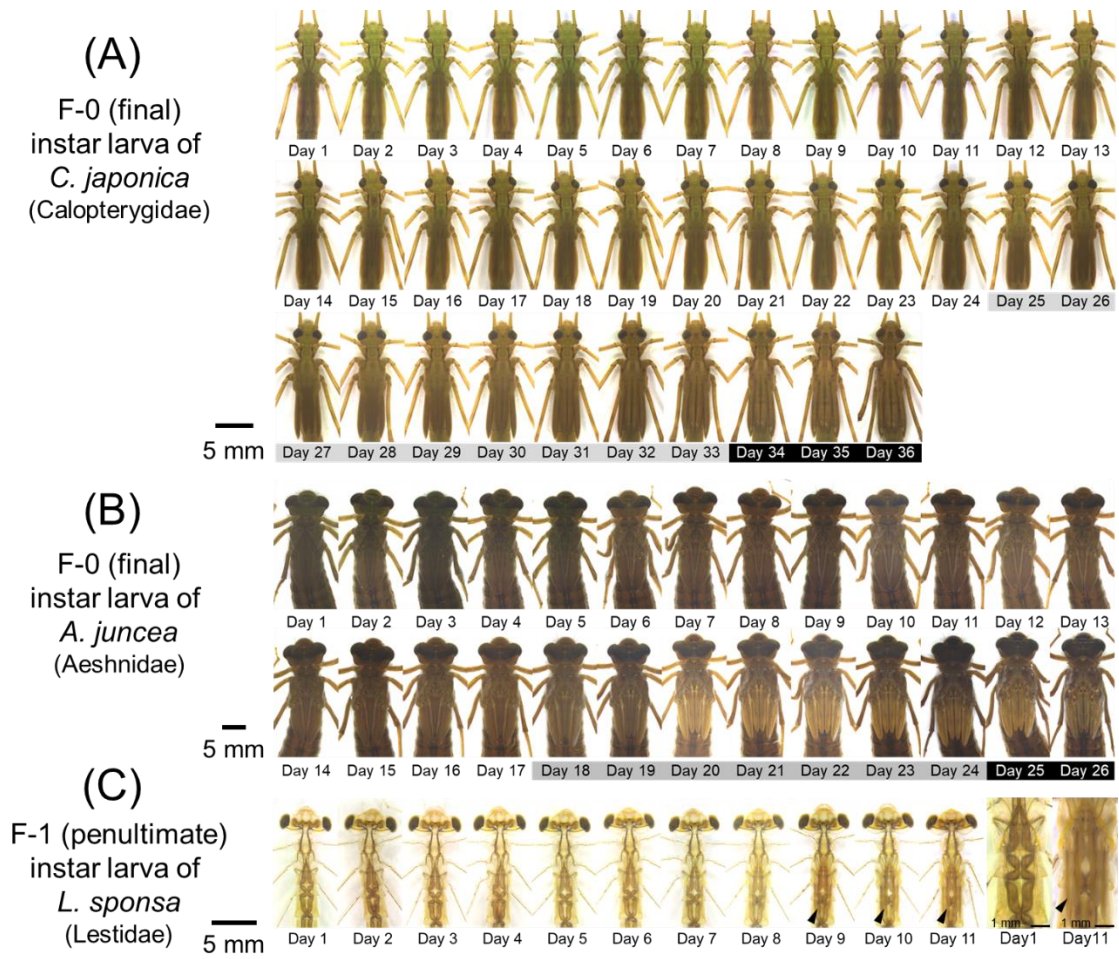


Figure 1-2.

Examples of daily photos obtained in this study. For all photos, see Supplementary Figs. S1 and S2. (A) F-0 instar female larva of *Calopteryx japonica* (Calopterygidae, Zygoptera). Adult emergence was observed on Day 37. (B) F-0 instar female larva of *Aeshna juncea* (Aeshnidae, Anisoptera). Adult emergence was observed on Day 27. (C) F-1 instar female larva of *Lestes sponsa* (Lestidae, Zygoptera). Ecdysis to F-0 instar was observed on Day 12. Black arrowheads indicate the expansion of the wing sheaths. Day numbers shaded in gray or black indicate stage 2 or 3, respectively.

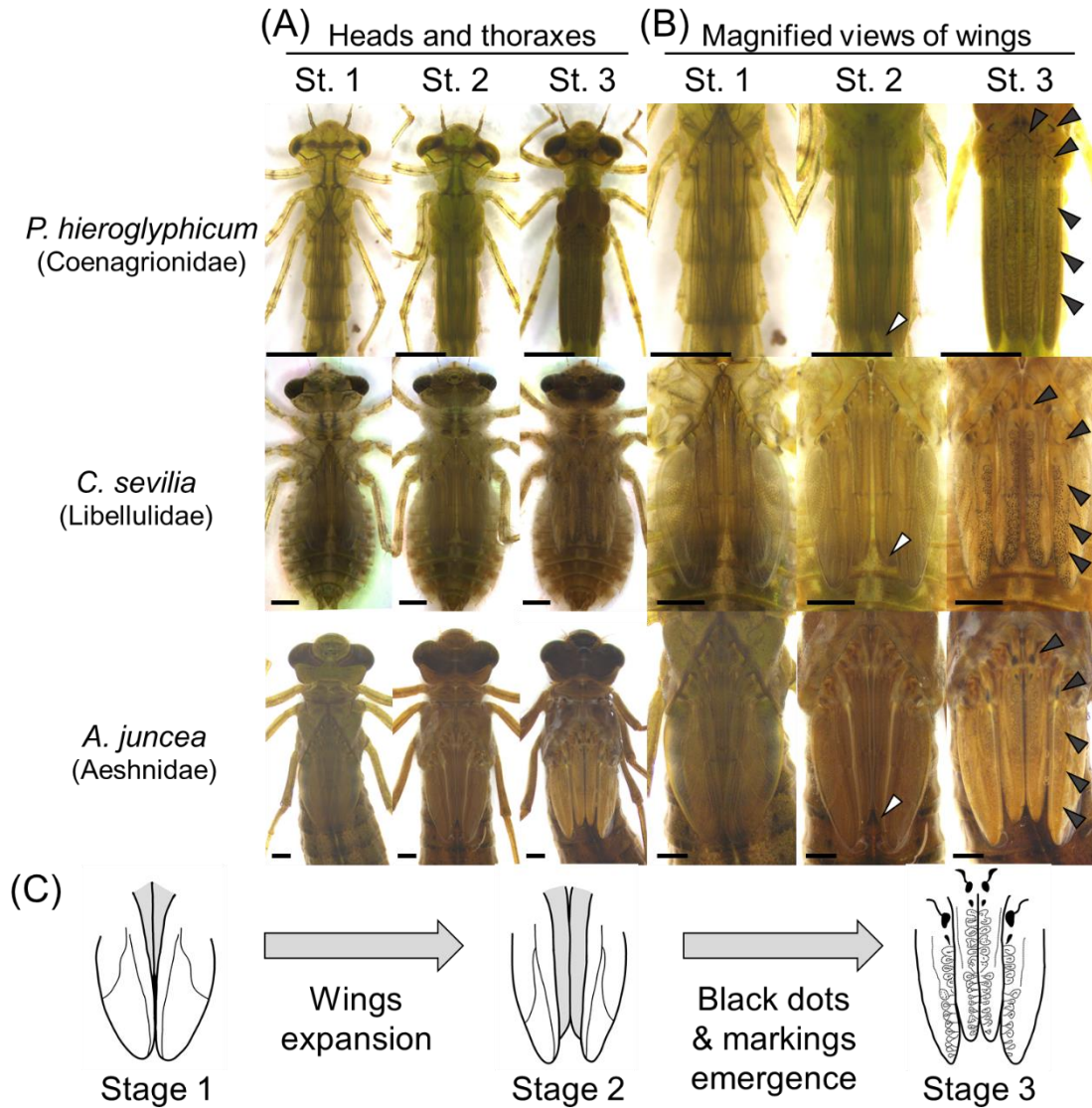


Figure 1-3.

Summary of three developmental stages commonly observed in F-0 instar larvae among diverse Odonata species. (A) Dorsal views of heads, thoraxes, and wings. (B) Magnified views of wing sheaths. White arrowheads indicate the dorsal tips of forewings (defining the onset of stage 2). Black arrowheads indicate the black dots and markings on the wing sheaths (defining the onset of stage 3). All scale bars show 2 mm. All the photos were taken on the first day of each stage. (C) Schematic diagrams of three developmental stages.

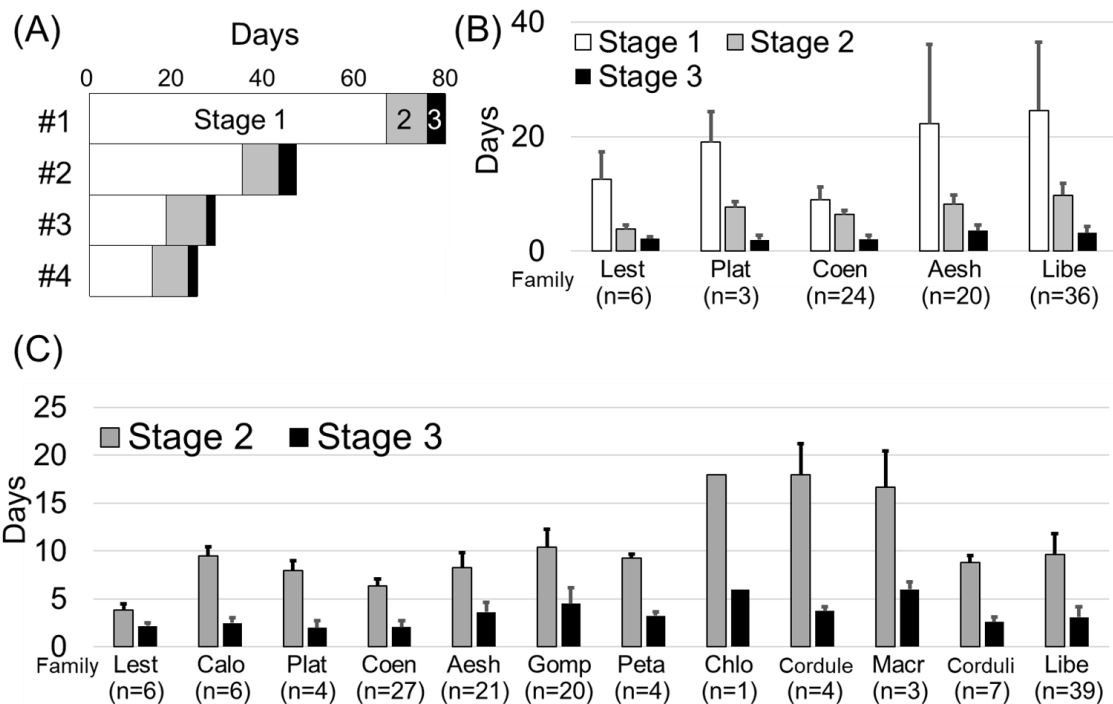


Figure 1-4.

Durations of stages 1, 2 and 3 of observed larvae. (A) Durations of stages 1, 2 and 3 of four individuals of *Aeshna crenata* (Aeshnidae), highlighting varied lengths of stage 1 compared with relatively short and constant lengths of stages 2 and 3 (also see Table 1-2). (B) Durations of stages 1, 2 and 3 of F-0 instar larvae representing different Odonata families. (C) Durations of stage 2 and stage 3 of observed larvae. Duration of Stage 1 is not included in this figure because we started to photograph in the middle of stage 1 for most individuals of river dwelling species. Error bars show standard deviations. Abbreviations: Lest, Lestidae; Calo, Calopterygidae; Plat, Platycnemididae; Coen, Coenagrionidae; Aesh, Aeshnidae; Gomp, Gomphidae; Peta, Petaluridae; Chlo, Chlorogomphidae; Cordule, Cordulegastridae; Macr, Macromiidae; Corduli, Corduliidae; Libe, Libellulidae.

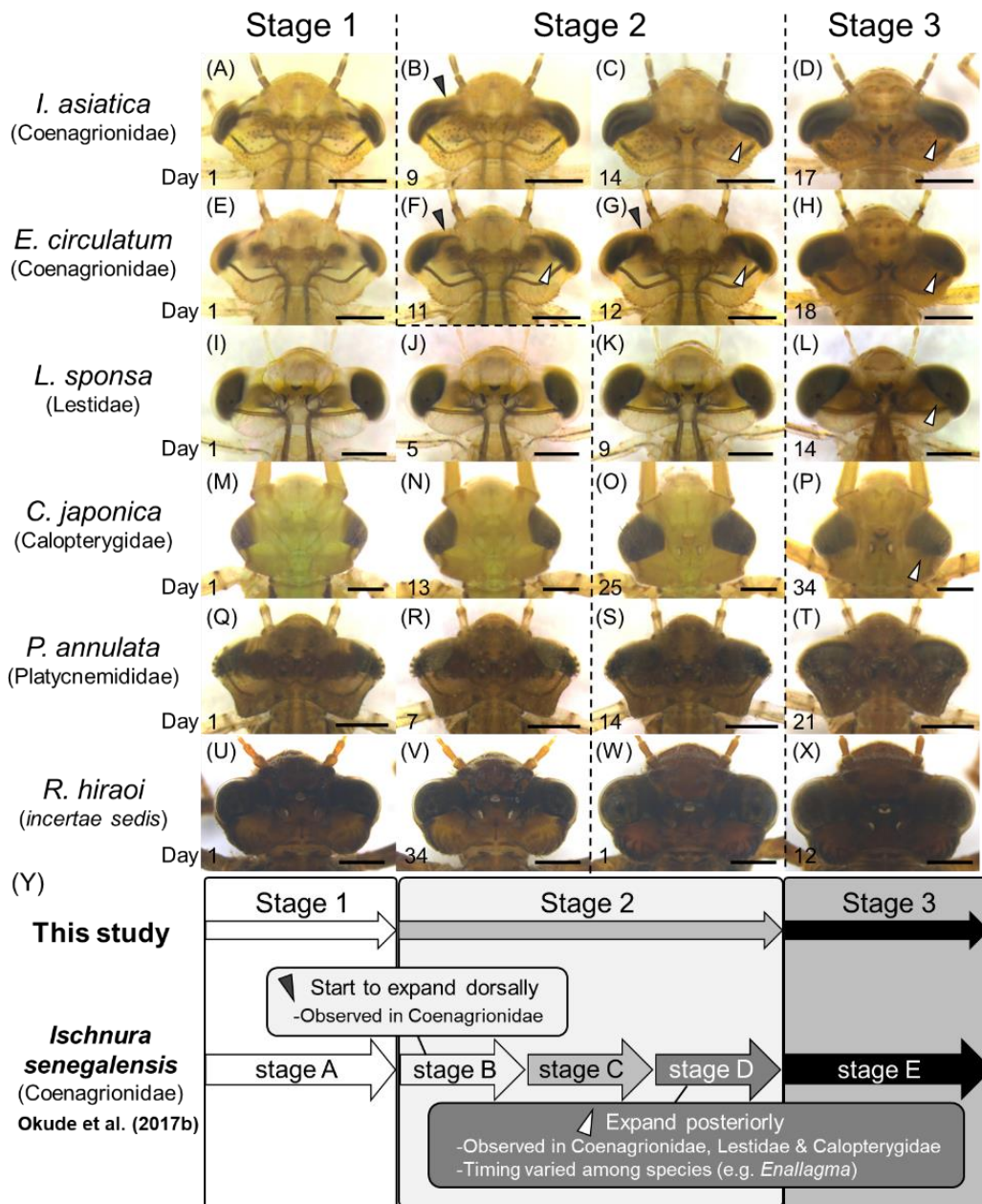


Figure 1-5.

Morphological changes during F-0 instar observed in the compound eyes of damselfly (Zygoptera) larvae. (A-X) Dorsal views of the heads. All scale bars show 1 mm. Species and family names are provided on the left side. The number shown on the lower left of each image indicates the number of days after ecdysis to F-0 instar (A-T) and after starting of photographing (U-X). Black arrowheads indicate the dorsal expansion of the compound eyes, whereas white arrowheads indicate the posterior expansion of the compound eyes. (A, E, I, M, and Q) The first day of stage 1. (B, F, K, O, and S) The first day of stage 2. (C) The first day of stage D (my master's thesis, Okude et al. 2017b) in which posterior expansion begin. (D, H, L, P, and T) The first day of stage 3. (U) The first day of photographing in individual No. 5-1 (stage 1). (V) The 34th day of the photographing in individual No. 5-1 (stage 1). This individual No. 5-1 died before entering stage 2. (W) The first day of the photographing in individual No.5-2 (early stage 2). (X) The first day of stage 3 in individual No. 5-2. (Y) Schematic diagrams of the comparison of the developmental stages during F-0 larval instar defined in this study and those proposed by my master's thesis (Okude et al. 2017b).

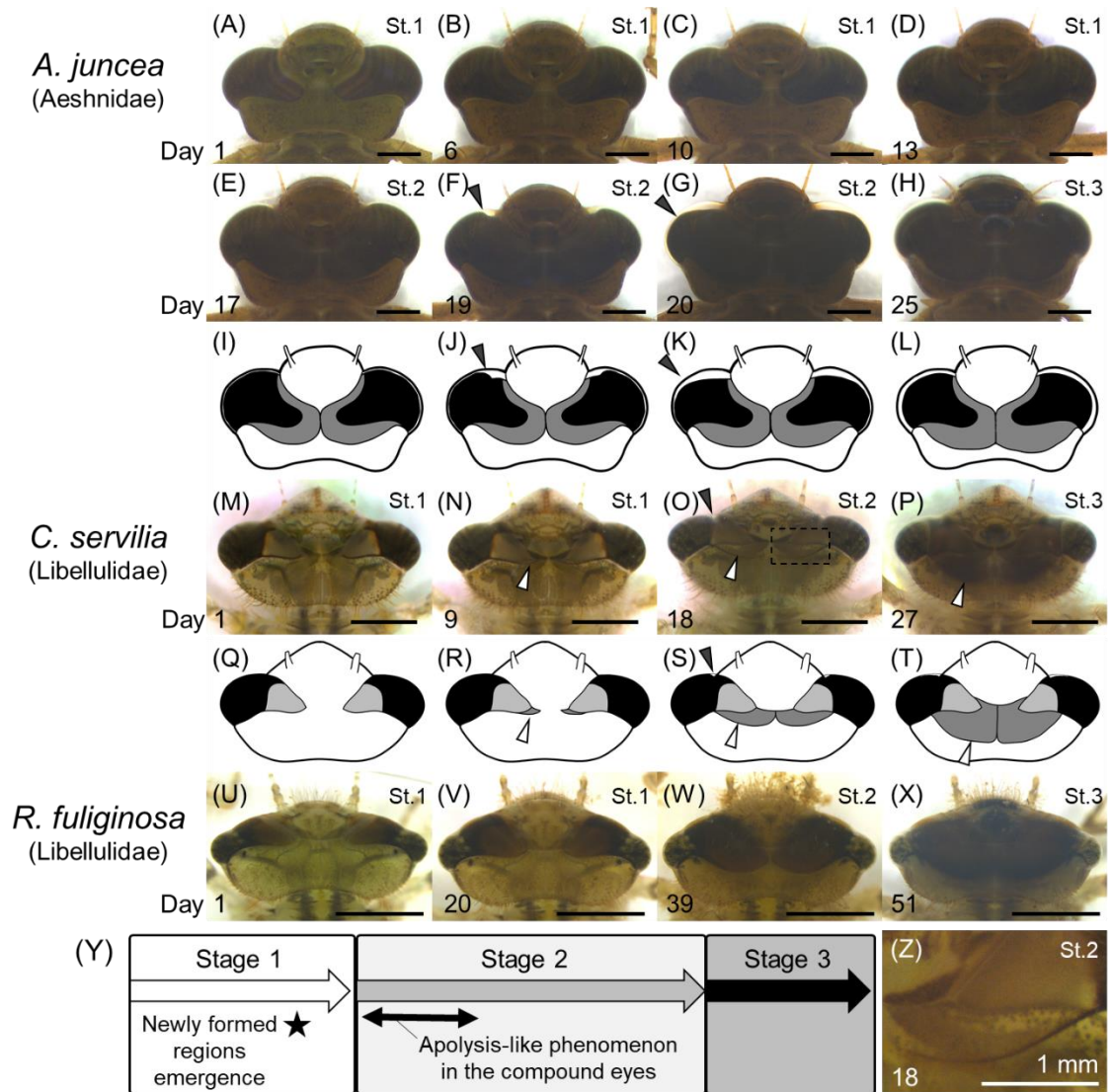


Figure 1-6.

Morphological changes of the compound eyes during F-0 instar in Aeshnidae and Libellulidae larvae. (A-X) Dorsal views of the heads. All scale bars show 2 mm. Species and family names are provided on the left side. The number shown on the lower left of each image indicates the number of days after ecdysis to F-0 instar. Black arrowheads indicate the progression of the apolysis-like phenomenon in the compound eyes. White arrowheads indicate the newly formed regions of the compound eyes. (I-L, and Q-T) Schematic illustration of changes in shape and size of compound eyes. (I-L) or (Q-T) correspond to (E-H) or (M-P), respectively. (A, M, and U) The first day of stage 1. (E, I, O, S, and W) The first day of stage 2. (H, L, P, T, and X) The first day of stage 3. (N, R) First day when the newly formed regions appeared. (Y) Schematic diagrams on the timing of the morphological changes during F-0 larval instar. (Z) Magnified view of the newly formed region in Fig. 1-6O.

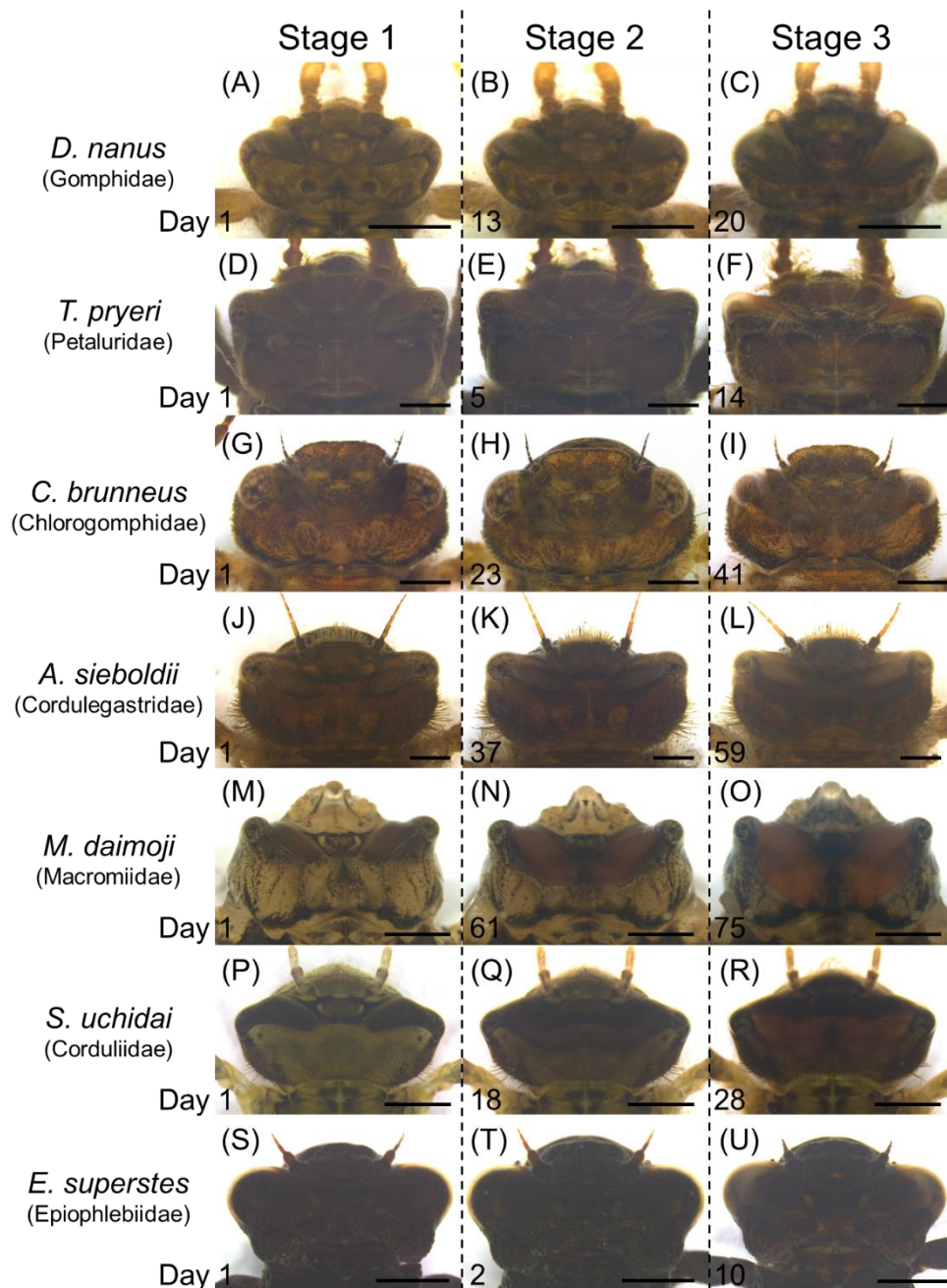


Figure 1-7.

Morphological changes of the compound eyes during F-0 instar in Gomphidae, Petaluridae, Chlorogomphidae, Cordulegastridae, Macromiidae, Corduliidae, and Epiophlebiidae species. (A-U) Dorsal views of the heads. All scale bars show 2 mm. Species and family names are provided on the left side. The number shown on the lower left of each image indicates the number of days from the day of ecdysis or collection. (A, D, G, J, and M) The first day of starting photographing. (P) The first day of stage 1. (B, E, H, K, N, Q, and T) The first day of stage 2. (C, F, I, L, O, and R) The first day of stage 3. (U) The day before adult emergence.

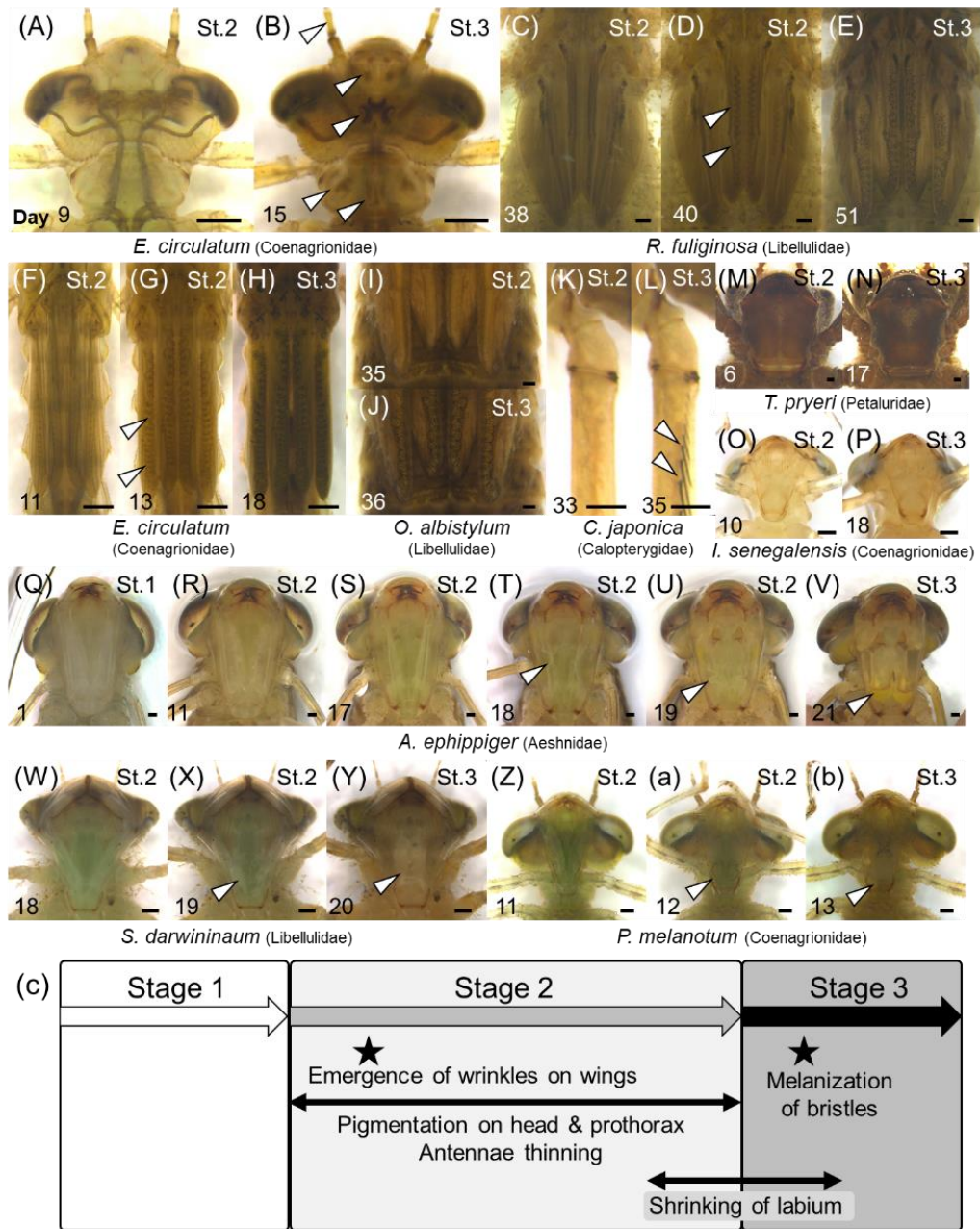


Figure 1-8.

Morphological changes other than compound eyes during F-0 larval instar. The number on each photo indicates the number of days after ecdysis or starting photographing. All scale bars show 0.5 mm. Species and family names are indicated at the bottom. Developmental stage is shown on the upper right of each photo. (A-B) Dorsal views of the heads. White arrowheads indicate specific pigmentation that appeared during stage 2. (C-J) Magnified views of wing sheaths. White arrowheads indicate wrinkles in the wing sheaths. (C, F) The first day of stage 2. (D, G) The day on which the wrinkles on the wing sheaths appeared. (E, H) The first day of stage 3. (K-L) Magnified views of right foreleg. White arrowheads indicate melanized bristles. Adult emergence was observed on Day 37. (M-b) Ventral views of the heads. White arrowheads indicate the degraded larval labia. (Q) The first day of stage 1. (M, O, R). The first day of stage 2. (T, W, and Z) Two days before the onset of stage 3. (U, X, and a) One day before the onset of stage 3. (Y, b) The first day of stage 3. (N, P, and V) The last day of stage 3. (c) Schematic diagrams on the timing of the morphological changes during F-0 larval instar.

Table 1-1.

Interspecific diversity of morphological changes during F-0 instar larvae. (*1) Difficult to determine the start point when the newly formed regions appear. (*2) Gradually expand since stage 1. Ref. 1: Okude et al. (2017b). Ref. 2: Okude et al. (2020), see Chapter 2.

Species No.	Family	Species	The number of individuals		Clear emergence of newly formed regions	Compound eyes expansion to dorsal side	Wing sheaths Expansion	Wrinkles on the wings	Pigmentation on the head	Apolyses on compound eyes	Degradation of larval labrum	Black markings on the basal wings	Black dots emergence		Bristles melanization
			F-1	F-0									3-1	3-2	
						Stage 1		Stage 2						Stage 3	
1	Lestidae	<i>Lestes sponsa</i>	1	1	X	Δ(*2)	○	○	○	X	-	○		X	X
2	Lestidae	<i>Lestes temporalis</i>	1	5	X	Δ(*2)	○	○	○	X	-	○		X	X
3	Calopterygidae	<i>Mnais costalis</i>	0	6	X	Δ(*2)	○	○	X	X	-	○		○	X
4	Calopterygidae	<i>Calopteryx japonica</i>	0	1	X	Δ(*2)	○	○	○	X	-	○		○	○
5	(family status uncertain)	<i>Rhipidolestes hirai</i>	0	3	X	-	○	○	X	X	-	○		○	X
6	Platycnemididae	<i>Pseudocoptera annulata</i>	0	4	X	Δ(*2)	○	○	○	X	-	○		○	○
7	Coenagrionidae	<i>Paracercion calamorum</i>	4	7	X	○	○	○	○	X	-	○		○	○
8	Coenagrionidae	<i>Paracercion hieroglyphicum</i>	0	3	X	○	○	○	○	X	-	○		○	○
9	Coenagrionidae	<i>Paracercion sieboldii</i>	1	3	X	○	○	○	○	X	-	○		○	○
10	Coenagrionidae	<i>Paracercion melanotum</i>	0	2	X	○	○	○	○	X	Δ	○		○	○
11	Coenagrionidae	<i>Agrionemis pygmaea</i>	0	1	X	○	○	X	○	X	-	○		○	○
12	Coenagrionidae	<i>Mortonagrion selenion</i>	0	1	X	○	○	X	○	X	-	○		-	-
13	Coenagrionidae	<i>Enallagma circulatum</i>	1	5	X	○	○	○	○	X	-	○		○	○
14	Coenagrionidae	<i>Ischnura senegalensis</i>	0	2	X	○	○	X	○	X	X	○		○	○
15	Coenagrionidae	<i>Ischnura asiatica</i>	0	3	X	○	○	○	○	X	-	○		○	○
Ref. 1	Coenagrionidae	<i>Ischnura senegalensis</i>	3	6	X	○	○	X	○	X	-	○		○	○
Ref. 2	Coenagrionidae	<i>Ischnura elegans x I. senegalensis</i>	4	6	X	○	○	X	○	X	-	○		○	○
16	Epiophlebiidae	<i>Epiophlebia superstes</i>	0	2	X	X	○	X	X	X	-	X		X	X
17	Aeshnidae	<i>Boyeria maclachlani</i>	0	2	X	X	○	X	X	○	-	X		○	X
18	Aeshnidae	<i>Planaeschna milnei</i>	0	3	X	X	○	Δ	X	○	-	○		○	X
19	Aeshnidae	<i>Gynacantha japonica</i>	1	4	X	X	○	○	X	○	-	X		○	X
20	Aeshnidae	<i>Aeshna crenata</i>	0	4	X	X	○	○	X	○	-	○		○	X
21	Aeshnidae	<i>Aeshna juncea</i>	0	1	X	X	○	○	X	○	-	○		○	X
22	Aeshnidae	<i>Anax ephippiger</i>	4	5	X	X	○	X	X	○	○	X		○	○
23	Aeshnidae	<i>Anax parthenope</i>	1	1	X	X	○	Δ	X	○	-	X		○	○
24	Aeshnidae	<i>Anax nigrofasciatus</i>	1	1	X	X	○	Δ	X	○	-	○		○	X
25	Gomphidae	<i>Sieboldius albardae</i>	0	3	Δ(*1)	X	○	X	X	X	-	X		○	X
26	Gomphidae	<i>Meligomphus viridicostus</i>	0	3	Δ(*1)	X	○	○	X	X	-	○		○	X
27	Gomphidae	<i>Nihonogomphus viridis</i>	0	1	Δ(*1)	X	○	X	X	X	-	○		○	X
28	Gomphidae	<i>Davidius nanus</i>	0	5	Δ(*1)	X	○	○	X	X	-	○		○	X
29	Gomphidae	<i>Singomphus flavolimbatus</i>	0	2	Δ(*1)	X	○	X	X	X	-	X		X	X
30	Gomphidae	<i>Stylogomphus suzuki</i>	0	4	Δ(*1)	X	○	○	X	X	-	○		○	X
31	Gomphidae	<i>Asiagomphus metaenops</i>	0	4	Δ(*1)	X	○	X	X	X	-	○		○	X
32	Petaluridae	<i>Tanypteryx pryeri</i>	0	4	X	X	○	X	X	X	X	X		○	X
33	Chlorogomphidae	<i>Chlorogomphus brunneus</i>	0	1	Δ(*1)	X	○	X	X	X	-	○		○	X
34	Cordulegastridae	<i>Anotogaster sieboldii</i>	0	4	Δ(*1)	X	○	X	X	X	-	○		○	X
35	Macromiidae	<i>Macromia daimoji</i>	0	3	Δ(*1)	X	○	○	X	X	-	○		○	X
36	Cordulidae	<i>Epithea bimaculata</i>	0	1	-	X	○	X	X	X	-	○		○	X
37	Cordulidae	<i>Somatochlora uchidai</i>	0	6	Δ(*1)	X	○	○	X	X	-	○		○	X
38	Libellulidae	<i>Rhyothemis fuliginosa</i>	0	7	Δ(*1)	X	○	○	X	X	-	○		○	○
39	Libellulidae	<i>Sympetrum darwinianum</i>	0	3	○	X	○	○	X	○	○	○		○	○
40	Libellulidae	<i>Sympetrum maculatum</i>	0	4	○	X	○	○	X	○	○	○		○	○
41	Libellulidae	<i>Sympetrum infuscatum</i>	0	3	○	X	○	○	X	○	-	○		○	○
42	Libellulidae	<i>Sympetrum frequens</i>	0	1	○	X	○	○	X	○	-	○		○	○
43	Libellulidae	<i>Sympetrum kunczei</i>	0	3	○	X	○	○	X	○	-	○		○	○
44	Libellulidae	<i>Sympetrum uniforme</i>	3	3	○	X	○	○	X	○	-	X		○	○
45	Libellulidae	<i>Pseudothemis zonata</i>	0	4	Δ(*1)	X	○	X	X	○	-	X		○	○
46	Libellulidae	<i>Deileia phaon</i>	0	1	○	X	○	X	X	X	-	X		○	○
47	Libellulidae	<i>Acisoma panorpoides</i>	0	1	Δ(*1)	X	○	X	X	○	-	○		○	○
48	Libellulidae	<i>Crocothemis servilia</i>	1	5	○	X	○	○	X	○	-	○		○	○
49	Libellulidae	<i>Orthetrum albistylum</i>	3	5	○	X	○	X	X	X	-	○		○	X

Table 1-2. (next page)

Data of all Odonata individuals whose daily photos were taken in this study. (*1) Unidentifiable because we started to photograph from the middle of the stage. (*2) We could not identify the morphological stage due to very dark pigmentation on the body surface.

Family	Species	Start photographing	Ecdysis to F-1	F-1 duration	F-1 Photos	Ecdysis to F-0	F-0 duration	Stage 1	Stage 2	Stage 3	F-0 photos	Ventral photos	Adult emergence	Sex	Collection	Location	Collector
1-1	Lestidae	2019-05-18	2019-05-22	11	11	2019-06-02	15	8	5	2	15		2019-06-17	Female	2019-04-16	Tsukuba, Ibaraki	Genita Okude & Ryo Futahashi
2-1	Lestidae	2017-06-09				2017-06-09	22	17	3	2	21		2017-07-01	No data	2017-06-06	Tsukuba, Ibaraki	Genita Okude & Ryo Futahashi
2-2	Lestidae	2017-06-10				2017-06-10	21	16	3	2	21		2017-07-01	No data	2017-06-06	Tsukuba, Ibaraki	Genita Okude & Ryo Futahashi
2-3	Lestidae	2017-06-10				2017-06-10	21	15	4	2	21		2017-07-01	No data	2017-06-06	Tsukuba, Ibaraki	Genita Okude & Ryo Futahashi
2-4	Lestidae	2017-06-10				2017-06-10	21	15	4	2	21		2017-07-01	No data	2017-06-06	Tsukuba, Ibaraki	Genita Okude & Ryo Futahashi
2-5	Lestidae	2017-06-11				2017-06-28	11	4	4	3	11		2017-07-09	Female	2017-06-16	Tsukuba, Ibaraki	Genita Okude & Ryo Futahashi
3-1	Calopterygidae	2019-03-02					16	(*)	11	2	16		2019-05-18	Male	2019-03-02	Tsukuba, Ibaraki	Genita Okude & Ryo Futahashi
3-2	Calopterygidae	2019-03-06					17	(*)	10	2	17		2019-05-23	Female	2019-03-06	Tsukuba, Ibaraki	Genita Okude & Ryo Futahashi
3-3	Calopterygidae	2019-03-06					28	(*)	10	3	28		2019-04-03	Female	2019-03-06	Tsukuba, Ibaraki	Genita Okude & Ryo Futahashi
3-4	Calopterygidae	2019-03-06					16	(*)	(*)	(*)	16		2019-04-11	Female	2019-03-06	Tsukuba, Ibaraki	Genita Okude & Ryo Futahashi
3-5	Calopterygidae	2019-03-20					22	(*)	9	2	22		2019-04-12	Female	2019-03-19	Hiachiomiya, Ibaraki	Genita Okude & Ryo Futahashi
3-6	Calopterygidae	2019-03-20					23	(*)	8	3	23		2019-04-12	Female	2019-03-19	Hiachiomiya, Ibaraki	Genita Okude & Ryo Futahashi
4-1	Calopterygidae	2019-04-04				2019-04-04	36	24	9	3	36		2019-05-10	Female	2019-03-19	Hiachiomiya, Ibaraki	Genita Okude & Ryo Futahashi
5-1	(family status uncl.)	2020-02-28					34				34			Male	2020-02-24	Shimanto, Kochi	Sae Nomura
5-2	(family status uncl.)	2020-04-11					15	(*)	(*)	4	15		2020-04-28	Male	2020-04-09	Mihara, Kochi	Mitsutoshi Sugimura
5-3	(family status uncl.)	2020-04-11					13	(*)	(*)	3	13		2020-04-24	Male	2020-04-09	Mihara, Kochi	Mitsutoshi Sugimura
6-1	Platycnemididae	2017-11-21				2017-11-21	38	26	9	3	37		2017-12-29	Female	2017-10-30	Kitahiroshima, Hiroshima	Akira Ozono
6-2	Platycnemididae	2019-05-27				2019-05-27	26	18	7	1	26		2019-06-22	Male	2019-05-26	Etsetsu, Hokkaido	Genita Okude & Jun Okude
6-3	Platycnemididae	2019-05-29					34	(*)	9	2	34		2019-07-02	Male	2019-05-26	Etsetsu, Hokkaido	Genita Okude & Jun Okude
6-4	Platycnemididae	2019-06-06					22	13	7	2	22		2019-06-28	Female	2019-05-26	Etsetsu, Hokkaido	Genita Okude & Jun Okude
7-1	Coenagrionidae	2017-09-13				2017-09-13	9	9	7	2	16		2017-10-08	Female	2017-08-20	Ikeda, Hokkaido	Genita Okude & Jun Okude
7-2	Coenagrionidae	2017-09-05				2017-09-05	16	8	6	2	16		2017-10-05	Female	2017-08-20	Ikeda, Hokkaido	Genita Okude & Jun Okude
7-3	Coenagrionidae	2017-09-06				2017-09-06	21	12	7	2	21		2017-10-07	Female	2017-08-20	Ikeda, Hokkaido	Genita Okude & Jun Okude
7-4	Coenagrionidae	2017-09-08				2017-09-08	17	9	7	1	17		2017-10-04	Female	2017-08-20	Ikeda, Hokkaido	Genita Okude & Jun Okude
7-5	Coenagrionidae	2017-09-24				2017-09-24	14	6	6	2	14		2017-10-08	Male	2017-08-20	Ikeda, Hokkaido	Genita Okude & Jun Okude
7-6	Coenagrionidae	2019-05-30				2019-05-30	17	8	7	2	17		2019-06-16	Female	2019-05-26	Sapporo, Hokkaido	Genita Okude & Jun Okude
7-7	Coenagrionidae	2019-06-02				2019-06-02	15	6	6	3	15		2019-06-17	Female	2019-05-26	Sapporo, Hokkaido	Genita Okude & Jun Okude
8-1	Coenagrionidae	2019-05-30				2019-05-30	17	8	7	2	17		2019-06-16	Female	2019-05-26	Sapporo, Hokkaido	Genita Okude & Jun Okude
8-2	Coenagrionidae	2019-06-01				2019-06-01	15	8	6	1	15		2019-06-16	Female	2019-05-26	Sapporo, Hokkaido	Genita Okude & Jun Okude
8-3	Coenagrionidae	2019-06-01				2019-06-01	18	11	5	2	18		2019-06-19	Female	2019-05-26	Sapporo, Hokkaido	Genita Okude & Jun Okude
9-1	Coenagrionidae	2017-11-08				2017-11-08	17	8	7	2	17		2017-12-08	Male	2017-10-30	Kitahiroshima, Hiroshima	Akira Ozono
9-2	Coenagrionidae	2019-05-30				2019-05-30	22	(*)	7	3	22		2019-06-21	Female	2019-05-26	Etsetsu, Hokkaido	Genita Okude & Jun Okude
9-3	Coenagrionidae	2019-06-06				2019-06-06	25	(*)	7	3	25		2019-07-01	Female	2019-05-26	Etsetsu, Hokkaido	Genita Okude & Jun Okude
10-1	Coenagrionidae	2020-03-22				2020-03-22	13	6	5	2	13	9	2020-04-04	Female	2020-03-09	Tsukuba, Ibaraki	Genita Okude & Ryo Futahashi
10-2	Coenagrionidae	2020-03-21				2020-03-21	13	5	6	2	13	8	2020-04-03	Female	2020-03-09	Tsukuba, Ibaraki	Genita Okude & Ryo Futahashi
11-1	Coenagrionidae	2018-11-23				2018-11-23	23	12	8	3	23		2018-12-16	Male	2018-11-05	Taketomi, Okinawa	Bin Hirota
12-1	Coenagrionidae	2017-10-31				2017-10-31	9	(*)	5	1	9		2017-06-29	No data	2017-06-20	Kitaaraki, Ibaraki	Genita Okude & Ryo Futahashi
13-1	Coenagrionidae	2019-05-29				2019-05-29	16	9	6	1	16		2017-11-25	Female	2017-10-12	Nakashibetsu, Hokkaido	Hiroyuki Koga
13-2	Coenagrionidae	2019-05-29				2019-05-29	19	11	6	2	19		2019-06-17	Female	2019-05-26	Etsetsu, Hokkaido	Genita Okude & Jun Okude
13-3	Coenagrionidae	2019-05-29				2019-05-29	17	9	6	2	17		2019-06-15	Female	2019-05-26	Etsetsu, Hokkaido	Genita Okude & Jun Okude
13-4	Coenagrionidae	2019-05-29				2019-05-29	16	8	6	2	16		2019-06-14	Female	2019-05-26	Etsetsu, Hokkaido	Genita Okude & Jun Okude
13-5	Coenagrionidae	2019-05-30				2019-05-30	18	10	7	1	18		2019-06-17	Male	2019-05-26	Etsetsu, Hokkaido	Genita Okude & Jun Okude
14-1	Coenagrionidae	2019-11-16				2019-11-16	22	12	7	3	22	22	2019-12-08	Male	2019-08-01	Tsukuba, Ibaraki	Genita Okude & Ryo Futahashi
14-2	Coenagrionidae	2019-11-16				2019-11-16	18	9	6	3	18	18	2019-12-04	Female	2019-03-06	Tsukuba, Ibaraki	Genita Okude & Ryo Futahashi
15-1	Coenagrionidae	2019-03-11				2019-03-11	18	9	7	2	18		2019-03-29	Female	2019-03-06	Tsukuba, Ibaraki	Genita Okude & Ryo Futahashi
15-2	Coenagrionidae	2019-06-19				2019-06-19	17	9	7	2	17		2019-06-26	Female	2019-06-19	Tsukuba, Ibaraki	Genita Okude & Ryo Futahashi
15-3	Coenagrionidae	2020-02-04				2020-02-04	9	(*)	(*)	5	1	9	2020-02-13	Female	2020-02-04	Hiachiomiya, Ibaraki	Genita Okude & Ryo Futahashi
16-1	Epiophlebiidae	2020-02-04				2020-02-04	10	(*)	(*)	(*)	10		2020-02-14	Female	2020-02-04	Hiachiomiya, Ibaraki	Genita Okude & Ryo Futahashi
17-1	Aeshnidae	2019-04-20				2019-04-20	42	29	10	3	42		2019-06-01	Female	2019-03-19	Hiachiomiya, Ibaraki	Genita Okude & Ryo Futahashi
17-2	Aeshnidae	2019-04-20				2019-04-20	42	29	9	4	42		2019-06-01	Male	2019-03-19	Hiachiomiya, Ibaraki	Genita Okude & Ryo Futahashi

Family	Species	Start photographing	Ecdysis to F-1	F-1 duration	F-1 Photos	Ecdysis to F.0	F.0 duration	Stage 1	Stage 2	Stage 3	F.0 photos	Ventral photos	Adult emergence	Sex	Collection	Location	Collector
18-1 Aeshmidae	<i>Planaeschna miniei</i>	2018-02-12				2018-01-04	16	(*)	10	5	16		2018-02-28	Female	2018-02-28	Wajima, Ishikawa	Ryo Futahashi & Hiroyuki Futahashi
18-2 Aeshmidae	<i>Planaeschna miniei</i>	2018-01-04				2018-01-09	58	42	11	5	58		2018-03-03	Male	2017-10-28	Wajima, Ishikawa	Ryo Futahashi & Hiroyuki Futahashi
18-3 Aeshmidae	<i>Planaeschna miniei</i>	2018-01-09				2017-06-09	54	37	12	5	53		2018-03-04	Male	2017-10-28	Wajima, Ishikawa	Ryo Futahashi & Hiroyuki Futahashi
19-1 Aeshmidae	<i>Gynacantha japonica</i>	2017-06-09				2017-06-16	19	11	6	2	19		2017-06-28	Male	2017-06-28	Tsukuba, Ibaraki	Genta Okude & Ryo Futahashi
19-2 Aeshmidae	<i>Gynacantha japonica</i>	2019-06-03	2019-06-03	15	15	2019-06-18	21	12	6	3	21		2017-07-07	Male	2019-05-30	Tsukuba, Ibaraki	Genta Okude & Ryo Futahashi
19-3 Aeshmidae	<i>Gynacantha japonica</i>	2019-06-14				2019-06-18	25	14	8	3	25		2019-07-09	Female	2019-05-30	Tsukuba, Ibaraki	Genta Okude & Ryo Futahashi
19-4 Aeshmidae	<i>Gynacantha japonica</i>	2019-06-17				2019-06-17	34	22	7	5	34		2019-07-21	Male	2019-05-30	Tsukuba, Ibaraki	Genta Okude & Ryo Futahashi
20-1 Aeshmidae	<i>Aeschna crenta</i>	2019-05-29				2019-05-29	79	66	9	4	79		2018-08-16	Male	2019-05-26	Ehetsu, Hokkaido	Genta Okude & Jun Okude
20-2 Aeshmidae	<i>Aeschna crenta</i>	2019-06-04				2019-06-04	45	34	8	3	45		2019-07-19	Female	2019-05-26	Ehetsu, Hokkaido	Genta Okude & Jun Okude
20-3 Aeshmidae	<i>Aeschna crenta</i>	2019-06-09				2019-06-09	29	17	9	3	29		2019-07-08	Male	2019-05-26	Ehetsu, Hokkaido	Genta Okude & Jun Okude
20-4 Aeshmidae	<i>Aeschna crenta</i>	2019-06-10				2019-06-09	24	14	8	2	24		2019-07-03	Male	2019-05-26	Ehetsu, Hokkaido	Genta Okude & Jun Okude
21-1 Aeshmidae	<i>Aeschna iinca</i>	2019-05-29				2019-05-29	26	17	7	2	26		2019-06-24	Female	2019-05-25	Sapporo, Hokkaido	Genta Okude & Jun Okude
22-1 Aeshmidae	<i>Anax ephippiger</i>	2020-01-30	2020-01-30	11	11	2020-02-11								Male	2019-11-05	Hamamatsu, Shizuoka	Akira Konabe
22-2 Aeshmidae	<i>Anax ephippiger</i>	2020-01-30	2020-01-31	18	18	2020-02-11	26	14	8	4	26	26	2020-03-10	Female	2019-11-05	Hamamatsu, Shizuoka	Akira Konabe
22-3 Aeshmidae	<i>Anax ephippiger</i>	2020-02-01	2020-02-02	11	10	2020-02-13	22	11	7	4	22	21	2020-02-23	Female	2019-11-05	Hamamatsu, Shizuoka	Akira Konabe
22-4 Aeshmidae	<i>Anax ephippiger</i>	2020-02-01				2020-02-13	22	11	7	4	22	22	2020-02-24	Female	2019-11-05	Hamamatsu, Shizuoka	Akira Konabe
22-5 Aeshmidae	<i>Anax ephippiger</i>	2020-02-02				2020-02-02	21	10	8	3	21	21	2020-02-24	Female	2019-11-05	Hamamatsu, Shizuoka	Akira Konabe
22-6 Aeshmidae	<i>Anax ephippiger</i>	2020-02-03				2020-02-02	21	9	7	5	21	21	2020-02-23	Male	2019-11-05	Hamamatsu, Shizuoka	Akira Konabe
22-7 Aeshmidae	<i>Anax ephippiger</i>	2020-02-03				2020-02-02	36	26	7	3	36		2018-11-12	Male	2019-05-15	Tsukuba, Ibaraki	Genta Okude & Ryo Futahashi
22-8 Aeshmidae	<i>Anax ephippiger</i>	2019-05-18	2019-05-18	15	14	2019-06-02	34	20	10	4	33		2018-11-12	Male	2019-04-11	Tsukuba, Ibaraki	Genta Okude & Ryo Futahashi
24-1 Aeshmidae	<i>Anax nigrofasciatus</i>	2018-09-19	2018-09-19	20	20	2018-10-09	57	(*)	13	8	57		2019-05-24	Male	2019-03-02	Tsukuba, Ibaraki	Genta Okude & Ryo Futahashi
25-1 Gomphidae	<i>Setodellus albarde</i>	2018-04-20					50	(*)	14	7	50		2019-04-23	Male	2019-03-02	Tsukuba, Ibaraki	Genta Okude & Ryo Futahashi
25-2 Gomphidae	<i>Setodellus albarde</i>	2019-03-04					37	(*)	12	6	37		2019-06-08	Male	2019-05-01	Chofu, Tokyo	Tomohito Noda
25-3 Gomphidae	<i>Setodellus albarde</i>	2019-03-04					38	(*)	13	5	38		2019-06-09	Male	2019-05-01	Chofu, Tokyo	Tomohito Noda
26-1 Gomphidae	<i>Meligomphus vindocostus</i>	2018-05-02					37	(*)	13	5	38		2018-06-07	Male	2018-05-01	Chofu, Tokyo	Tomohito Noda
26-2 Gomphidae	<i>Meligomphus vindocostus</i>	2018-05-02					38	(*)	12	5	38		2018-06-07	Male	2018-05-01	Chofu, Tokyo	Tomohito Noda
27-1 Gomphidae	<i>Meligomphus vindocostus</i>	2018-05-02					15	(*)	12	3	15		2018-03-20	Female	2018-03-02	Tsukuba, Ibaraki	Genta Okude & Ryo Futahashi
28-1 Gomphidae	<i>Meligomphus vindocostus</i>	2018-03-05					23	(*)	10	2	17		2018-03-27	Female	2019-03-02	Tsukuba, Ibaraki	Genta Okude & Ryo Futahashi
28-2 Gomphidae	<i>Meligomphus vindocostus</i>	2018-03-04					19	(*)	9	3	16		2018-03-20	Female	2019-03-02	Tsukuba, Ibaraki	Genta Okude & Ryo Futahashi
28-3 Gomphidae	<i>Meligomphus vindocostus</i>	2018-03-04					19	(*)	9	3	16		2018-03-20	Female	2019-03-02	Tsukuba, Ibaraki	Genta Okude & Ryo Futahashi
28-4 Gomphidae	<i>Meligomphus vindocostus</i>	2018-03-04					19	(*)	9	3	16		2018-03-20	Female	2019-03-02	Tsukuba, Ibaraki	Genta Okude & Ryo Futahashi
28-5 Gomphidae	<i>Meligomphus vindocostus</i>	2018-03-04					19	(*)	9	3	16		2018-03-20	Female	2019-03-02	Tsukuba, Ibaraki	Genta Okude & Ryo Futahashi
28-6 Gomphidae	<i>Meligomphus vindocostus</i>	2018-03-04					19	(*)	9	3	16		2018-03-20	Female	2019-03-02	Tsukuba, Ibaraki	Genta Okude & Ryo Futahashi
28-7 Gomphidae	<i>Meligomphus vindocostus</i>	2018-03-04					19	(*)	9	3	16		2018-03-20	Female	2019-03-02	Tsukuba, Ibaraki	Genta Okude & Ryo Futahashi
28-8 Gomphidae	<i>Meligomphus vindocostus</i>	2018-03-04					19	(*)	9	3	16		2018-03-20	Female	2019-03-02	Tsukuba, Ibaraki	Genta Okude & Ryo Futahashi
28-9 Gomphidae	<i>Meligomphus vindocostus</i>	2018-03-04					19	(*)	9	3	16		2018-03-20	Female	2019-03-02	Tsukuba, Ibaraki	Genta Okude & Ryo Futahashi
28-10 Gomphidae	<i>Meligomphus vindocostus</i>	2018-03-04					19	(*)	9	3	16		2018-03-20	Female	2019-03-02	Tsukuba, Ibaraki	Genta Okude & Ryo Futahashi
29-1 Gomphidae	<i>Meligomphus vindocostus</i>	2018-03-04					19	(*)	9	3	16		2018-03-20	Female	2019-03-02	Tsukuba, Ibaraki	Genta Okude & Ryo Futahashi
29-2 Gomphidae	<i>Meligomphus vindocostus</i>	2018-03-04					19	(*)	9	3	16		2018-03-20	Female	2019-03-02	Tsukuba, Ibaraki	Genta Okude & Ryo Futahashi
29-3 Gomphidae	<i>Meligomphus vindocostus</i>	2018-03-04					19	(*)	9	3	16		2018-03-20	Female	2019-03-02	Tsukuba, Ibaraki	Genta Okude & Ryo Futahashi
29-4 Gomphidae	<i>Meligomphus vindocostus</i>	2018-03-04					19	(*)	9	3	16		2018-03-20	Female	2019-03-02	Tsukuba, Ibaraki	Genta Okude & Ryo Futahashi
29-5 Gomphidae	<i>Meligomphus vindocostus</i>	2018-03-04					19	(*)	9	3	16		2018-03-20	Female	2019-03-02	Tsukuba, Ibaraki	Genta Okude & Ryo Futahashi
29-6 Gomphidae	<i>Meligomphus vindocostus</i>	2018-03-04					19	(*)	9	3	16		2018-03-20	Female	2019-03-02	Tsukuba, Ibaraki	Genta Okude & Ryo Futahashi
29-7 Gomphidae	<i>Meligomphus vindocostus</i>	2018-03-04					19	(*)	9	3	16		2018-03-20	Female	2019-03-02	Tsukuba, Ibaraki	Genta Okude & Ryo Futahashi
29-8 Gomphidae	<i>Meligomphus vindocostus</i>	2018-03-04					19	(*)	9	3	16		2018-03-20	Female	2019-03-02	Tsukuba, Ibaraki	Genta Okude & Ryo Futahashi
29-9 Gomphidae	<i>Meligomphus vindocostus</i>	2018-03-04					19	(*)	9	3	16		2018-03-20	Female	2019-03-02	Tsukuba, Ibaraki	Genta Okude & Ryo Futahashi
29-10 Gomphidae	<i>Meligomphus vindocostus</i>	2018-03-04					19	(*)	9	3	16		2018-03-20	Female	2019-03-02	Tsukuba, Ibaraki	Genta Okude & Ryo Futahashi
30-1 Gomphidae	<i>Meligomphus vindocostus</i>	2018-03-04					19	(*)	9	3	16		2018-03-20	Female	2019-03-02	Tsukuba, Ibaraki	Genta Okude & Ryo Futahashi
30-2 Gomphidae	<i>Meligomphus vindocostus</i>	2018-03-04					19	(*)	9	3	16		2018-03-20	Female	2019-03-02	Tsukuba, Ibaraki	Genta Okude & Ryo Futahashi
30-3 Gomphidae	<i>Meligomphus vindocostus</i>	2018-03-04					19	(*)	9	3	16		2018-03-20	Female	2019-03-02	Tsukuba, Ibaraki	Genta Okude & Ryo Futahashi
30-4 Gomphidae	<i>Meligomphus vindocostus</i>	2018-03-04					19	(*)	9	3	16		2018-03-20	Female	2019-03-02	Tsukuba, Ibaraki	Genta Okude & Ryo Futahashi
31-1 Gomphidae	<i>Meligomphus vindocostus</i>	2018-03-04					19	(*)	9	3	16		2018-03-20	Female	2019-03-02	Tsukuba, Ibaraki	Genta Okude & Ryo Futahashi
31-2 Gomphidae	<i>Meligomphus vindocostus</i>	2018-03-04					19	(*)	9	3	16		2018-03-20	Female	2019-03-02	Tsukuba, Ibaraki	Genta Okude & Ryo Futahashi
31-3 Gomphidae	<i>Meligomphus vindocostus</i>	2018-03-04					19	(*)	9	3	16		2018-03-20	Female	2019-03-02	Tsukuba, Ibaraki	Genta Okude & Ryo Futahashi
31-4 Gomphidae	<i>Meligomphus vindocostus</i>	2018-03-04					19	(*)	9	3	16		2018-03-20	Female	2019-03-02	Tsukuba, Ibaraki	Genta Okude & Ryo Futahashi
32-1 Petaluridae	<i>Tanypteryx pryer</i>	2020-02-24					14	(*)	7	5	13		2018-04-06	Female	2018-03-16	Tsukuba, Ibaraki	Genta Okude & Ryo Futahashi
32-2 Petaluridae	<i>Tanypteryx pryer</i>	2020-02-24					14	(*)	7	5	13		2018-04-06	Female	2018-03-16	Tsukuba, Ibaraki	Genta Okude & Ryo Futahashi
32-3 Petaluridae	<i>Tanypteryx pryer</i>	2020-02-26					17	(*)	10	3	16	15	2020-03-12	Female	2020-02-23	Fuchu, Toyama	Naoki Futahashi & Ryo Futahashi
32-4 Petaluridae	<i>Tanypteryx pryer</i>	2020-03-09					16	(*)	9	3	16	15	2020-03-13	Female	2020-02-23	Fuchu, Toyama	Naoki Futahashi & Ryo Futahashi
33-1 Chordilegastriidae	<i>Chlorogomphus brunneus</i>	2020-02-08					14	(*)	9	4	16	15	2020-03-25	Female	2020-03-05	Kosai, Shizuoka	Motoharu Fuku
33-2 Chordilegastriidae	<i>Chlorogomphus brunneus</i>	2020-02-08					14	(*)	9	3	14	11	2020-03-23	Female	2020-02-13	Kosai, Shizuoka	Motoharu Fuku
33-3 Chordilegastriidae	<i>Chlorogomphus brunneus</i>	2020-02-28					46	(*)	18	6	46	11	2020-04-14	Male	2020-02-13	Shimanto, Kochi	Sae Nomura
34-1 Cordilegastriidae	<i>Anotogaster seboldi</i>	2018-04-20					39	(*)	18	3	39		2018-05-29	Male	2018-04-11	Tsukuba, Ibaraki	Genta Okude & Ryo Futahashi
34-2 Cordilegastriidae	<i>Anotogaster seboldi</i>	2019-03-05					62	(*)	22	4	62		2019-05-06	Male	2018-03-16	Tsukuba, Ibaraki	Genta Okude & Ryo Futahashi
34-3 Cordilegastriidae	<i>Anotogaster seboldi</i>	2019-03-08					70	(*)									

Family	Species	Start photographing	Ecdysis to F-1	F-1 duration	F-1 Photos	Ecdysis to F-0	F-0 duration	Stage 1	Stage 2	Stage 3	F-0 photos	Ventral photos	Adult emergence	Sex	Collection	Location	Collector
35-1 Macromiidae	<i>Macromia damoji</i>	2018-03-05					62	(*)	22	5	61		2018-05-06	Female	2018-03-04	Tsukuba, Ibaraki	Genta Okude & Ryo Furuhashi
35-2 Macromiidae	<i>Macromia damoji</i>	2018-04-18					118	(*)	14	6	118		2018-07-01	Female	2018-03-04	Tsukuba, Ibaraki	Genta Okude & Ryo Furuhashi
35-3 Macromiidae	<i>Macromia damoji</i>	2018-04-18					81	60	14	7	81		2018-07-08	Female	2018-03-16	Tsukuba, Ibaraki	Genta Okude & Ryo Furuhashi
36-1 Corduliidae	<i>Epilloca bimaculata</i>	2020-02-11					7	(*)	(*)	3	7		2020-02-18	Female	2019-05-26	Sapporo, Hokkaido	Genta Okude & Jun Okude
37-1 Corduliidae	<i>Somatochlora uchidaï</i>	2019-05-30					11	(*)	(*)	3	11		2019-06-10	Male	2019-05-25	Sapporo, Hokkaido	Genta Okude & Jun Okude
37-2 Corduliidae	<i>Somatochlora uchidaï</i>	2019-05-27					12	(*)	(*)	2	12		2019-06-08	Female	2019-05-25	Sapporo, Hokkaido	Genta Okude & Jun Okude
37-3 Corduliidae	<i>Somatochlora uchidaï</i>	2019-05-27					25	(*)	8	3	25		2019-06-21	Male	2019-05-25	Sapporo, Hokkaido	Genta Okude & Jun Okude
37-4 Corduliidae	<i>Somatochlora uchidaï</i>	2019-05-27					28	(*)	8	3	28		2019-06-24	Male	2019-05-25	Sapporo, Hokkaido	Genta Okude & Jun Okude
37-5 Corduliidae	<i>Somatochlora uchidaï</i>	2019-05-29				2019-05-29	30	17	10	3	30		2019-06-28	Male	2019-05-25	Sapporo, Hokkaido	Genta Okude & Jun Okude
37-6 Corduliidae	<i>Somatochlora uchidaï</i>	2019-05-29					20	17	10	3	20		2019-06-28	Female	2019-05-25	Sapporo, Hokkaido	Genta Okude & Jun Okude
38-1 Libellulidae	<i>Rhyothemis fuliginosa</i>	2018-05-02					53	38	11	4	53		2018-06-24	Male	2018-04-27	Tsukuba, Ibaraki	Genta Okude & Ryo Furuhashi
38-2 Libellulidae	<i>Rhyothemis fuliginosa</i>	2018-05-02					52	37	11	4	52		2018-06-23	Female	2018-04-27	Tsukuba, Ibaraki	Genta Okude & Ryo Furuhashi
38-3 Libellulidae	<i>Rhyothemis fuliginosa</i>	2018-05-03					53	38	12	3	53		2018-06-25	Male	2018-04-27	Tsukuba, Ibaraki	Genta Okude & Ryo Furuhashi
38-4 Libellulidae	<i>Rhyothemis fuliginosa</i>	2018-05-04					55	40	11	4	55		2018-06-28	Female	2018-04-27	Tsukuba, Ibaraki	Genta Okude & Ryo Furuhashi
38-5 Libellulidae	<i>Rhyothemis fuliginosa</i>	2018-05-06					51	36	11	4	51		2018-06-26	Female	2018-04-27	Tsukuba, Ibaraki	Genta Okude & Ryo Furuhashi
38-6 Libellulidae	<i>Rhyothemis fuliginosa</i>	2018-05-09					61	48	9	3	59		2018-07-09	Male	2018-04-27	Tsukuba, Ibaraki	Genta Okude & Ryo Furuhashi
38-7 Libellulidae	<i>Rhyothemis fuliginosa</i>	2018-06-13					61	48	10	3	61		2018-08-13	Female	2018-05-29	Tsukuba, Ibaraki	Genta Okude & Ryo Furuhashi
39-1 Libellulidae	<i>Sympetrum damianum</i>	2017-06-28					19	9	7	3	19		2017-07-15	Male	2017-06-16	Tsukuba, Ibaraki	Genta Okude & Ryo Furuhashi
39-2 Libellulidae	<i>Sympetrum damianum</i>	2017-06-27					18	10	7	1	18		2017-07-15	Male	2017-06-06	Tsukuba, Ibaraki	Genta Okude & Ryo Furuhashi
39-3 Libellulidae	<i>Sympetrum damianum</i>	2020-02-13				2020-02-13	22	9	10	3	22	14	2020-03-06	Male	2019-09-25	Tsukuba, Ibaraki	Genta Okude & Ryo Furuhashi
40-1 Libellulidae	<i>Sympetrum maculatum</i>	2020-10-02					9	(*)	(*)	2	9		2020-10-11	Male	2019-10-26	Nanao, Ishikawa	Genta Okude & Ryo Furuhashi
40-2 Libellulidae	<i>Sympetrum maculatum</i>	2020-10-02					17	(*)	(*)	2	17		2020-10-19	Female	2019-10-26	Nanao, Ishikawa	Ryo Furuhashi
40-3 Libellulidae	<i>Sympetrum maculatum</i>	2020-10-02					20	(*)	(*)	2	20		2020-10-22	Female	2019-10-26	Nanao, Ishikawa	Hiroyuki Furuhashi
40-4 Libellulidae	<i>Sympetrum maculatum</i>	2020-10-02					11	(*)	(*)	6	11		2020-10-13	Male	2019-10-26	Nanao, Ishikawa	Hiroyuki Furuhashi
41-1 Libellulidae	<i>Sympetrum infuscatum</i>	2018-06-01				2018-06-01	26	14	8	4	26		2018-06-27	Female	2018-05-29	Tsukuba, Ibaraki	Genta Okude & Ryo Furuhashi
41-2 Libellulidae	<i>Sympetrum infuscatum</i>	2018-06-01					23	12	9	2	23		2018-06-24	Male	2018-05-29	Tsukuba, Ibaraki	Genta Okude & Ryo Furuhashi
41-3 Libellulidae	<i>Sympetrum frequens</i>	2019-06-11					25	13	9	3	23		2019-07-01	Female	2018-05-29	Tsukuba, Ibaraki	Genta Okude & Ryo Furuhashi
42-1 Libellulidae	<i>Sympetrum kurckel</i>	2019-06-29					20	9	9	2	20		2019-07-18	Male	2018-05-29	Tsukuba, Ibaraki	Genta Okude & Ryo Furuhashi
43-1 Libellulidae	<i>Sympetrum kurckel</i>	2019-06-10					19	11	6	2	19		2019-07-07	Female	2018-05-29	Tsukuba, Ibaraki	Genta Okude & Ryo Furuhashi
43-2 Libellulidae	<i>Sympetrum kurckel</i>	2019-06-10					27	14	10	3	27		2019-07-07	Female	2018-05-29	Tsukuba, Ibaraki	Genta Okude & Ryo Furuhashi
43-3 Libellulidae	<i>Sympetrum kurckel</i>	2019-06-11					26	16	8	2	26		2019-07-07	Female	2018-05-29	Tsukuba, Ibaraki	Genta Okude & Ryo Furuhashi
44-1 Libellulidae	<i>Sympetrum uniforme</i>	2017-06-21	2017-06-21				24	16	6	2	24		2017-07-28	Male	2017-06-17	Matsuyama, Ehime	Akira Ozono
44-2 Libellulidae	<i>Sympetrum uniforme</i>	2017-06-21	2017-06-21				22	14	7	1	22		2017-08-02	Female	2017-06-17	Matsuyama, Ehime	Akira Ozono
44-3 Libellulidae	<i>Sympetrum uniforme</i>	2017-06-30	2017-06-30				21	12	7	2	21		2017-08-02	Female	2017-06-17	Matsuyama, Ehime	Akira Ozono
45-1 Libellulidae	<i>Pseudothemis zonata</i>	2018-05-01					54	36	14	4	54		2018-06-24	Female	2018-04-27	Tsukuba, Ibaraki	Genta Okude & Ryo Furuhashi
45-2 Libellulidae	<i>Pseudothemis zonata</i>	2018-05-01					57	41	11	5	57		2018-06-28	Male	2018-04-27	Tsukuba, Ibaraki	Genta Okude & Ryo Furuhashi
45-3 Libellulidae	<i>Pseudothemis zonata</i>	2018-05-03					53	38	11	4	53		2018-06-25	Female	2018-04-27	Tsukuba, Ibaraki	Genta Okude & Ryo Furuhashi
45-4 Libellulidae	<i>Pseudothemis zonata</i>	2018-05-06					46	30	10	6	46		2018-06-21	Female	2018-04-27	Tsukuba, Ibaraki	Genta Okude & Ryo Furuhashi
46-1 Libellulidae	<i>Acisoma panorpoides</i>	2019-05-19					46	31	12	3	46		2019-07-04	Female	2018-05-15	Sapporo, Hokkaido	Genta Okude & Ryo Furuhashi
46-2 Libellulidae	<i>Crocothemis servila</i>	2018-11-16					52	34	14	4	52		2019-01-07	Female	2018-11-05	Taketomi, Okinawa	Genta Okude & Ryo Furuhashi
46-3 Libellulidae	<i>Crocothemis servila</i>	2018-10-11					29	18	8	3	27		2017-11-09	Female	2017-09-07	Tsukuba, Ibaraki	Genta Okude & Ryo Furuhashi
46-4 Libellulidae	<i>Crocothemis servila</i>	2018-04-30					46	35	8	3	46		2018-06-15	Male	2018-04-27	Tsukuba, Ibaraki	Genta Okude & Ryo Furuhashi
46-5 Libellulidae	<i>Crocothemis servila</i>	2019-04-07	2019-04-07				32	21	10	1	32		2019-05-17	Female	2019-04-01	Tsukuba, Ibaraki	Genta Okude & Ryo Furuhashi
46-6 Libellulidae	<i>Crocothemis servila</i>	2019-04-15					27	17	7	3	27		2019-06-27	Male	2019-04-05	Tsukuba, Ibaraki	Genta Okude & Ryo Furuhashi
46-7 Libellulidae	<i>Crocothemis servila</i>	2019-05-31					32	18	10	4	32		2019-07-05	Male	2019-05-26	Sapporo, Hokkaido	Genta Okude & Jun Okude
46-8 Libellulidae	<i>Crocothemis servila</i>	2019-06-03					44	28	12	4	44		2018-10-20	Female	2018-08-14	Tsukuba, Ibaraki	Genta Okude & Jun Okude
46-9 Libellulidae	<i>Orithrum albistylum</i>	2018-08-20	2018-08-20				41	25	13	3	41		2019-05-04	Male	2018-08-14	Tsukuba, Ibaraki	Genta Okude & Ryo Furuhashi
46-10 Libellulidae	<i>Orithrum albistylum</i>	2018-08-23	2018-08-23				41	25	13	3	41		2019-05-04	Male	2018-08-14	Tsukuba, Ibaraki	Genta Okude & Ryo Furuhashi
46-11 Libellulidae	<i>Orithrum albistylum</i>	2019-04-10					35	18	13	4	35		2019-05-15	Female	2019-03-06	Tsukuba, Ibaraki	Genta Okude & Ryo Furuhashi
46-12 Libellulidae	<i>Orithrum albistylum</i>	2019-04-10					39	25	10	4	39		2019-06-23	Male	2019-04-05	Tsukuba, Ibaraki	Genta Okude & Ryo Furuhashi
46-13 Libellulidae	<i>Orithrum albistylum</i>	2019-05-15					26	11	4	4	26		2019-06-27	Male	2019-05-08	Tsukuba, Ibaraki	Genta Okude & Ryo Furuhashi
46-14 Libellulidae	<i>Orithrum albistylum</i>	2019-05-17					41	26	11	4	41		2019-06-27	Male	2019-05-08	Tsukuba, Ibaraki	Genta Okude & Ryo Furuhashi
46-15 Libellulidae	<i>Orithrum albistylum</i>	2019-05-17					26	11	4	4	26		2019-06-12	Male	2019-05-08	Tsukuba, Ibaraki	Genta Okude & Ryo Furuhashi

Chapter 2: Improvement of electroporation-mediated RNA interference method in Odonata.

The content of this chapter has been published in; Okude G, Fukatsu T, Futahashi R. (2021). Electroporation-mediated RNA interference method in Odonata. *Journal of Visualized Experiments* **168**: e61952.

Abstract

Dragonflies and damselflies (order Odonata) represent one of the most ancestral insects with metamorphosis, in which they change their habitat, morphology, and behavior drastically from aquatic larvae to terrestrial/aerial adults without pupal stage. Adult Odonata have a well-developed color vision and show a remarkable diversity in body colors and patterns across sexes, stages, and species. While many ecological and behavioral studies on Odonata have been conducted, molecular genetic studies have been scarce mainly due to the difficulty in applying gene functional analysis to Odonata. For instance, RNA interference (RNAi) is less effective in the Odonata, as reported in the Lepidoptera. To overcome this problem, I established an RNAi method combined with *in vivo* electroporation, but the small interfering RNA (siRNA) used in my master's thesis was expensive, and the effect was confirmed using the relatively rare species *Nannophya pygmaea* (Libellulidae: Anisoptera). In this chapter, I improved the RNAi method by using double-stranded RNA (dsRNA) and optimized it for the blue-tailed damselfly *Ischnura senegalensis* (Coenagrionidae) as a representative damselfly species and the pied skimmer dragonfly *Pseudothemis zonata* (Libellulidae) as a representative of dragonfly species. As a model RNAi target gene, I adopted the melanin synthesis gene

multicopper oxidase 2 (MCO2), whose suppression causes a clear visible phenotype. Also, I confirmed that this RNAi method can be applicable to other dragonfly species including *Ischnura asiatica* (Coenagrionidae), *Lestes temporalis* (Lestidae), *Mnais costalis* (Calopterygidae), *Sympetrum frequens* (Libellulidae), *Davidius nanus* (Gomphidae), *Shaogomphus postocularis* (Gomphidae), whereas RNAi phenotypes were not observed in *Asiagomphus melaenops* (Gomphidae). This RNAi method will facilitate understanding of various gene functions involved in metamorphosis, morphogenesis, color pattern formation, and other biological features of Odonata.

Introduction

Dragonflies and damselflies (the order Odonata) are among the most ancestral groups of insects that exhibit “metamorphosis” (Misof et al. 2014, Wipfler et al. 2019). By metamorphosis, they change their habitat, morphology, and behavior drastically from aquatic larvae to terrestrial/aerial adults (Corbet 1999). Adult dragonflies and damselflies have a well-developed color vision and represent a remarkable diversity in body colors and patterns across sexes, stages, and species (Corbet 1999, Futahashi 2016, Futahashi 2020). While many ecological and behavioral studies on Odonata have been conducted (Córdoba-Aguilar 2008, Bybee et al. 2016), molecular genetic studies have been hindered mainly by the difficulty in applying gene functional analysis to Odonata species.

The conventional RNA interference (RNAi) method, in which double-stranded RNA (dsRNA) is injected to suppress the function of the gene of interest (Linz et al. 2014), turned out to be ineffective in Odonata insects (my master's thesis, Okude et al. 2017a), as reported in Lepidopteran insects (Terenius et al. 2011). On the other hand, previous

reports have suggested that electroporation-mediated RNAi is effective in Lepidopteran species, especially in epidermal tissues (Ando and Fujiwara 2013, Nishikawa et al. 2015, Osanai-Futahashi et al. 2016). In my master's thesis, I found that the electroporation-mediated RNAi works effectively in the tiny dragonfly *Nannophya pygmaea* (Libellulidae: Anisoptera) (Okude et al. 2017a), but *N. pygmaea* is a relatively rare species and therefore not suitable for molecular genetic studies. In addition, small interfering RNA (siRNA) used in my master's thesis (Okude et al. 2017a) was expensive, so the alternative RNAi method is needed for RNAi screen experiment.

Most Odonata species are classified into either of the two suborders, Zygoptera (damselflies) or Anisoptera (true dragonflies) (Corbet 1999). In this Chapter, I focused on the blue-tailed damselfly *Ischnura senegalensis* (Coenagrionidae; Fig. 2-1A) as a representative of Zygopteran species and the pied skimmer dragonfly *Pseudothemis zonata* (Libellulidae; Fig. 2-1B) as a representative of Anisopteran species. The two species are among the most common Odonata species in natural and urban ponds in Japan, including those in Tsukuba City, and I can collect many larvae of the two species in the field. Here I report the improved RNAi method and the success of RNAi in various damselfly and dragonfly species.

Materials and Methods

The overall scheme of the electroporation-mediated RNAi method is shown in Fig. 2-1C.

1. Preparation of larvae of dragonflies or damselflies

Larvae used in this study were captured in Tsukuba city, Ibaraki Prefecture, Japan. *I.*

senegalensis larvae often cling onto water plants floating on the water surface, while *P. zonata* larvae often stay among leaf litter at the bottom. In Tsukuba City, the final instar larvae of *I. senegalensis* are found mainly from March to June, and those of *P. zonata* from May to June.

For *Ischnura* species, the collected larvae were placed separately into each well of a 12-well plate with approximately 3 mL of water until use for RNAi. *L. temporalis* and *S. frequens* larvae were kept individually in the petri dish (5 cm diameter) because they frequently cannibalize each other, while *P. zonata* larvae can be kept in a group because they rarely cannibalize. I fed Zygopteran larvae with *Artemia* brine shrimp every day and Anisopteran larvae with bloodworms and/or *Tubifex* worms at least twice a week until they grow to the suitable developmental stage for RNAi.

2. Species identification

Most Japanese Odonata species were identified by their morphological characters (Ozono et al. 2019). However, in Japan, *I. senegalensis* and *Ischnura asiatica*, which are genetically close, are often found sympatrically (Ozono et al. 2017), and they are difficult to distinguish in larvae (Ozono et al. 2019). Two *Ischnura* species were identified by restriction fragment length polymorphism (RFLP) as follows (see Fig. 2-2).

Larvae of Zygopteran damselflies usually have three caudal gills (Fig. 2-1A). When they are attacked by a predator, they can take off their own caudal gills to escape. After one of the caudal gills of a larva was held using forceps, the larva falls off its caudal gill itself (causing autotomy). If the caudal gill is not available, a portion of the leg is dissected.

One caudal gill was put into 100 μ L of PBS solution [0.8% NaCl, 0.02% KCl, 0.115% Na₂HPO₄, and 0.02% KH₂PO₄ (w/v)] and homogenized with a hand mixer using a deposit

pestle. The mixture was spined down at 5,000 x g for 10 seconds, and 0.5 µL of the supernatant is subjected to PCR-amplification using Tks Gflex DNA polymerase (Takara Bio) and primers (ITS-F0: 5'- GGA AAG ATG GCC AAA CTT GA -3' and 5.8S-AS1: 5'- GCC GGC CCT CAG CCA G -3' Futahashi et al. 2018) to amplify the internal transcribed spacer 1 (ITS1) region of the nuclear DNA. The mixture of 1 µL of PCR-amplified product, 0.3 µL of 10 x M Buffer, 0.1 µL of DraI restriction enzyme (Takara Bio), and 1.6 µL of water was incubated at 37 °C for an hour. 2 µL of the products with loading dye were loaded on 2 % agarose gel and electrophoresis was conducted for about 30 minutes. Then, the electrophoresis pattern was checked to identify the species (Fig. 2-2).

It should be noted that RFLP patterns are species- and population-dependent. In Tsukuba population, *I. asiatica* has a major band of 400–500 bp, whereas *I. senegalensis* has a major band of approximately 200 bp and an additional band of less than 100 bp (an arrowhead in Fig. 2-2). The ITS1 region exists in multiple copies in the genome, and in *Ischnura* species, microsatellite polymorphism within the ITS1 region is often present in the same individual, affecting the pattern of RFLPs.

3. Preparation of dsRNA/siRNA solution for RNAi

As for small interfering RNA (siRNA), siRNA sequence was determined by using siDirect program version 2.0 (<http://sidirect2.rnai.jp/>) (Naito et al. 2009), following the guidelines previously reported in Lepidopteran insects (Yamaguchi et al. 2011). The sequences of siRNA targeting *MCO2* gene of *I. senegalensis* used in this study were as follows: 5'- GCA CUU UCC GUU AUC AAU AUA -3' for sense strand and 5'- UAU UGA UAA CGG AAA GUG CUC -3' for antisense strand. As a negative control, the

sequences of siRNA targeting *enhanced green fluorescent protein (EGFP)* gene were as follows: 5'- GCA UCA AGG UGA ACU UCA AGA -3' for sense strand and 5'- UUG AAG UUC ACC UUG AUG CCG -3' for antisense strand (Ando and Fujiwara 2013). Commercially synthesized siRNA was diluted to 100 μ M with injection buffer [100 mM CH₃COOK, 2 mM Mg(CH₃COO)₂, 30 mM HEPES-KOH, pH 7.4] (Yamaguchi et al. 2011) and stored at -80 °C until use.

As for double-stranded RNA (dsRNA), 300-400 bp region was selected using the primer3 program version 4.1.0 (<http://bioinfo.ut.ee/primer3/>) (Untergasser et al. 2012) and the primer sets were designed. Primer sets to produce templates for dsRNA synthesis are shown in Supplementary Table 2 (no. 1–10). Total RNA was extracted from the freshly prepared samples using RNAiso Plus (Takara Bio) and RNeasy Mini Kit (Qiagen) following the manufacturer's protocol. Using 1 μ g of total RNA per sample as template, cDNA was synthesized using SuperScript II Reverse Transcriptase (Thermo Fisher Scientific) or SuperScript IV Reverse Transcriptase (Thermo Fisher Scientific). The target sequences were amplified using the synthesized cDNA and the designed primer set and cloned into the pT7Blue T-vector (Novagen) using the DNA Ligation Kit Ver. 2.1 (Takara Bio). The plasmid was transformed into *E. coli* competent cells and a single colony after overnight incubation was picked up. The insert region was PCR-amplified using primers on the vector (uni19: 5'-GTT TTC CCA GTC ACG ACG T-3' and rev20: 5'-AGC TAT GAC CAT GAT TAC GC-3'). After the cloned sequence was confirmed by Sanger sequencing using BigDye Terminator v3.1 Cycle Sequencing Kit (Applied Biosystems) and 3130xl Genetic Analyzer (Applied Biosystems), the insert was PCR-amplified using vector primers containing the T7 polymerase promoter sequence (T7-F: 5' - TAA TAC GAC TCA CTA TAG GGA GAC TAG TCA TAT GGA T - 3' and T7-R: 5'- TAA TAC

GAC TCA CTA TAG GGA GAC CCG GGG ATC CGA T - 3'; Futahashi 2011, Matsuura et al. 2015).

The PCR product was purified using the QIAquick PCR purification Kit (QIAGEN) and eluted with 50 μ L of distilled water. The eluted DNA solution was concentrated to approximately 10 μ L using a centrifugal evaporator. A total of 1000 ng template DNA was used, and dsRNA was synthesized by *in vitro* transcription using MEGAscript RNAi kit (Thermo Fisher Scientific). Synthesized dsRNA was eluted with 100 μ L elution buffer, and diluted to 1000 ng/ μ L with elution buffer. The quality of dsRNA was confirmed by electrophoresis on a 1.5% agarose gel, and dsRNA was stored at -20 °C until use.

4. siRNA/dsRNA injection

First, a glass capillary (calibrated micropipette 1-5 μ L; Drummond) was pulled by using a glass needle puller (PN-3, NARISHIGE). The tip of the pulled capillary was placed onto a double-sided adhesive tape and was broken with forceps. The capillary was set to an injector (IM-12, NARISHIGE) and siRNA/dsRNA solution was loaded to the prepared capillary. I did not use the capillary repeatedly since the tip of the injected capillary may become clogged with dirt because the larvae collected in the field lived in the mud.

As for Zygopteran damselflies, a larva was anesthetized covered with a wet paper on crushed ice for 50-70 seconds (Fig. 2-3A-3C). Duration of cold anesthesia depends on the condition of the larva, and if the larva begins to move after 70 seconds of cold anesthesia, an additional 70 seconds of cold anesthesia was applied. Two pins were attached to both sides of the prothorax and fix the larva to a fixed stand (e.g., a piece of styrofoam) (Fig. 2-3D). The inter-segmental membrane between the 7th and 8th abdominal segment for RNAi in the abdomen or between the prothorax and synthorax

(fused mesothorax and metathorax) for RNAi in the thorax was stretched using hands and forceps. The inter-segmental membrane was kept stretched by hand. The tip of the prepared capillary was inserted into the stretched inter-segmental membrane (Fig. 2-3D, 3F), and 1 μ L of siRNA/dsRNA solution was injected.

As for Anisopteran dragonflies, the water on the larval surface was wiped off with a paper towel. For *P. zonata*, two pins were attached to both sides of the prothorax and fix the larva to a fixed stand (Fig. 2-3H). The inter-segmental membrane between the 4th and 5th abdominal segment was stretched by hand, and a small hole was made with a fine needle in the inter-segmental membrane between the 4th and 5th abdominal segment. The tip of the prepared capillary was inserted into the prepared hole (Fig. 2-3I), and 1 μ L of siRNA/dsRNA solution was injected.

5. *in vivo* electroporation

For *P. zonata*, more pins were added to fix the larva to a fixed stand (e.g., a piece of styrofoam). Following the injection of the siRNA/dsRNA solution, two droplets of LOGIQLEAN Gel for Ultrasound Hard type (GE Healthcare) were applied to the larval surface using forceps. The electrode (1 mm ϕ , NEPAGENE) was placed on the ultrasound gel, with a positive electrode on the side injected with the siRNA/dsRNA solution and a negative electrode on the opposite side (Fig. 2-3E, 3G, 3J). 10-times electroporation pulses (280 ms/s each) were generated using the Cure-gene electroporator (CellProduce). In this study, 25 V was applied to Zygopteran species and 45 V to Anisopteran species. The remaining gel on the surface was wiped off with a paper towel. The treated larvae were kept resting on a wet paper towel for approximately one day and transferred to a rearing case on the following day.

6. Site-specific phenotypic analysis.

For Zygopteran damselfly species, the treated larvae were kept individually in a petri dish (5 cm in diameter) containing approximately 10 mL of water and a piece of paper towel. After the larvae stop eating (when entering stage 3 of final larval instar), move them individually into a plastic cage (10 cm × 15 cm, 3 cm water depth) with a disposable non-woven mesh for assisting adult emergence. For Anisopteran dragonfly species, the treated larvae were kept in a plastic cage (10 cm × 15 cm, 3 cm water depth) with a disposable non-woven mesh.

After the emergence of the adult, the phenotype around the region where the positive electrode was placed for electroporation was observed and photographed using a stereoscopic microscope S8APO (Leica Microsystems) with a digital high definition microscope camera MC120HD (Leica) or a stereoscopic microscope S9D (Leica Microsystems) with a digital high definition microscope camera MC190HD (Leica). The emerged adults were preserved in 100 % ethanol for future analyses.

Results

For evaluating the effectiveness of the electroporation-mediated RNAi, I select *multicopper oxidase 2* gene (*MCO2*; also known as *laccase2*) as a representative target gene, on account of the visible phenotype of paler cuticle color upon knockdown of the gene expression (Okude et al. 2017a). *MCO2* is known to be essential for darkening of the epidermis in a variety of insect species (Arakane et al. 2016, Asano et al. 2019).

First, I conducted the electroporation-mediated RNAi targeting *MCO2* gene and

negative control genes (*EGFP* for siRNA and *bla* for dsRNA) (i) in the abdomen of *I. senegalensis* (Fig. 2-4), (ii) in the thorax of *I. senegalensis* (Fig. 2-5), and (iii) in the abdomen of *P. zonata* (Fig. 2-6).

In both *I. senegalensis* and *P. zonata*, inhibition of melanin pigmentation (i.e., black, brown, and reddish brown) appeared in patches around the region where positive electrode was placed (white arrowheads and dotted lines in Figs. 2-4, 2-5, 2-6) when *MCO2* RNAi was performed in combination with electroporation (Table 2-1), as previously reported in *N. pygmaea* (my master's thesis, Okude et al. 2017a). By contrast, no phenotypic effects were observed around the electroporation site when the control gene was injected (*EGFP* siRNA or *bla* dsRNA) (Figs. 2-4, 2-5, 2-6, Table 1). In addition, injecting the *MCO2* gene without electroporation had no effect on adult pigmentation (Fig. 2-4, Table 1), indicating that electroporation is essential for RNAi in Odonata. It should be noted that the blue, green, and yellow colorations are not affected by the RNAi of *MCO2* gene that is involved in melanin synthesis in the cuticle, which plausibly reflect the fact that these body colors are attributed to pigment granules present in the epidermal cells that are visible through the transparent cuticle (see Chapter 5). As shown in Fig. 2-4, no remarkable phenotypic differences were recognized between the individuals subjected to siRNA treatment and dsRNA treatment, whereas considerable variation in size and location of the RNAi phenotype was observed among different individuals subjected to the same RNAi treatment (i.e., compare two examples of *IsMCO2* dsRNA in Fig. 2-4). In addition, as shown in Fig. 2-3H, part of the dorsal side of the larvae corresponds to the ventral side of the adult, so the phenotype appears ventrally in *P. zonata* (Fig. 2-6) when treated as shown in Figure 2-3H-3J.

To determine the developmental stage most suitable for the RNAi treatment, I compared

the phenotypic consequences of the RNAi treatment at five morphological stages (stage A-E, Okude et al. 2017b, see Chapter 1) in the final larval instar of *I. senegalensis* (Fig. 2-7A). Inhibition of melanin pigmentation caused by *MCO2* RNAi was observed in all emerged adults when injected at the stages A and B (Fig. 2-7C). When injected at the stages C and D, suppression of melanin pigmentation was certainly observed in some emerged adults, but other adults exhibited abnormal coloration caused by wounds (Fig. 2-7B).

To examine whether this RNAi method can be applicable to other Odonata species, I conducted *MCO2* RNAi in the larval abdomen of *Lestes temporalis* (Lestidae), in the adult abdomen of *Ischnura asiatica* (Coenagrionidae), *Mnais costalis* (Calopterygidae) and *Davidius nanus* (Gomphidae) (Fig. 2-8), and in the adult thorax of *Sympetrum frequens* (Libellulidae), *Shagomphus postocularis* (Gomphidae), and *Asiagomphus melaenops* (Gomphidae) (Fig. 2-9). As a result, the suppression of melanin pigmentation was observed in most of the species, but RNAi was less effective in Gomphidae species, *S. postocularis* (1/4 = 25%) and *A. melaenops* (0/4 = 0%) (Fig. 2-9). As in *I. senegalensis*, abnormal coloration caused by wounds was sometimes observed (Fig. 2-9, black arrowheads).

Discussion

1. Efficiency of RNAi treatment

As described above, the levels of RNAi phenotype, namely size and location of the cuticle decolorization, often exhibited considerable variation between individuals subjected to the same RNAi treatment (e.g., Fig. 2-4), but the levels of the phenotypic

penetrance seem to be remarkably different between the Odonata species. The observed phenotypic regions were larger and more prominent in *I. senegalensis* (Figs. 2-4, 2-5) and *I. asitatica* (Fig. 2-7B) than in *P. zonata* (Fig. 2-6) and *N. pygmaea* (my master's thesis, Okude et al. 2017a). In summary, RNAi is more effective in Zygopteran species than in Anisopteran species. This difference may be due to the thickness of the cuticle on the larval surface, considering that the cuticle of Zygopteran species is thinner than the cuticle of Anisopteran species. Especially, RNAi did not affect effectively in two Gomphidae species (*S. postocularis* and *A. melaenops*) probably due to their large bodies and hard cuticles. As far as I examined, no clear difference was recognized between the effects of siRNA and dsRNA (Fig. 2-4, Table 2-1).

2. Appropriate developmental stage for RNAi

I found that proper larval staging is important for performing RNAi efficiently. Inhibition of adult pigmentation was caused by *MCO2* RNAi before the stage D (approximately 3 days before adult emergence) in *I. senegalensis*, which is consistent with the previous report on *N. pygmaea* (Okude et al. 2017a). The RNAi phenotypes observed when injected at the stages C and D were less conspicuous than those treated at the stages A and B, which indicate that the stages C and D may be too late to sufficiently suppress the gene expression. The appropriate timing for RNAi treatment depends on the timing of gene expression, and *MCO2* gene exhibits transiently high expression during adult emergence (see Chapter 4, Fig. 4-8, Okude et al. 2017a), as in other insects (Arakane et al. 2016, Asano et al. 2019). In the stinkbug *Plautia stali*, RNAi knockdown of *MCO2* gene was observed from day 4 onwards after injection (Nishide et al. 2020), which is consistent with the present results.

In Chapter 1, I revealed that after the stage 2 (the stage B in *I. senegalensis*), days to adult emergence exhibit relatively small variation among the majority of final instar larvae, suggesting that the stage 2 may correspond to the onset of the process toward adult emergence, after which the developmental processes for metamorphosis proceed in a prefixed and coordinated manner (see Chapter 1, Okude et al. 2017b). Morphological abnormalities caused by wounds were often observed when the larvae were RNAi-treated at the stages C and D (Fig. 2-7B, 7C). This is likely to be associated with a dramatic progression of metamorphosis during these stages, suggesting that RNAi treatment should be avoided from the stage C and on. In summary, I found that final instar larvae at the stage A or B (or stage 1 in Chapter 1) should be used for RNAi experiments.

3. Usefulness and superiority of electroporation-mediated RNAi method

The conventional RNAi is a simple and powerful experimental method, but some insect lineages like butterflies (Terenius et al. 2011), aphids (Christiaens et al. 2014) and dragonflies (Okude et al. 2017b) exhibit low RNAi efficiency, for which establishment of gene function analysis is a major challenge. In this study, I found that electroporation-mediated RNAi can induce local gene suppression in most Odonata species with almost 100% efficiency, at least in epidermis, if treated at appropriate developmental stages (Table 2-1). Recently, CRISPR/Cas9-based gene knockouts have been successfully applied to a variety of insects, providing a powerful molecular genetic tool for non-model organisms (Sun et al. 2017). Here, however, I point out that CRISPR/Cas9 is certainly great but the electroporation-mediated RNAi method may be superior to CRISPR/Cas9 in some respects.

Firstly, in the electroporation-mediated RNAi method, the body region where RNAi

phenotypes appear can be easily controlled experimentally by the position of positive electrode upon electroporation. In addition, since the region where the gene expression is suppressed is limited around the region where positive electrode was placed, the RNAi phenotypes can be easily compared with the control phenotypes side by side in the same individual. Secondly, compared to CRISPR/Cas9 method in which injected eggs have to be reared to adulthood to observe the knockout phenotypes, the electroporation-mediated RNAi is superior in that the gene knockdown phenotypes can usually be observed in much shorter time. For example, it takes three to four months for *I. senegalensis* and one to two years for *P. zonata* from eggs to adults (Miyakawa 1969, Okude et al. 2017b). However, in order to observe RNAi phenotypes within the adult epidermis, it takes less than one month from dsRNA injection into final instar larvae at the stage B to adult emergence for both *I. senegalensis* and *P. zonata* (Fig. 2-7, see Chapter 1). Thirdly, the electroporation-mediated RNAi method entails dsRNA injection into large larvae, which is easier than microinjection into tiny eggs required for CRISPR/Cas9 method. In addition, the electroporation-mediated RNAi is applicable to insect species whose newly laid eggs are difficult to collect. For example, females of *P. zonata* lay eggs onto floating plants on water surface during flight (Ozono et al. 2017), and thus it is difficult to collect their eggs both in the field and in the laboratory. Hence, I expect that this protocol may be generally applicable to not only all the Odonata species but also non-model organisms in which the conventional RNAi method does not work efficiently.

References

- Ando T, Fujiwara H (2013). Electroporation-mediated somatic transgenesis for rapid functional analysis in insects. *Development* **140**: 454–458.
- Arakane Y, Noh MY, Asano T, Kramer KJ (2016). Tyrosine metabolism for insect cuticle

pigmentation and sclerotization. in *Extracellular Composite Matrices in Arthropods* (eds Cohen E and Moussian B) 165–220, Springer.

Asano T, Seto Y, Hashimoto K, Kurushima H (2019). Mini-review an insect-specific system for terrestrialization: Laccase-mediated cuticle formation. *Insect Biochem Mol Biol* **108**: 61–70.

Bybee S, Córdoba-Aguilar A, Duryea MC, Futahashi R, Hansson B, Lorenzo-Carballea MO, et al. (2016). Odonata (dragonflies and damselflies) as a bridge between ecology and evolutionary genomics. *Front Zool* **13**: 46.

Christiaens O, Swevers L, Smaghe G (2014). DsRNA degradation in the pea aphid (*Acyrtosiphon pisum*) associated with lack of response in RNAi feeding and injection assay. *Peptides*. **53**: 307–314.

Corbet PS (1999). *Dragonflies, Behavior and Ecology of Odonata*. Cornell University Press.

Córdoba-Aguilar A (2008). Dragonflies and damselflies. *Model organisms for ecological and evolutionary research*. Oxford University Press.

Futahashi R (2011). Whole-mount *in situ* hybridization of sectioned tissues of species hybrids to detect *cis*-regulatory changes in gene expression pattern. *Methods Mol Biol* **772**: 319–328.

Futahashi R (2016). Color vision and color formation in dragonflies. *Curr Opin Insect Sci*: **17**: 32–39.

Futahashi R (2020). Diversity of UV reflection patterns in Odonata. *Front Eco Evol* **8**: 201.

Futahashi R, Okude G, Sugimura M, Ugai S (2018). Interspecific hybrids in Japanese Odonata. *Tombo* **60**: 1–49.

Henze MJ, Lind O, Wilts BD, Kelber A (2019). Pterin-pigmented nanospheres create the colours of the polymorphic damselfly *Ischnura elegans*. *J R Soc Interface* **16**: 20180785.

Linz DM, Clark-Hachtel CM, Borràs-Castelles F, Tomoyasu Y (2014). Larval RNA interference in the red flour beetle, *Tribolium castaneum*. *J Vis Exp* **92**: 52059.

Matsuura Y, Kikuchi Y, Miura T, Fukatsu T (2015). Ultrabithorax is essential for bacteriocyte development. *Proc Natl Acad Sci USA* **112**: 9376–9381.

Misof B, Liu S, Meusemann K, Peters RS, Donath A, Mayer C, et al. (2014). Phylogenomics resolves the timing and pattern of insect evolution. *Science* **346**: 763–767.

Miyakawa K (1969). A study of the life-history of *Pseudothemis zonata* (Burm.) (Odonata, Libellulidae) II. Immature stage. *Kontyû* **37**: 409–422. In Japanese.

Naito Y, Yoshimura J, Morishita S, Ui-Tei K (2009). siDirect 2.0: updated software for designing functional siRNA with reduced seed-dependent off-target effect. *BMC Bioinformatics* **10**: 392.

Nishide Y, Kageyama D, Hatakeyama M, Yokoi K, Jouraku A, Tanaka H, et al. (2020). Diversity and function of multicopper oxidase genes in the stinkbug *Plautia stali*. *Sci Rep* **10**, 3464.

Nishikawa H, Iijima T, Kajitani R, Yamaguchi J, Ando T, Suzuki Y, et al. (2015). A genetic mechanism for female-limited Batesian mimicry in *Papilio* butterfly. *Nat Genet* **47**: 405–409.

Okude G, Futahashi R, Kawahara-Miki R, Yoshitake K, Yajima S, Fukatsu T (2017a).

Electroporation-mediated RNA interference reveals a role of the multicopper oxidase 2 gene in dragonfly cuticular pigmentation. *Appl Entomol Zool* **52**: 379–387.

Okude G, Futahashi R, Tanahashi M, Fukatsu T (2017b). Laboratory rearing system for *Ischnura senegalensis* (Insecta: Odonata) enables detailed description of larval development and morphogenesis in dragonfly. *Zool Sci* **34**: 386–397.

Okude G, Fukatsu T, Futahashi R (2020). Interspecific crossing between blue-tailed damselflies *Ischnura elegans* and *I. senegalensis* in the laboratory. *Entomol Sci* **23**: 165–172.

Osanai-Futahashi M, Tatematsu K, Futahashi R, Narukawa J, Takasu Y, Kayukawa T, *et al.* (2016). Positional cloning of a *Bombyx pink-eyed white egg* locus reveals the major role of *cardinal* in ommochrome synthesis. *Heredity* **116**, 135–145.

Ozono A, Kawashima I, Futahashi R (2017). *Dragonflies of Japan*. (3rd edition) Bunichi-Sogo Syuppan, Co Ltd. (in Japanese)

Ozono A, Kawashima I, Futahashi R (2019). *The handbook of Japanese aquatic insects. Volume 3: dragonfly larvae*. Bunichi-Sogo Syuppan, Co Ltd. (in Japanese)

Sun D, Guo Z, Liu Y, Zhang Y (2017). Progress and prospects of CRISPR/Cas systems in insects and other arthropods. *Front Physiol* **8**: 608.

Terenius O, Papanicolaou A, Garbutt JS, Eleftherianos I, Huvenne H, Kanginakudru S, *et al.* (2011). RNA interference in Lepidoptera: An overview of successful and unsuccessful studies and implications for experimental design. *J Insect Physiol* **57**: 231–245.

Untergasser A, Cutcutache I, Koressaar T, Ye J, Faircloth BC, Remm M, *et al.* (2012). Primer3--new capabilities and interfaces. *Nucleic Acids Res* **40**: e115.

Wipfler B, Letsch H, Frandsen PB, Kapli P, Mayer C, Bartel D, *et al.* (2019). Evolutionary history of Polyneoptera and its implications for our understanding of early winged insects. *Proc Natl Acad Sci USA* **116**: 3024–3029.

Yamaguchi J, Mizoguchi T, Fujiwara H (2011). siRNAs induce efficient RNAi response in *Bombyx mori* embryos. *PLoS ONE* **6**: e25469.

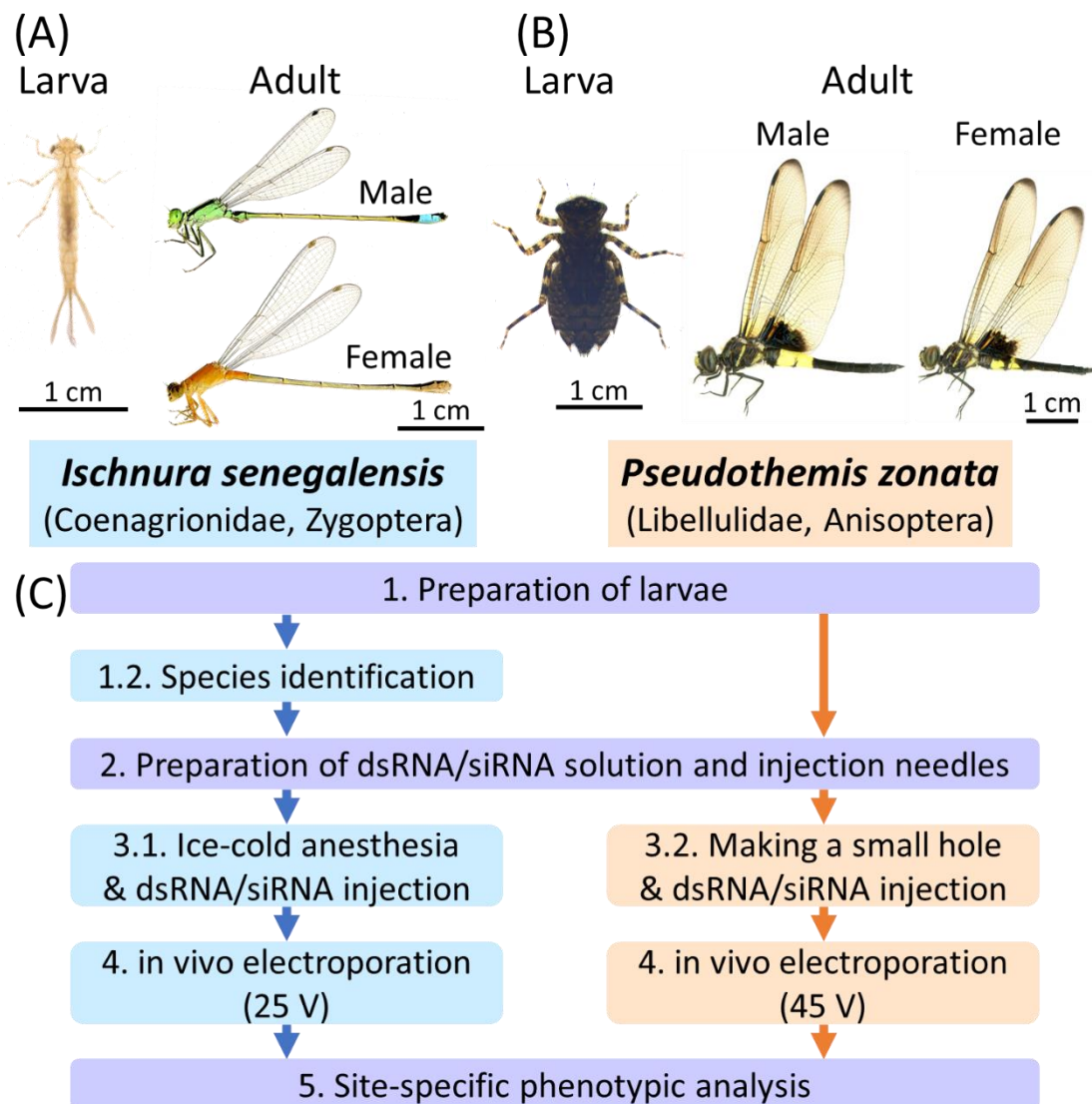


Figure 2-1.

Electroporation-mediated RNAi method in Odonata. (A) *Ischnura senegalensis* (Coenagrionidae) as a representative damselfly species. (B) *Pseudothemis zonata* (Libellulidae) as a representative dragonfly species. (C) The overall scheme of the RNAi method. Blue and orange boxes indicate the methods for *I. senegalensis* and *P. zonata*, respectively. The purple boxes indicate the common methods applied to both species.

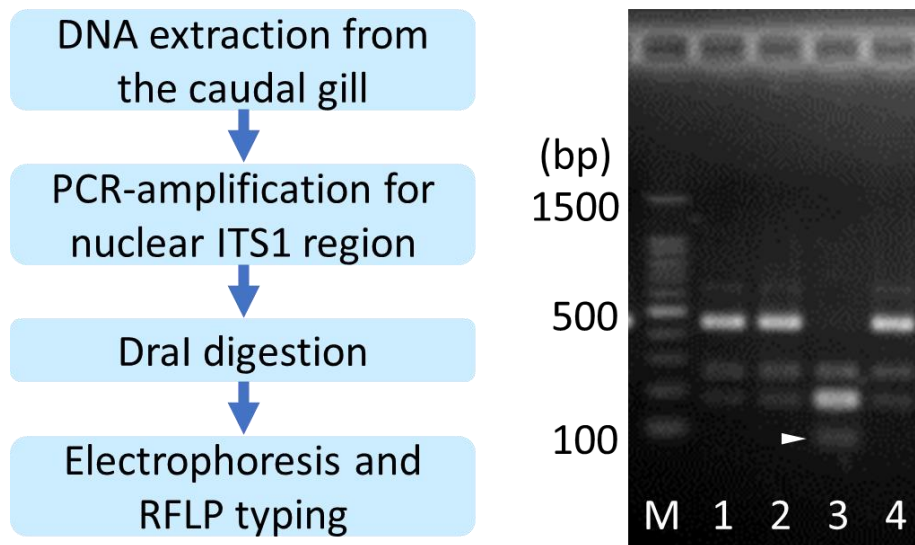


Figure 2-2.

A representative result of restriction fragment length polymorphism (RFLP)-based species identification for *Ischnura* species. Arrowhead indicates the *I. senegalensis*-specific band. 1, 2, 4: *I. asiatica*, 3: *I. senegalensis*, M: 100-base pair ladder marker.

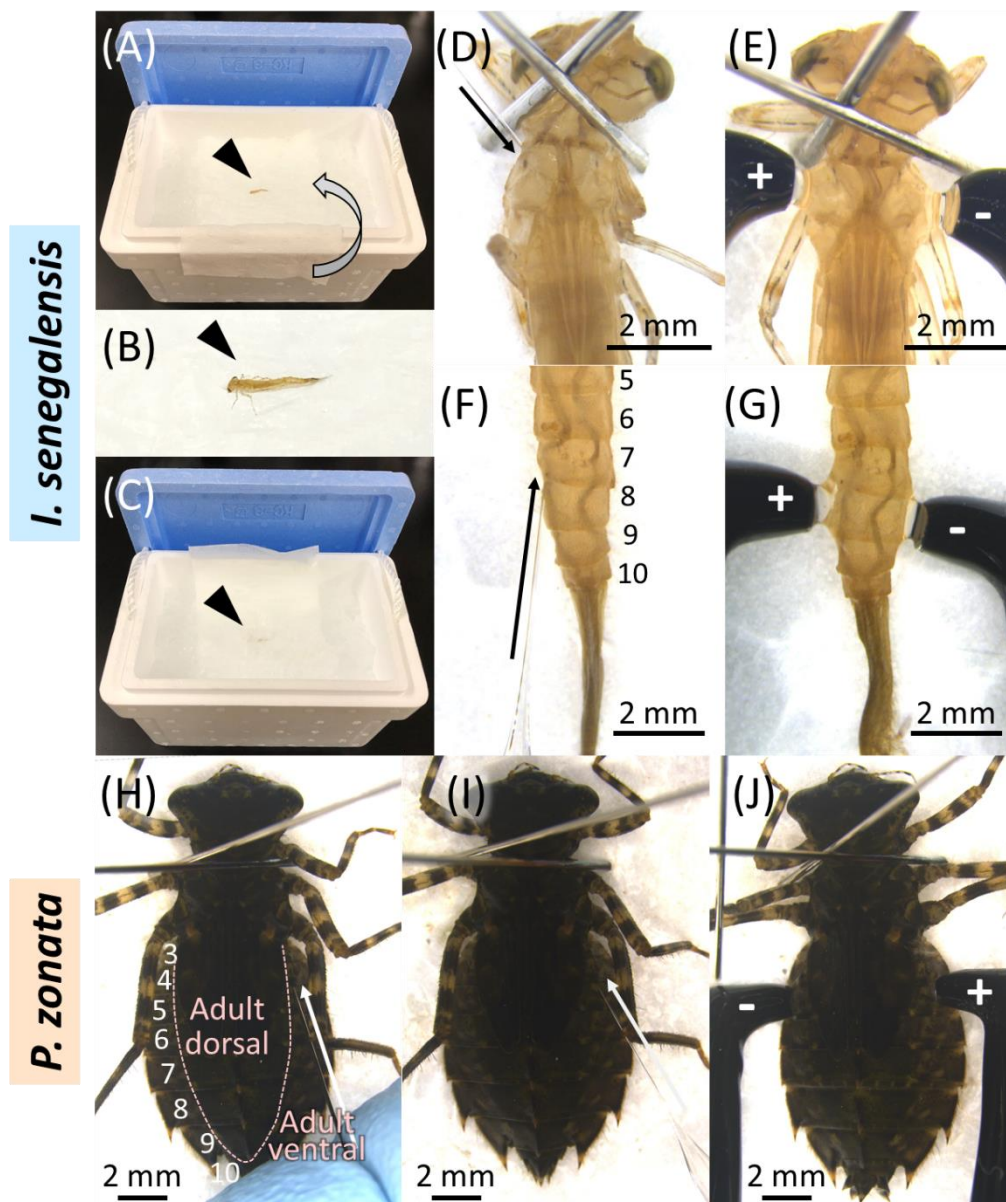


Figure 2-3.

Electroporation-mediated RNAi method in Odonata. (A)-(C). Cold anesthesia of *I. senegalensis*. Arrowheads indicate a larva. (A) Putting a larva on crushed ice with a wet paper. (B) Magnified view of a larva on ice. (C) A larva covered with a wet paper on ice. (D)-(G) RNAi method for *I. senegalensis*. (D) Injection into the thorax. (E) Electroporation on the thorax. (F) Injection into the abdomen. (G) Electroporation on the abdomen. (H)-(J) RNAi method for *P. zonata*. (H) Making a small hole on the abdomen. (I) Injection into the abdomen. (J) Electroporation on the abdomen. Arrows indicate the point of making a hole or injection. +, -: Positive/negative side of an electrode. Numbers indicate the abdominal segment.

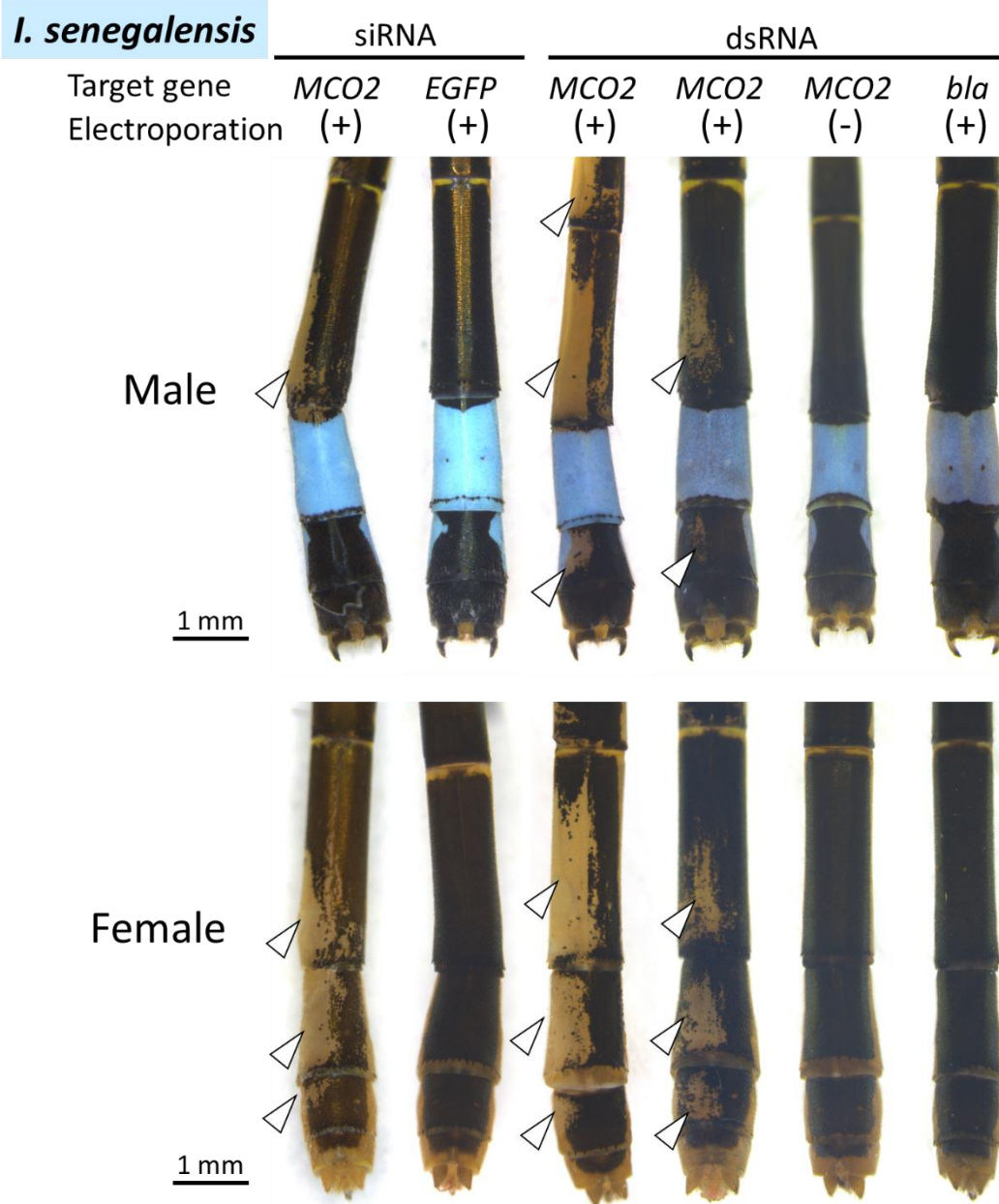


Figure 2-4.

Dorsal views of RNAi phenotypes on the abdomen of *I. senegalensis*. White arrowheads indicate the regions of suppressed melanization.

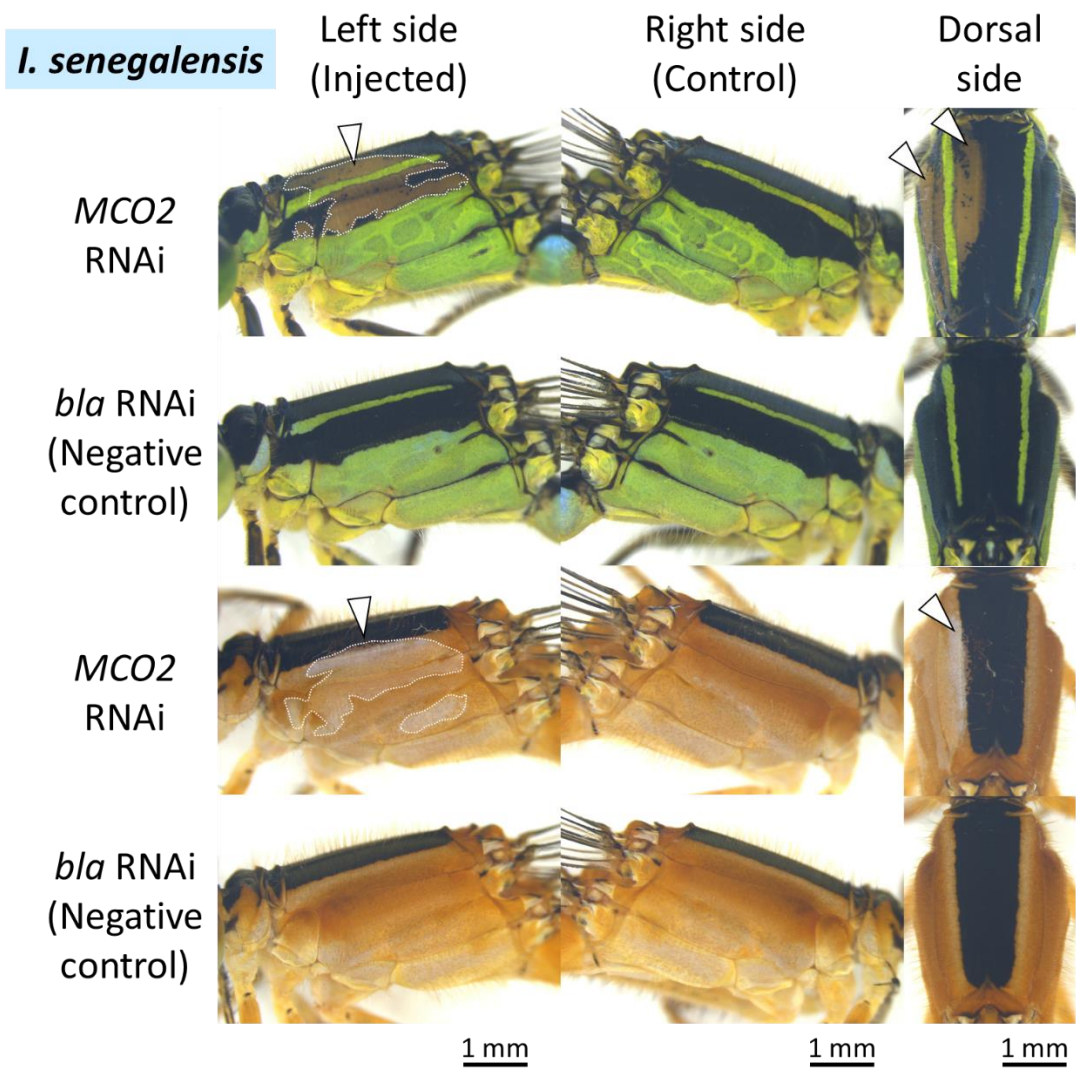


Figure 2-5.

Lateral and dorsal views of RNAi phenotypes on the thorax of *I. senegalensis*. White arrowheads and dotted lines indicate the regions of suppressed pigmentation.

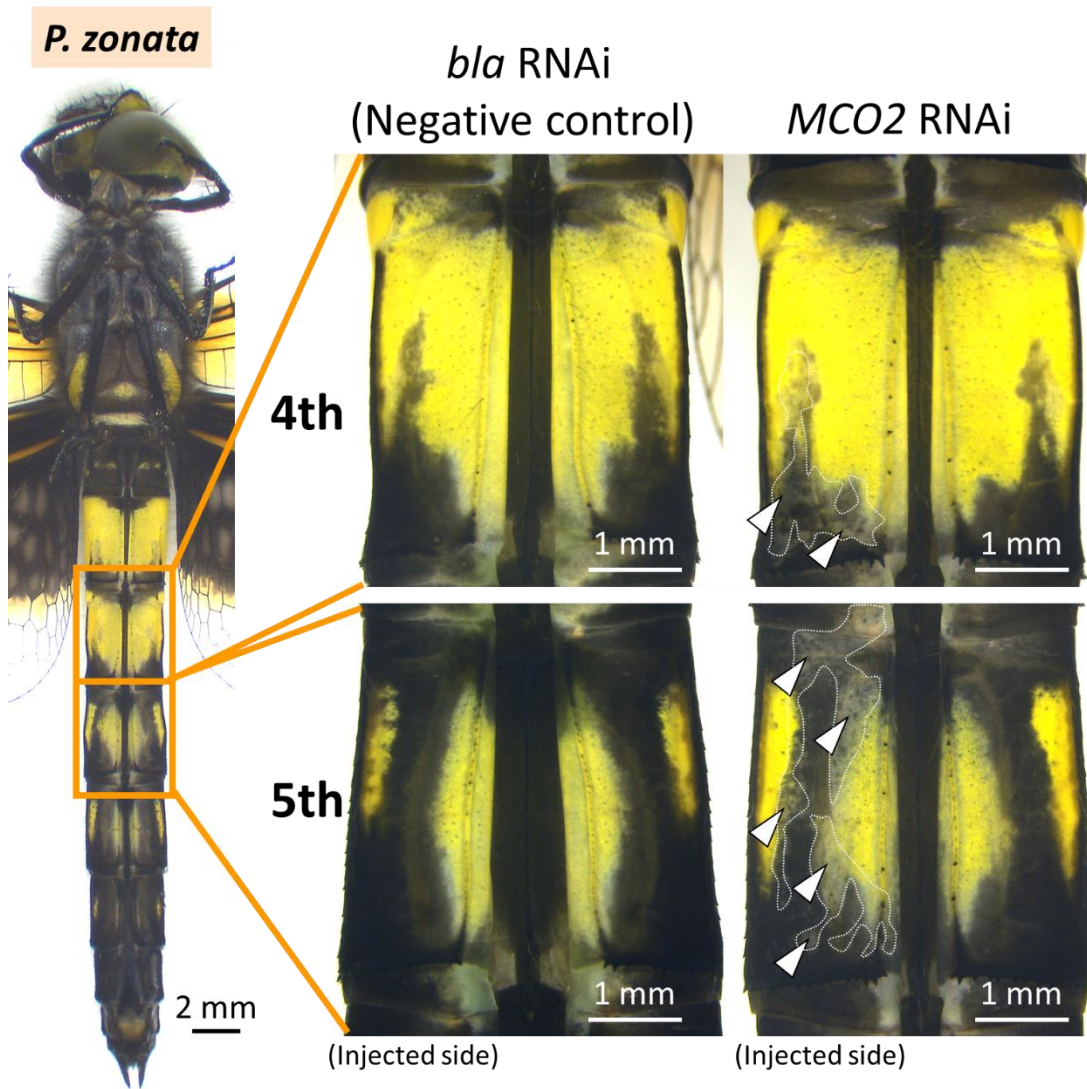


Figure 2-6.

Ventral views of RNAi phenotypes in the abdomen of *P. zonata*. White arrowheads and dotted lines indicate the regions of suppressed melanization.

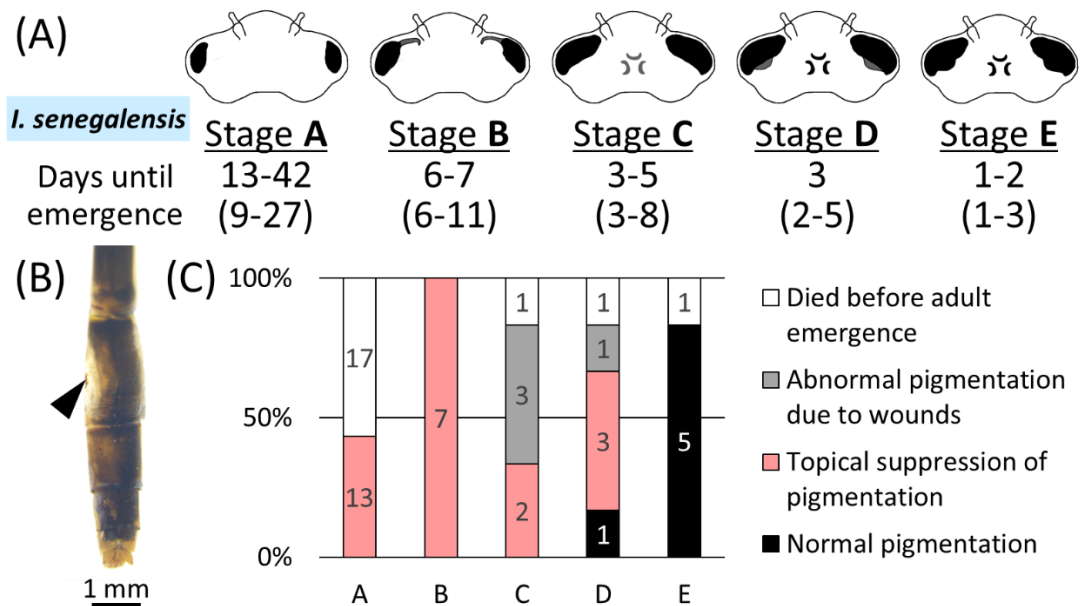


Figure 2-7.

Stage dependent *IsMCO2* RNAi effects during the final larval instar of *I. senegalensis*.

(A) Morphological changes in the compound eyes at five morphological stages (stage A–E) and the number of days to adult emergence in this study. Numbers in parentheses are from previous report (Okude et al. 2017b). (B) Abnormal pigmentation due to wounds. Arrowhead indicates electroporation site. (C) The effect of RNAi at five morphological stages on adult pigmentation in *I. senegalensis*. The number on the bar indicates the number of individuals.

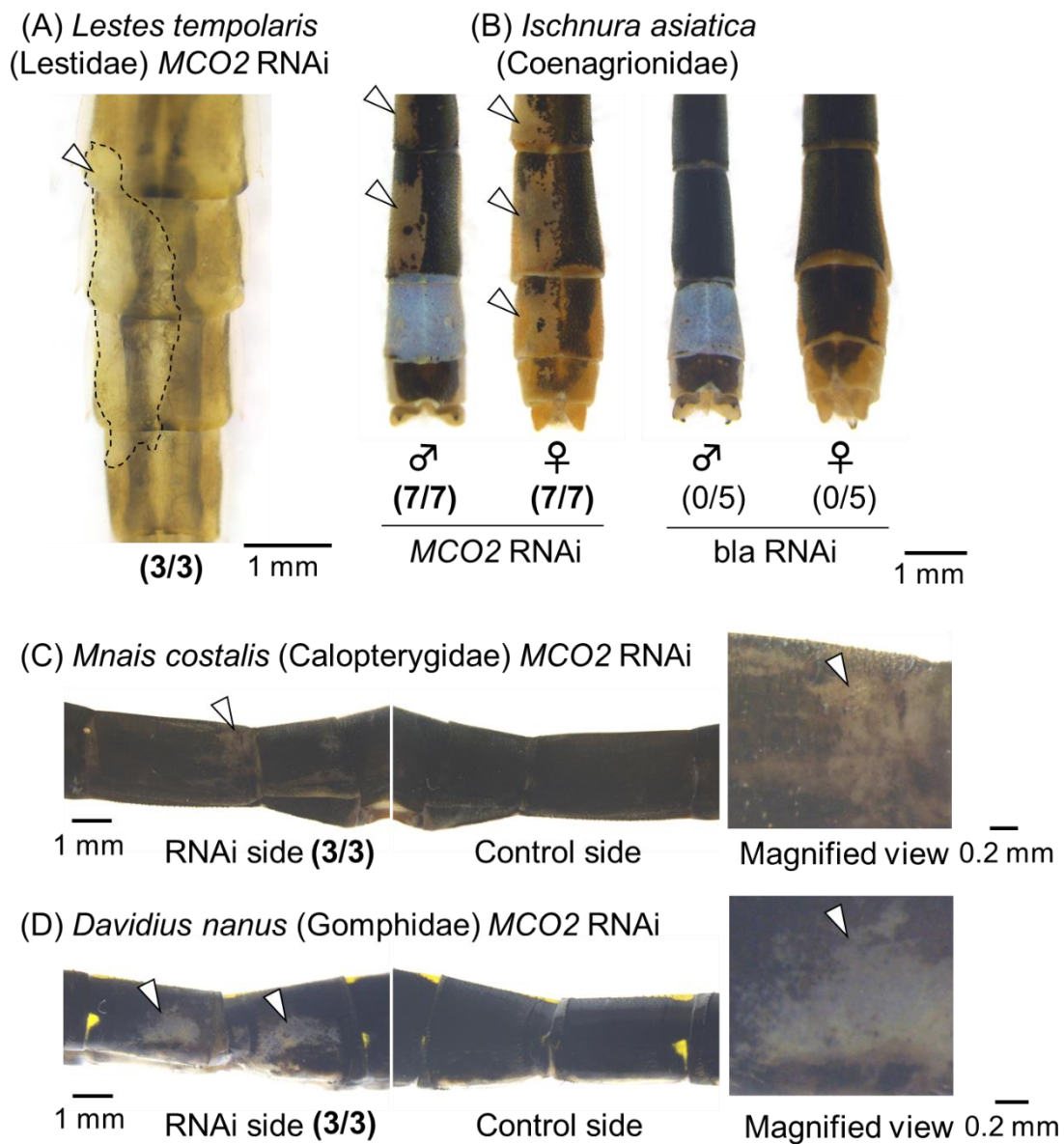


Figure 2-8.

RNAi phenotypes in the abdomen. (A) A F-0 larva of *Lestes tempolaris* (Lestidae). RNAi was conducted at the F-1 larval instar and RNAi phenotype was observed at the F-0 larval instar. (B) Adults of *Ischnura asiatica* (Coenagrionidae). (C) An adult of *Mnais costalis* (Calopterygidae). (D) An adult of *Davidius nanus* (Gomphidae). Arrowheads indicate the regions of suppressed melanization. Numbers of parentheses indicate (number of individuals affected by RNAi / number of emerged adults or molted larvae).

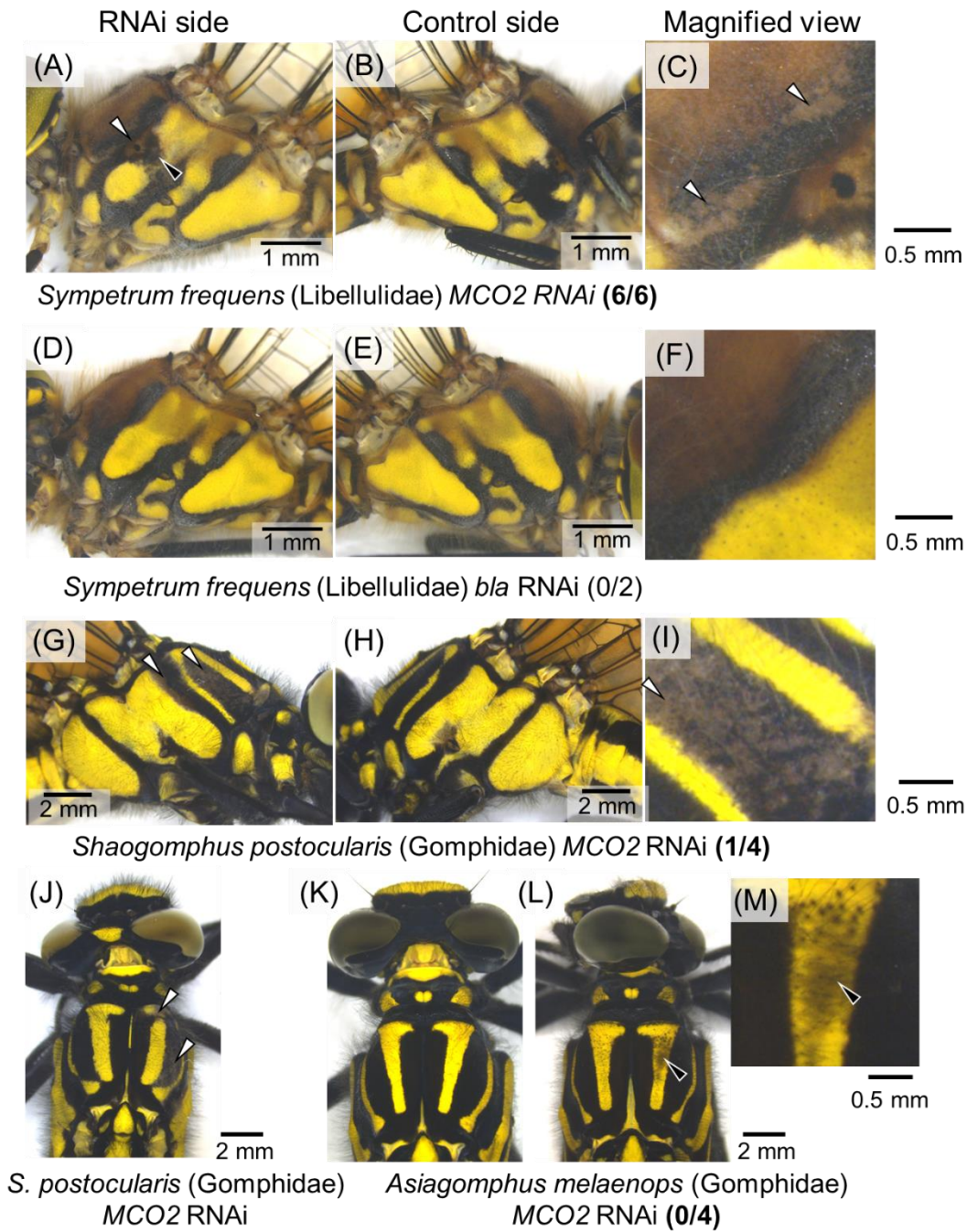


Figure 2-9.

RNAi phenotypes in the thorax of adults. (A)-(F) *Sympetrum frequens* (Libellulidae). (G)-(J) *Shaogomphus postocularis* (Gomphidae). (G)-(J) are the same individual. (M)(N) *Asiagomphus melaenops* (Gomphidae). White arrowheads indicate the regions of suppressed melanization. Numbers of parentheses indicate (number of individuals affected by RNAi / number of emerged adults). Black arrowheads indicate the blackened region due to the wound.

Species	<i>I. senegalensis</i>					<i>P. zonata</i>				
	Abdomen					Thorax		Abdomen		
	siRNA		dsRNA			dsRNA		dsRNA		
Target gene	<i>IsMCO2</i>	<i>EGFP</i>	<i>IsMCO2</i>	<i>IsMCO2</i>	<i>bla</i>	<i>IsMCO2</i>	<i>bla</i>	<i>PzMCO2</i>	<i>PzMCO2</i>	<i>bla</i>
Electroporation	+	+	+	-	+	+	+	+	-	+
Injected larvae	22	25	30	6	53	12	20	18	7	10
Emerged adults	7	6	13	4	40	11	14	11	2	4
Adults with unpigmented region (ratio)	7 (100%)	0 (0%)	13 (100%)	0 (0%)	0 (0%)	10 (91%)	0 (0%)	11 (100%)	0 (0%)	0 (0%)

Table 2-1.

The effect of RNAi on adult pigmentation in *I. senegalensis* and *P. zonata*. Results at stage A are shown in *I. senegalensis*. *IsMCO2*: multicopper oxidase 2 gene of *I. senegalensis*, *EGFP*: Enhanced green fluorescent protein gene, *bla*: beta lactamase gene from pGEM-T Easy Vector, *PzMCO2*: multicopper oxidase 2 gene of *P. zonata*.

Chapter 3: Molecular mechanisms underlying metamorphosis in Odonata.

(本章については、5年以内に雑誌等で刊行予定のため、非公開。)

Chapter 4: Functional analyses of ecdysone-related transcription factors in Odonata.

(本章については、5年以内に雑誌等で刊行予定のため、非公開。)

Chapter 5: Molecular mechanisms underlying yellow color pattern formation in Odonata.

(本章については、5年以内に雑誌等で刊行予定のため、非公開。)

**Chapter 6: Molecular mechanisms underlying light blue coloration in
Ischnura damselflies.**

(本章については、5年以内に雑誌等で刊行予定のため、非公開。)

Chapter 7: Interspecific crossing between blue-tailed damselflies and functional analysis of sex-differentiation genes.

The partial content of this chapter has been published in; Okude G, Fukatsu T, Futahashi R. (2020). Interspecific crossing between blue-tailed damselflies *Ischnura elegans* and *I. senegalensis* in the laboratory. *Entomological Science* **23**: 165–172.

(本章のうち、5年以内に雑誌等で刊行予定の部分の記述については、非公開。)

Abstract

Ischnura species (Odonata) are among the most common damselflies in the world, which often exhibit female color polymorphisms. One morph, called androchrome, is similar to males in its color pattern, while the other morphs, generally referred to as gynochromes, exhibit female-specific colors. In several *Ischnura* species, the female polymorphism is heritable, although molecular and genetic mechanisms remain largely unknown. The dominant-recessive patterns of the female color morphs may differ between species. For example, androchromic females are dominant to gynochromic females in *I. elegans*, whereas androchromic females are recessive in *I. senegalensis*. In this Chapter, I report a case of interspecific hybridization between a gynochrome female of *I. elegans* and a male of *I. senegalensis* in the laboratory. I obtained 61 hybrid adult offspring, of which all 31 females were of gynochrome morph. DNA analyses of the hybrids confirmed that nuclear DNA sequences were derived from both parent species, whereas mitochondrial DNA sequences were maternally inherited. In the hybrids, the pattern of abdominal light blue spots was similar to that of *I. senegalensis*. ... (5年以内に

雑誌等で刊行予定のため、非公開。)

Introduction

Odonata (dragonflies and damselflies) are among the winged insect groups of the most ancient evolutionary origin (Misof et al. 2014, Wipfler et al. 2019) and show diverse colors on their wings and bodies, which often exhibit conspicuous inter- and intra-specific diversity (Tillyard 1917, Corbet 1999, Bybee et al. 2016, Futahashi 2016). The diverse color patterns in Odonata, especially color polymorphism within the same species, have been mainly investigated from ecological and evolutionary points of view (Tillyard 1917, Corbet 1999, Córdoba-Aguilar 2008, Bybee et al. 2016, Futahashi 2016, Futahashi 2017, Svensson 2017). In Odonata, such color polymorphisms are often limited to females (Corbet 1999). The color morphs in female dragonflies are categorized into the male-mimicking color morph called androchrome and the female-specific color morph called gynochrome. The color polymorphisms of female Odonata have been mainly studied in blue-tailed damselflies of the genus *Ischnura*, which is one of the most common groups of damselflies in the world (Fincke 2005, Kunte 2009, Svensson 2017). Previous studies have suggested that the female color polymorphisms in *Ischnura* species are maintained by negative frequency-dependent selection to avoid sexual harassments by males (Gosden and Svensson 2009, Takahashi et al. 2010, Takahashi et al. 2014, Le Rouzic et al. 2015, Gering 2017, Willink 2019).

Laboratory crossing experiments showed that the female color polymorphisms are regulated by a single autosomal locus in all the *Ischnura* species examined thus far (Johnson 1964, Johnson 1966, Cordero 1990, Sánchez-Guillén et al. 2005, Takahashi et

al. 2014, Sanmartín-Villar et al. 2016). Notably, dominant-recessive patterns of the female color morphs differ between the *Ischnura* species. The androchrome allele is dominant to the gynochrome alleles in *I. graellsii* (Cordero 1990), *I. elegans* (Sánchez-Guillén et al. 2005) and *I. genei* (Sanmartín-Villar et al. 2016), whereas the androchrome allele is recessive in *I. damula* (Johnson 1964), *I. demorsa* (Johnson 1966) and *I. senegalensis* (Takahashi et al. 2014). Recently, some candidate genes, whose expression levels differ between color morphs in females, have been reported from *I. elegans* (Chauhan et al. 2016, Willink et al. 2019b) and *I. senegalensis* (Takahashi et al. 2019), but the molecular basis of this genetic color polymorphism is still unknown. Hybrid individuals between closely-related *Ischnura* species have been occasionally obtained from wild populations (Leong and Hafernik 1992, Schneider and Krupp 1996, Monetti et al. 2002) and laboratory crossing experiments (Leong and Hafernik 1992, Monetti et al. 2002, Sánchez-Guillén et al. 2005, Sánchez-Guillén et al. 2012, Sánchez-Guillén et al. 2014), but, to my knowledge, there has been no report on hybrids between two species with different dominant-recessive patterns of the female color morphs.

In Japan, *I. elegans* shows patchy distribution patterns restricted to the northern regions Hokkaido and Aomori Prefectures, *I. senegalensis* is widely distributed in the southwestern regions with the northernmost populations in Iwate Prefecture, and thus these two species are allopatric in the wild (Fig. 7-1, Ozono et al. 2017). In this study, I report a case of interspecific hybridization between *I. elegans* (androchromic female being dominant) and *I. senegalensis* (androchromic female being recessive) in the laboratory. I obtained 61 (30 males and 31 females) hybrid adults with phenotypes intermediate between the two parent species. In addition, to elucidate the molecular mechanisms underlying female color polymorphism in *I. senegalensis*, I conducted

electroporation-mediated RNAi for the sex-differentiation genes known in other insects.

Material and Methods

1. Insects collecting and mating in the laboratory

Four females of *I. elegans* were collected in Ikeda-town, Hokkaido, on Aug. 20th, 2017 (Fig. 7-1, Table 7-1). All these four females were of gynochrome morph (the form *infuscans-obsolata* which lacks black stripes on the anterior side of the thorax) with vivid abdominal blue spot indicating their immature state (Svensson et al. 2019, Willink et al. 2019). After five days, three mature males of *I. senegalensis* were collected in Tsukuba, Ibaraki on Aug. 25th, 2017 (Fig. 7-1, Table 7-1). I reared these damselflies together in an adult-rearing cage (17 cm × 27 cm, 18 cm high; purchased at a 100-yen store) and fed with *Drosophila* fruit flies. In the morning after three days, I observed a mating pair of an *I. elegans* female and an *I. senegalensis* male (Fig. 7-1, Table 7-1). After the copulation finished, I transferred the mated female to a petri dish in which a wet filter paper was placed for oviposition.

For RNAi experiments, larvae of *I. senegalensis* and *I. asiatica* were collected in Tsukuba, Ibaraki, Japan.

2. Larvae rearing

For rearing larvae of the hybrid between *I. senegalensis* and *I. elegans*, the post-copulation female was transferred from the adult-rearing cage to a petri dish in which a sheet of wet filter paper was placed for an oviposition substratum. Each newly hatched larva was transferred to each well of 48-well plates (about 1 ml water for each well) to

avoid cannibalism. As the larvae grew, we transferred them to 24-well plates (about 2 ml water for each well), and subsequently to 12-well plates (about 3 ml water for each well). The larvae were fed with *Artemia* brine shrimps.

During initial six or seven weeks, we checked whether each larva was alive or dead individually once a week (Fig. 7-2). After that, we started to record their ecdysis and death events individually every day. When the larvae approached to adult emergence and stopped feeding, we transferred them individually to a cage (10 cm × 15 cm, 3 cm water depth) covered with a disposable non-woven mesh for assisting adult emergence.

3. DNA sequencing analysis

I extracted DNA from a pair of forelegs of each insect using QIAamp DNA Mini Kit (Qiagen). Nuclear ITS2 region was PCR-amplified from the DNA samples using the primers 5.8S-S1 (5'-CGG TGG ATC ACT CGG CTC GT-3') and 28S-AS1 (5'-TTT CAC TCG CCG TTA CTA AGG GAA TC-3'), whereas mitochondrial 16S rRNA gene was amplified using the primers 16S-F0 (5'-TTA AAC CGG TYT GAA CTC AGA TC-3') and 16S-R1 (5'-CGC CTG TTT ATC AAA AAC AT-3') (Futahashi et al. 2018). PCR-amplified products were subjected to DNA sequencing using BigDye Terminator v3.1 Cycle Sequencing Kit (Applied Biosystems) and 3130xl Genetic Analyzer (Applied Biosystems).

4. Morphometry

Magnified photos of emerged adults were taken using a stereoscopic microscope S8APO (Leica Microsystems) with a digital high definition microscope camera MC120HD (Leica). The following characteristics were used in species identification because they are

stable within the species: the morphology of postocular spots of female heads, the shape of prothorax and male appendages, the size of abdominal blue spots, and the size of black markings on the 2nd abdominal segment (Sugimura et al. 2001, Ozono et al. 2017).

Following the majority of previously published literature on dragonflies, I described the final larval instar as F-0 or F (= Final), and the penultimate larval instar as F-1 (= F minus 1) because the final larval instar is generally not fixed in dragonflies (Corbet 1999, Okude et al. 2017b). For each instar, the “day 1” denotes the day on which ecdysis occurred. In order to investigate morphological changes during larval development in detail, six F-0 instar larvae and four F-1 instar larvae were photographed every day using a stereoscopic microscope SZ-6850T (Relyon) with a digital high definition microscope camera TrueChrome Metrics (Relyon). For measuring the angle of compound eyes, the average angle of the compound eyes was calculated for the left and right compound eyes. All the image processing operations and the measurements were conducted on the software Natsumushi version 1.00 (Tanahashi and Fukatsu 2018). Statistical analysis was performed by R software (version 3.3.1) (R Core Team 2016).

5. RNAi experiment

Electroporation-mediated RNAi was conducted as described in Chapter 2. The primer sets to produce templates for dsRNA synthesis are shown in Supplementary Table 2 (no. 202-215).

Results

1. Interspecific crossing and F1 hybrids between *I. elegans* and *I. senegalensis*

On the next day after the transfer into a petri dish with a wet filter paper, I observed 297 eggs laid into the filter paper. Since that day, the female laid no eggs. After nine days, 243 1st instar larvae hatched, of which three died soon, whereas 54 eggs were unhatched (Table 7-1). Each of the remaining 240 1st instar larvae was reared individually (plate A-E; Fig. 7-2). Finally, 61 adults (30 males and 31 females; $61/240 = 25.4\%$) emerged (Figs. 7-2, 7-3). All the emerged females were gynochromic without black stripes on the anterior side of the thorax, similar to gynochrome female of *I. senegalensis* and *I. elegans*. Although I tried to maintain these adult dragonflies for two weeks, I could not observe neither sexual maturation with color change nor copulation in the adult-rearing cage, and no F2 generation was obtained.

Considering that the original females of *I. elegans* were collected in the field and thus they might have already mated prior to collection, I conducted nuclear and mitochondrial DNA analyses of the F1 individuals as well as their parent individuals. When I focused on the species-specific nucleotides of nuclear DNA, all the sequences of the F1 individuals ($n = 8$) represented the sequences derived from both the parent individuals (Fig. 7-3C), indicating that these individuals were interspecific hybrids, which strongly suggests that the collected female was a virgin. Mitochondrial DNA sequences of the F1 hybrid individuals were identical to the sequences of their maternal species *I. elegans* (Fig. 7-3C), confirming maternal inheritance of mitochondrial DNA in Odonata as reported previously (Futahashi et al. 2018).

2. Description of external characteristics of hybrid adults

I compared the external characteristics of the F1 hybrid adults to those of their parent species in detail. In the hybrids, the postocular spots on the female head looked similar to

those of *I. elegans*, and the shape of posterior margin of the female prothorax was intermediate between the two species – it protrudes backward in *I. elegans* whereas it looks rather linear in *I. senegalensis* (Fig. 7-4A). In the hybrids, the abdominal blue spots did not spread to the 7th abdominal segment in males and did not exist in females, which are reminiscent of the phenotypes of *I. senegalensis* (Fig. 7-4B). It should be noted that the repression of pigment production in abdominal light blue spots acted dominantly between species, given that the light blue spots of gynochrome females appeared sporadically across *Ischnura* genus (Willink et al. 2019). The shape of the superior and inferior abdominal appendages in the hybrid males was not slender compared to *I. senegalensis*, and the dorsal side of the 10th abdominal segment did not protrude compared to *I. elegans* (Fig. 7-4B). The color of female's cerci was more blackish compared to *I. senegalensis*. The size of black markings of the 2nd abdominal segment was variable, being *I. elegans*-like in some hybrid individuals and *I. senegalensis*-like in others (Fig. 7-4C).

3. Duration of larval instars of hybrids

Among 61 emerged adults, total larval periods until adult emergence varied from 86 days to 130 days (Fig. 7-5A). Total larval periods were slightly longer in females (n = 31; 109.4 ± 1.6 days) than in males (n = 30; 101.2 ± 3.3 days) (Mann-Whitney U test, $P = 0.024$). I also checked the larval durations of F-2 instar, F-1 instar and F-0 instar, respectively (Fig. 7-5B). The durations of F-2 instar exhibited no significant difference between males (n = 29; 10.0 ± 0.4 days) and females (n = 31; 9.6 ± 0.3 days) (Mann-Whitney U test, $P = 0.40$). Meanwhile, there were significant differences in the larval durations between F-1 males (n = 30; 12.2 ± 0.4 days) and F-1 females (n = 31; $13.2 \pm$

0.3 days) (Mann-Whitney U test, $P = 0.0057$), and between F-0 males ($n = 30$; 24.2 ± 0.6 days) and F-0 females ($n = 31$; 27.0 ± 0.6 days) (Mann-Whitney U test, $P = 0.0014$). The total duration from hatching to ecdysis into the F-2 instar did not exhibit significant difference between males ($n = 43$; 59.4 ± 1.0 days) and females ($n = 62$; 62.9 ± 0.94 days) (Mann-Whitney U test, $P = 0.052$) (Fig. 7-5C).

4. Morphological changes in F-0 and F-1 instar larvae of hybrids

In the six F-0 instar larvae (Figs. 7-6A, 7-7A), of which I photographed and monitored morphological changes, the most evident changes were observed in the shape and size of the compound eyes and wing sheaths as previously reported in *I. senegalensis* (see Chapter 1, Okude et al. 2017b). The compound eyes expanded, and their angle changed as the adult emergence approached (Figs. 7-6A, 7-7A, 7C). The F-0 instar larvae of hybrids could be categorized into five metamorphic stages (stage A, B, C, D and E), as in *I. senegalensis* (see Chapter 1, Okude et al. 2017b). The durations of stage A varied from 11 days to 14 days, whereas total durations from stage B to stage E were almost constant around 10 days (Fig. 7-6C).

In the three F-1 instar larvae, of which I photographed and monitored morphological changes, compound eyes became tilted and wing sheaths expanded (Figs. 7-6B, 7-7B). The late stage of F-1 instar being defined as the stage at which expanded wing sheaths were observable, the durations of the late stage were almost constant for two days regardless of the total duration of F-1 instar (Fig. 7-6D). Overall, morphological changes in the F-0 instar and F-1 instar hybrid larvae were comparable to those of *I. senegalensis* (see Chapter 1, Okude et al. 2017b).

...(5年以内に雑誌等で刊行予定のため、非公開。)

Discussion

1. Establishment of the model interspecific hybridization for analyzing the mechanisms underlying female color polymorphism

In this study, I successfully obtained adult insects of the F1 hybrid between *I. elegans* and *I. senegalensis*. To my knowledge, this is the first report of hybrids between two damselfly species with different dominant-recessive patterns of female color morphs, which expands understanding of the genetic mechanisms of polymorphism. I obtained all 31 hybrid females as gynochrome morph, probably because the *I. elegans* female used in this crossing experiment was the recessive gynochrome genotype (Sánchez-Guillén et al. 2005). To gain further insight into the genetic mechanisms underlying the female polymorphisms, more hybrids should be generated using different combinations of the color morphs and, if possible, F2 generations should be obtained and examined.

Uniquely, adult male Odonata possess secondary genitalia on the abdominal 2nd-3rd segments, which is, oddly, not directly connected to the internal genital organ. Therefore, male Odonata transfer the sperm from the genital orifice of the abdominal 9th segment to the secondary genitalia before copulation (Corbet 1999). At least partly because of these complicated procedures for sperm transfer and copulation, artificial mating experiments (e.g., hand-pairing) using different dragonfly species to obtain hybrids are challenging, with only a few reports of successful interspecific hybridization under captivity (Leong and Hafernik 1992, Monetti et al. 2002, Sánchez-Guillén et al. 2005, Sánchez-Guillén et al. 2012, Sánchez-Guillén et al. 2014, Barnard et al. 2017). In damselfly species, the most important barriers against hybridization have been reported as premating behaviors (Sánchez-Guillén et al. 2012, Barnard et al. 2017), which suggest that the successful

copulation (Fig. 7-1) should be the key to hybrid formation. Linkage analysis of the *I. elegans*–*I. senegalensis* hybrids, together with the use of RNAi, will provide a clue to understanding not only the mechanism of color pattern formation including the female polymorphism at molecular levels, but also the evolution of the significant genomic loci that are maintained across broad species and affected their reproductive isolation.

It should be noted that, recently in Japan, the distribution area of *I. senegalensis* has expanded northward, reaching close to the distribution area of *I. elegans* (Fig. 7-1, Ozono et al. 2017). In near future, these two species may come across and make hybrids in the wild.

...(5年以内に雑誌等で刊行予定のため、非公開。)

References

(5年以内に雑誌等で刊行予定の部分の記述については非公開。)

Barnard AA, Fincke OM, McPeck MA, Masly JP (2017). Mechanical and tactile incompatibilities cause reproductive isolation between two young damselfly species. *Evolution* **71**: 2410–2427.

Bybee S, Córdoba-Aguilar A, Duryea MC, Futahashi R, Hansson B, Lorenzo-Carballa MO, et al. (2016). Odonata (dragonflies and damselflies) as a bridge between ecology and evolutionary genomics. *Front Zool* **13**: 46.

Corbet PS (1999). *Dragonflies, Behavior and Ecology of Odonata*. Cornell University Press.

Cordero A (1990) The inheritance of female polymorphism in the damselfly *Ischnura graellsii* (Rambur) (Odonata: Coenagrionidae). *Heredity* **64**: 341–346.

Córdoba-Aguilar A (2008) Dragonflies and damselflies: model organisms for ecological and evolutionary research. Oxford University Press.

Fincke OM, Jödicke R, Paulson DR, Schultz TD (2005). The evolution and frequency of female color morphs in Holarctic Odonata: why are male-like females typically the minority? *Int J Odonatol* **8**: 183–212.

Futahashi R (2016). Color vision and color formation in dragonflies. *Curr Opin Insect Sci* **17**: 32–39.

Futahashi R (2017). Molecular mechanisms underlying color vision and color formation in dragonflies. In *Diversity and Evolution of Butterfly Wing Patterns: An Integrative Approach* (eds

Sekimura T, Nijhout HF) 303–321, Springer.

Futahashi R, Okude G, Sugimura M, Ugai S (2018). Interspecific hybrids in Japanese Odonata. *Tombo* **60**, 1–49. (In Japanese with English abstract, figures and tables.)

Gering EJ (2017). Male-mimicking females increase male-male interactions, and decrease male survival and condition in a female-polymorphic damselfly. *Evolution* **71**: 1390–1396.

Gosden TP, Svensson EI (2009). Density-dependent male mating harassment, female resistance, and male mimicry. *Am Nat* **173**: 709–721.

Johnson C (1964). The inheritance of female dimorphism in the damselfly, *Ischnura damula*. *Genetics* **49**: 513–519.

Johnson C (1966). Genetics of female dimorphism in *Ischnura demorsa*. *Heredity* **21**: 453–459.

Kunte K (2009). Female-limited mimetic polymorphism: a review of theories and a critique of sexual selection as balancing selection. *Anim Behav* **78**: 1029–1036.

Leong JM, Hafernik JEH (1992). Hybridization between two damselfly species (Odonata: Coenagrionidae): Morphometric and genitalic differentiation. *Ann Entomol Soc Am* **85**: 662–670.

Le Rouzic A, Hansen TF, Gosden TP, Svensson EI (2015). Evolutionary time-series analysis reveals the signature of frequency-dependent selection on a female mating polymorphism. *Am Nat* **185**: E182–E196.

Misof B, Liu S, Meusemann K, Peters RS, Donath A, Mayer C, *et al.* (2014). Phylogenomics resolves the timing and pattern of insect evolution. *Science* **346**: 763–767.

Monetti L, Sánchez-Guillén RA, Cordero-Rivera A (2002). Hybridization between *Ischnura graellsii* (Vander Linder) and *I. elegans* (Rambur) (Odonata: Coenagrionidae): are they different species? *Biol J Linn Soc* **76**: 225–235.

Nishikawa H, Iijima T, Kajitani R, Yamaguchi J, Ando T, Suzuki Y, *et al.* (2015). A genetic mechanism for female-limited Batesian mimicry in *Papilio* butterfly. *Nat Genet* **47**: 405–409.

Okude G, Futahashi R, Kawahara-Miki R, Yoshitake K, Yajima S, Fukatsu T (2017a). Electroporation-mediated RNA interference reveals a role of the multicopper oxidase 2 gene in dragonfly cuticular pigmentation. *Appl Entomol Zool* **52**: 379–387.

Okude G, Futahashi R, Tanahashi M, Fukatsu T (2017b). Laboratory rearing system for *Ischnura senegalensis* (Insecta: Odonata) enables detailed description of larval development and morphogenesis in dragonfly. *Zool Sci* **34**: 386–397.

Ozono A, Kawashima I, Futahashi R (2017). *Dragonflies of Japan*. (3rd edition) Bunichi-Sogo Syuppan, Co Ltd. (in Japanese)

Prakash A, Monteiro A (2016). Molecular mechanisms of secondary sexual trait development in insects. *Curr Opin Insect Sci* **17**: 40–48.

R Core Team (2018). R: A language and environment for statistical computing. R Foundation for Statistical Computing, Vienna, Austria. Available from URL: <https://www.R-project.org/>.

Sánchez-Guillén RA, Van Gossum H, Cordero-Rivera A (2005). Hybridization and inheritance of female colour polymorphism in two ischnurid damselflies (Odonata: Coenagrionidae). *Biol J Linn Soc* **85**: 471–481.

Sánchez-Guillén RA, Wellenreuther M, Cordero-Rivera A (2012). Strong asymmetry in the relative strengths of prezygotic and postzygotic barriers between two damselfly sister species. *Evolution* **66**: 690–707.

Sánchez-Guillén RA, Córdoba-Aguilar A, Cordero-Rivera A, Wellenreuther M (2014). Genetic divergence predicts reproductive isolation in damselflies. *J Evol Biol* **27**: 76–87.

Sanmartín-Villar I, Cordero-Rivera A (2016). The inheritance of female colour polymorphism in *Ischnura genei* (Zygoptera: Coenagrionidae), with observations on melanism under laboratory conditions. *PeerJ* **4**: e2380.

Schneider W, Krupp F (1996). A possible natural hybrid between *Ischnura elegans ebneri* Schmidt, 1939 and *Ischnura fountainei* Morton, 1905 (Odonata: Coenagrionidae). *Zool Middle East* **12**: 75–82.

Sugimura M, Ishida S, Kojima K, Ishida K, Aoki T (2001). *Dragonflies of the Japanese Archipelago in Color*. Hokkaido Univ Press.

Svensson EI (2017). Back to basics: using colour polymorphisms to study evolutionary processes. *Mol Ecol* **26**: 2204–2211.

Svensson EI, Willink B, Duryea MC, Lancaster LT (2019). Temperature drives pre-reproductive selection and shapes the biogeography of a female polymorphism. *Ecol Lett* **23**: 149–159.

Takahashi M, Takahashi Y, Kawata M (2018). Candidate genes associated with color morphs of female-limited polymorphisms of the damselfly *Ischnura senegalensis*. *Heredity* **122**: 81–92.

Takahashi Y, Yoshimura J, Morita S, Watanabe M (2010). Negative frequency-dependent selection in female color polymorphism of a damselfly. *Evolution* **64**: 3620–3628.

Takahashi Y, Kagawa K, Svensson EI, Kawata M (2014). Evolution of increased phenotypic diversity enhances population performance by reducing sexual harassment in damselflies. *Nat Commun* **5**: 4468.

Tillyard RJ (1917) *The Biology of Dragonflies*. Cambridge Univ Press.

Willink B, Duryea MC, Svensson EI (2019). Macroevolutionary origin and adaptive function of a polymorphic female signal involved in sexual conflict. *Am Nat* **194**: 707–724.

Willink B, Duryea MC, Wheat C, Svensson EI (2020). Changes in gene expression during female reproductive development in a color polymorphic insect. *Evolution* **74**: 1063–1081.

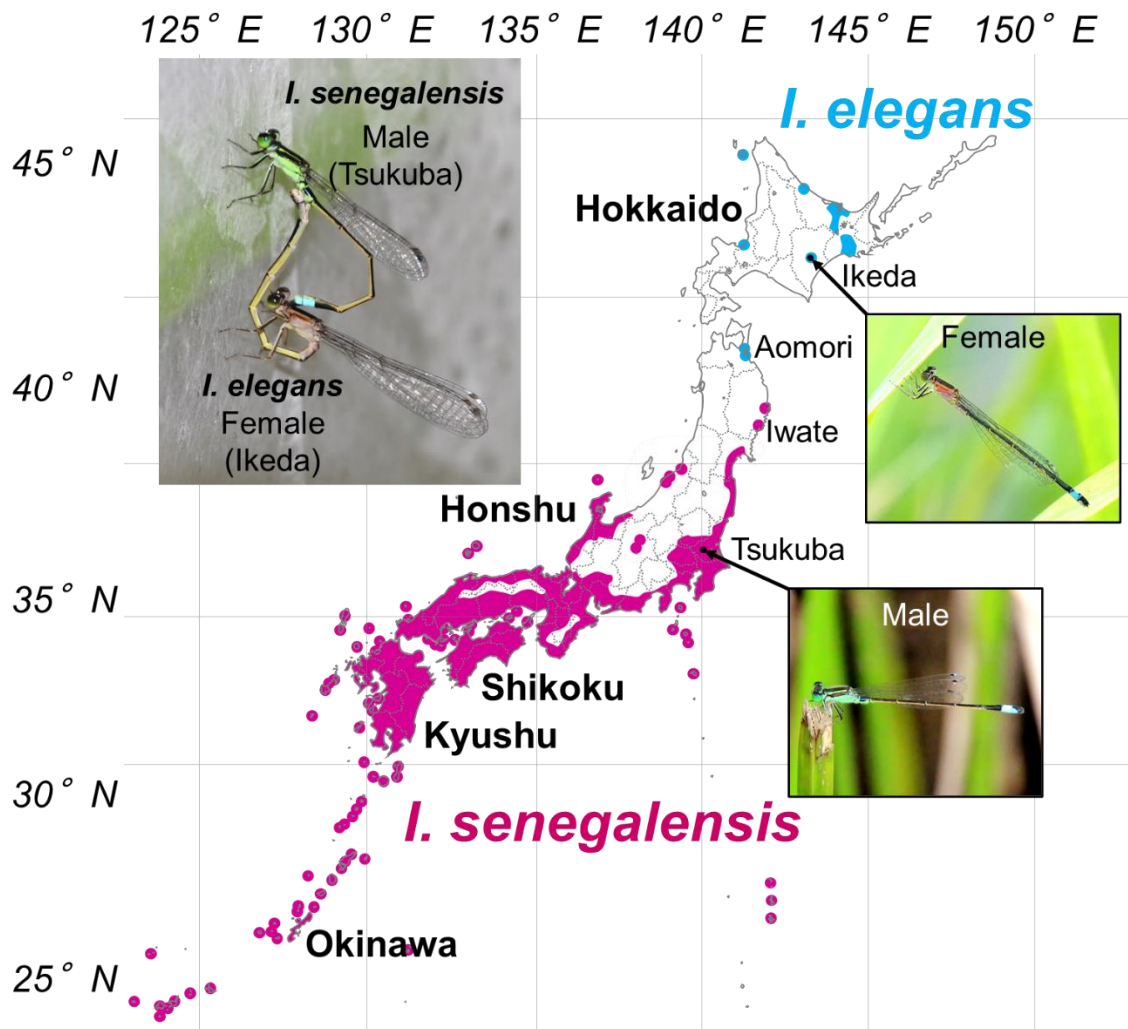


Figure 7-1.

Distribution patterns of *Ischnura elegans* (blue) and *I. senegalensis* (magenta) in Japan, on which the origins of *I. elegans* female (collected in Ikeda) and *I. senegalensis* male (collected in Tsukuba) hybridizing in the laboratory are highlighted. Distribution map is modified from Ozono et al. (2017). Photo of *I. elegans* female courtesy of Jun Okude.

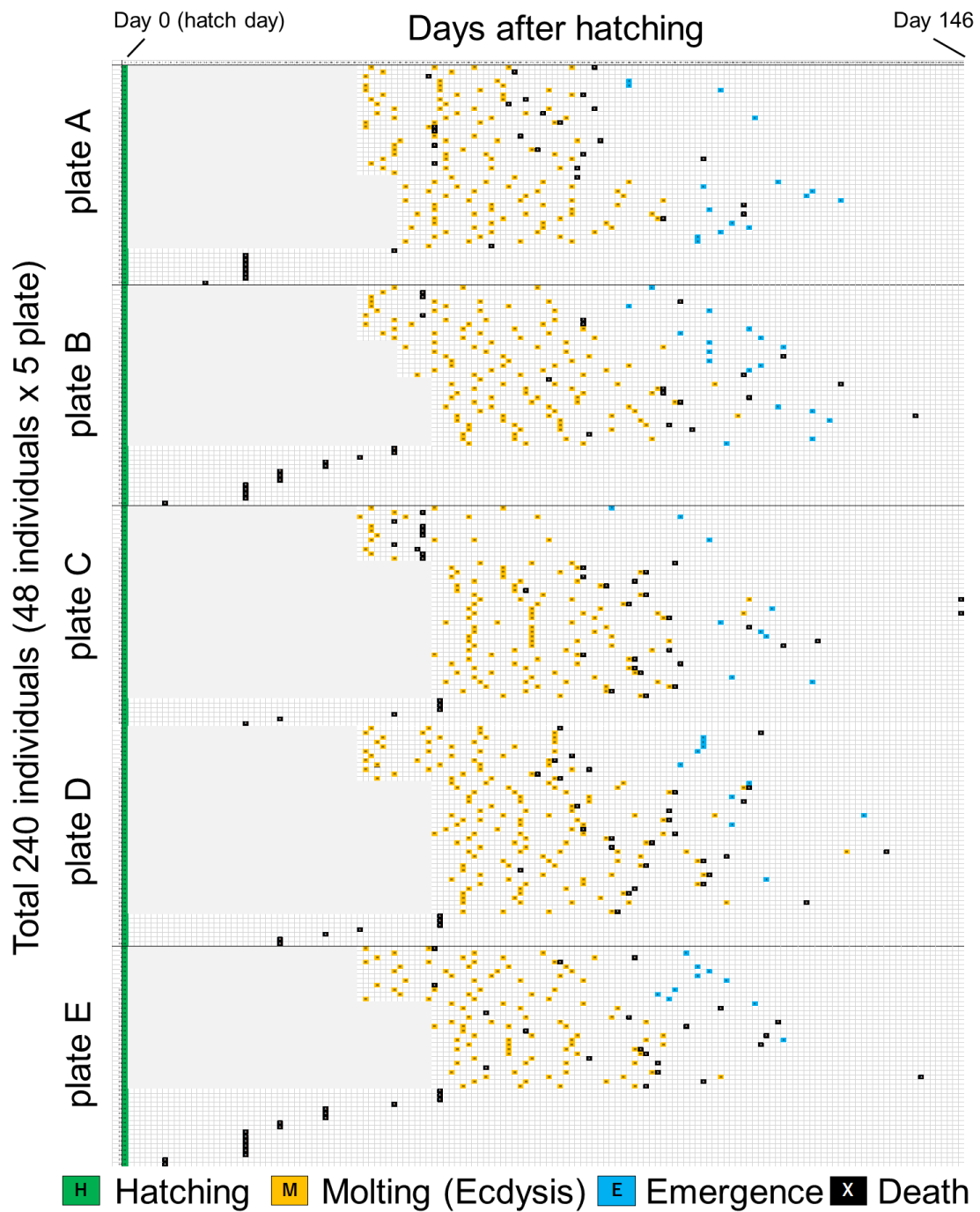


Figure 7-2.

Raw data of ecdysis, adult emergence and death events observed with 240 larvae of hybrids. Horizontal grids indicate days after hatching, whereas vertical grids show individuals we inspected in this study. During initial several weeks shown in the gray area, we recorded only if each larva is alive or dead once a week.

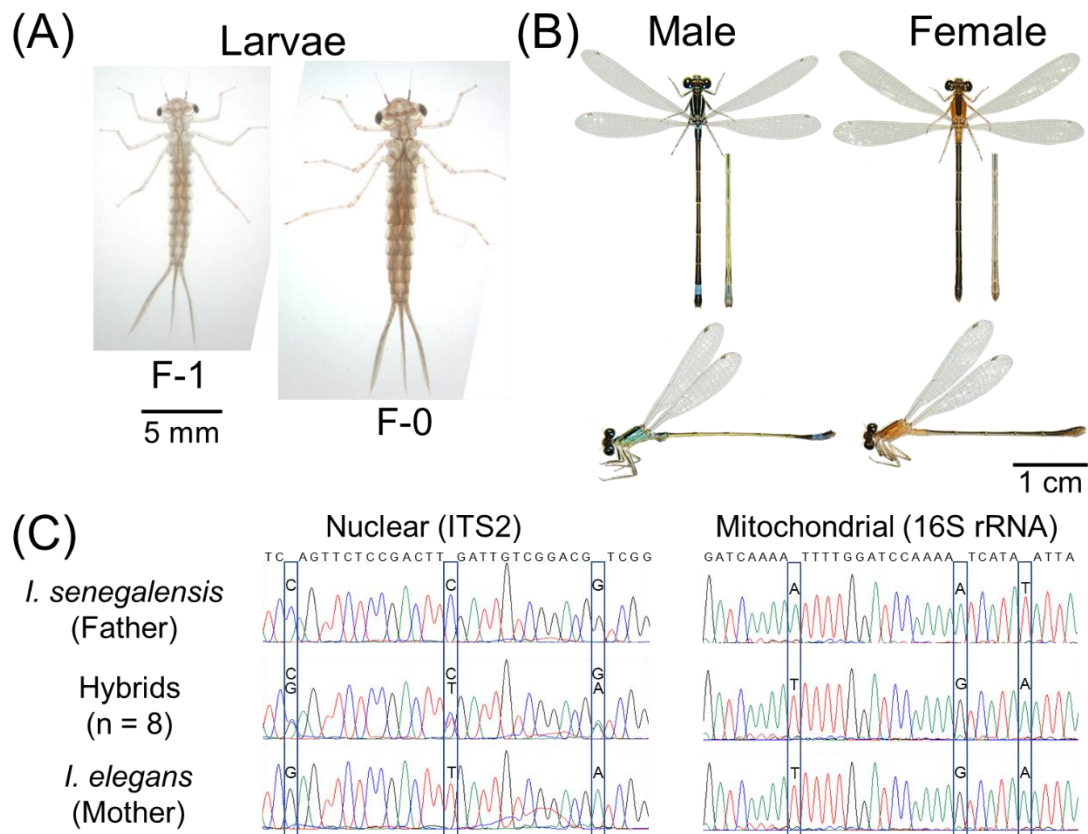


Figure 7-3.

Hybrids between *I. elegans* and *I. senegalensis*. (A) Penultimate (F-1) and final (F-0) instar larvae. (B) Adult male and female. Dorsal, ventral, and lateral views are shown. Photo courtesy of Mitsutoshi Sugimura. (C) Results of nuclear (ITS2 region) and mitochondrial (16S rRNA region) DNA analyses. Squares indicate species-specific nucleotides.

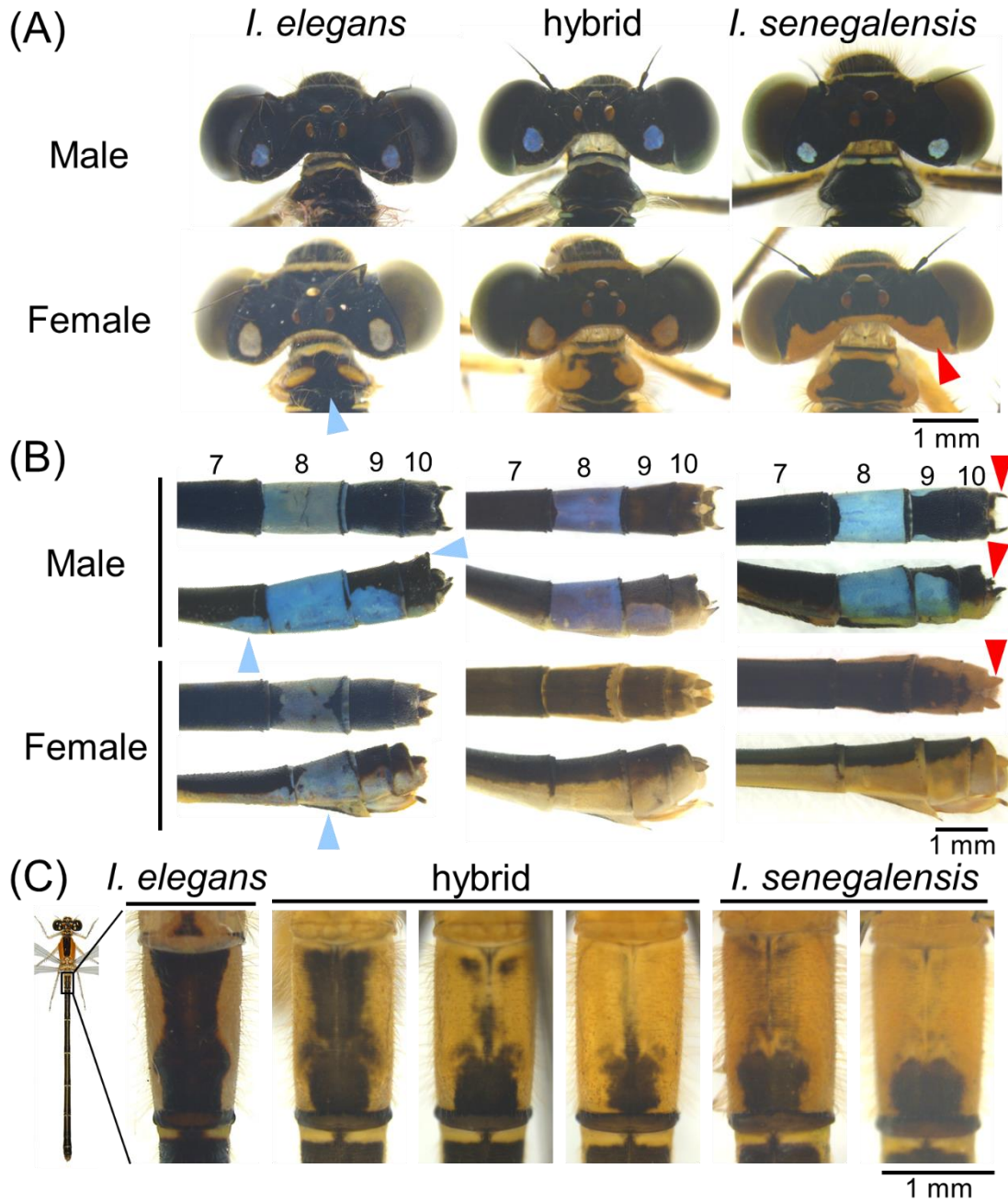


Figure 7-4.

Magnified views of *I. elegans*, *I. senegalensis* and their hybrids. (A) Dorsal views of heads and prothorax. (B) Dorsal and lateral views of 7th-10th abdominal segments. (C) Dorsal views of 2nd abdominal segments of females. Arrowheads indicate specific characteristics of *I. elegans* (blue) or *I. senegalensis* (red) that are different from hybrids.

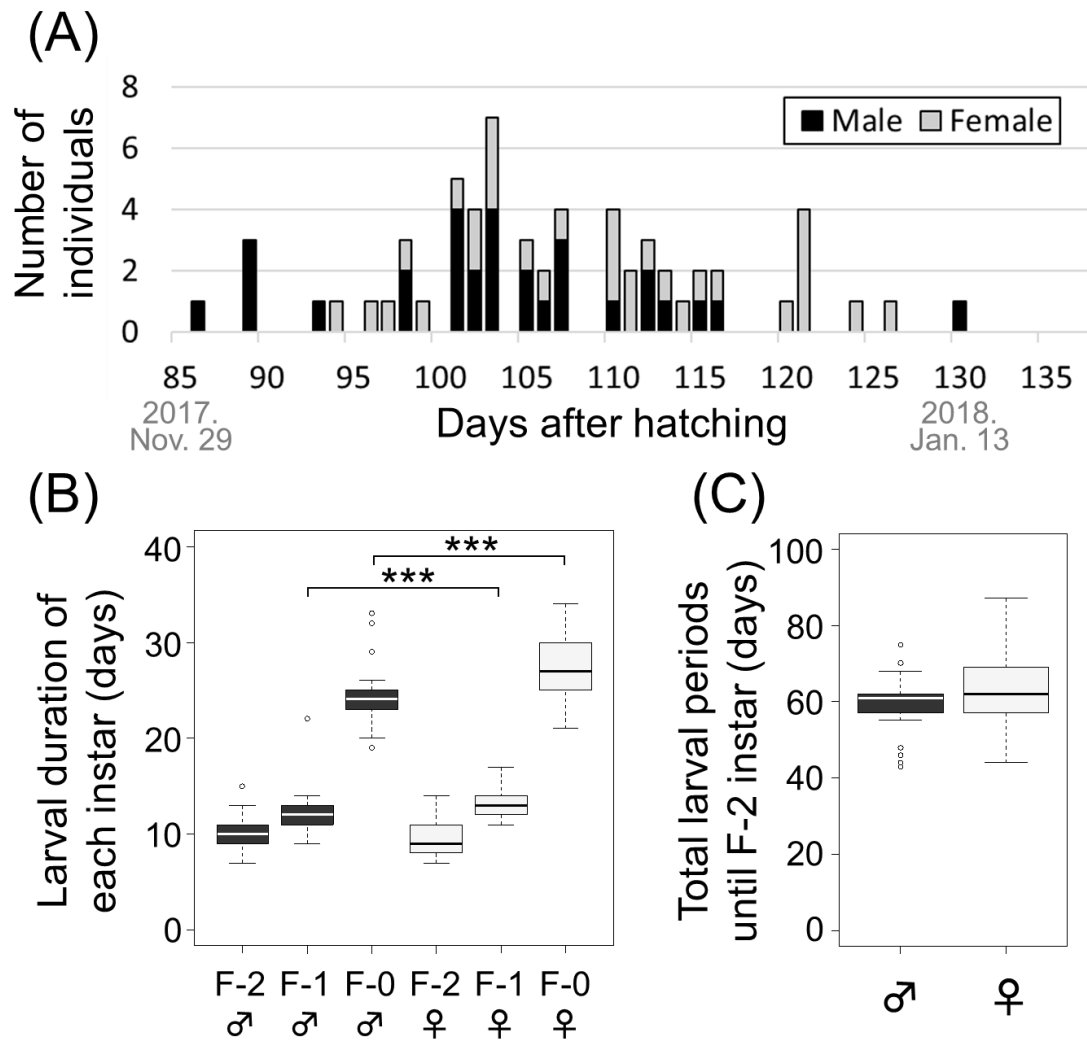


Figure 7-5.

Life history traits monitored during the larval development of hybrids. (A) Total larval periods until adult emergence. Black and gray indicate male and female, respectively. (B) Durations of F-2, F-1 and F-0 instars in larvae that reached adulthood. *** indicates $P < 0.01$ in Mann-Whitney test. (C) Total larval periods until ecdysis to F-2 instar.

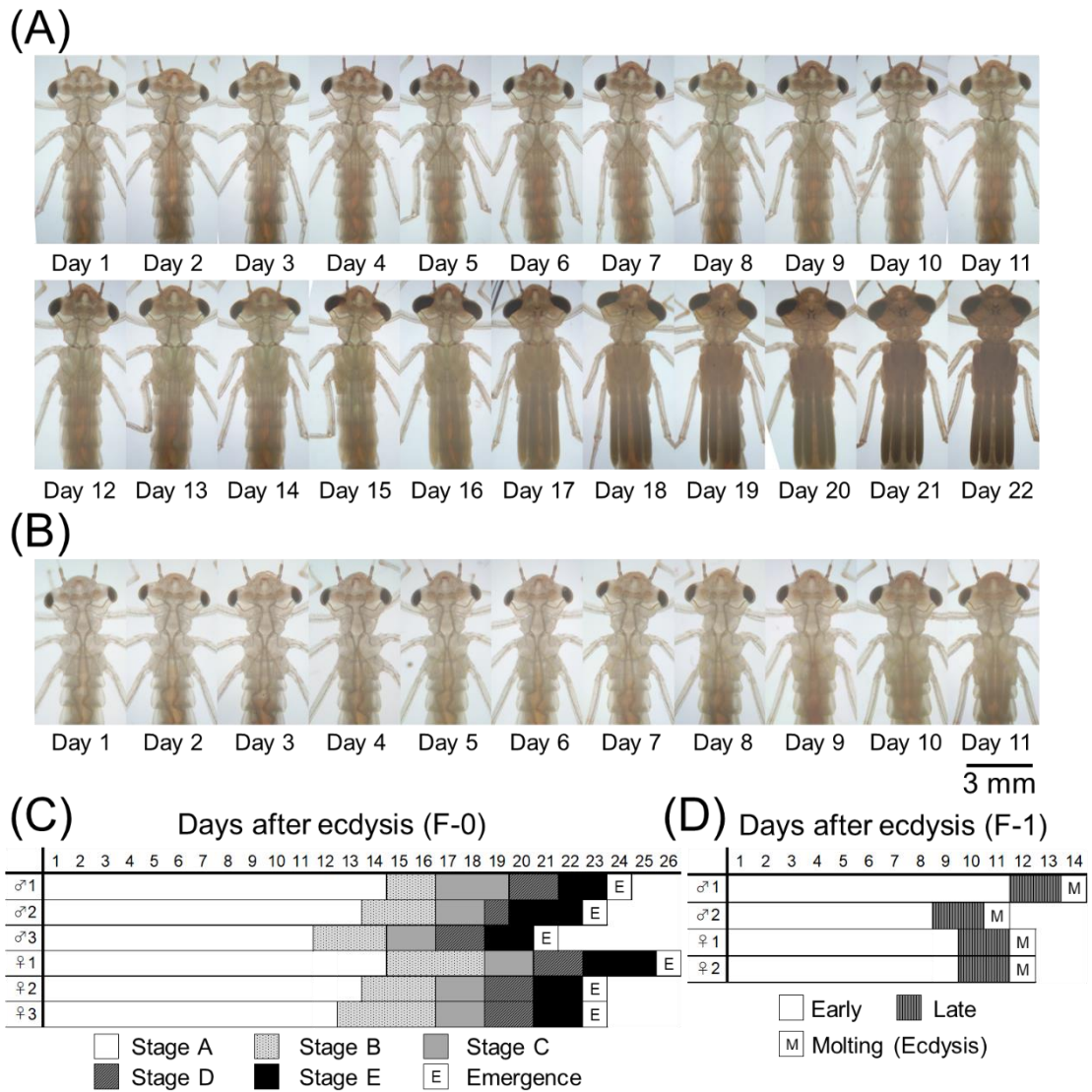


Figure 7-6.

Morphological changes in the final (F-0) and penultimate (F-1) instar larvae of hybrids. (A) Daily photos of the head-thorax region of a female larva (individual number: 3) in the final instar (F-0). (B) Daily photos of the head-thorax region of a female larva (individual number: 2) in the penultimate instar (F-1). (C) Developmental stages observed in the six F-0 instar larvae we examined. Five morphological stages (stage A-E) correspond to previous definitions in Okude et al. (2017). (d) Developmental stages observed in the four F-1 instar larvae we examined. In the late stage of F-1, we observed expansions of wing sheaths.

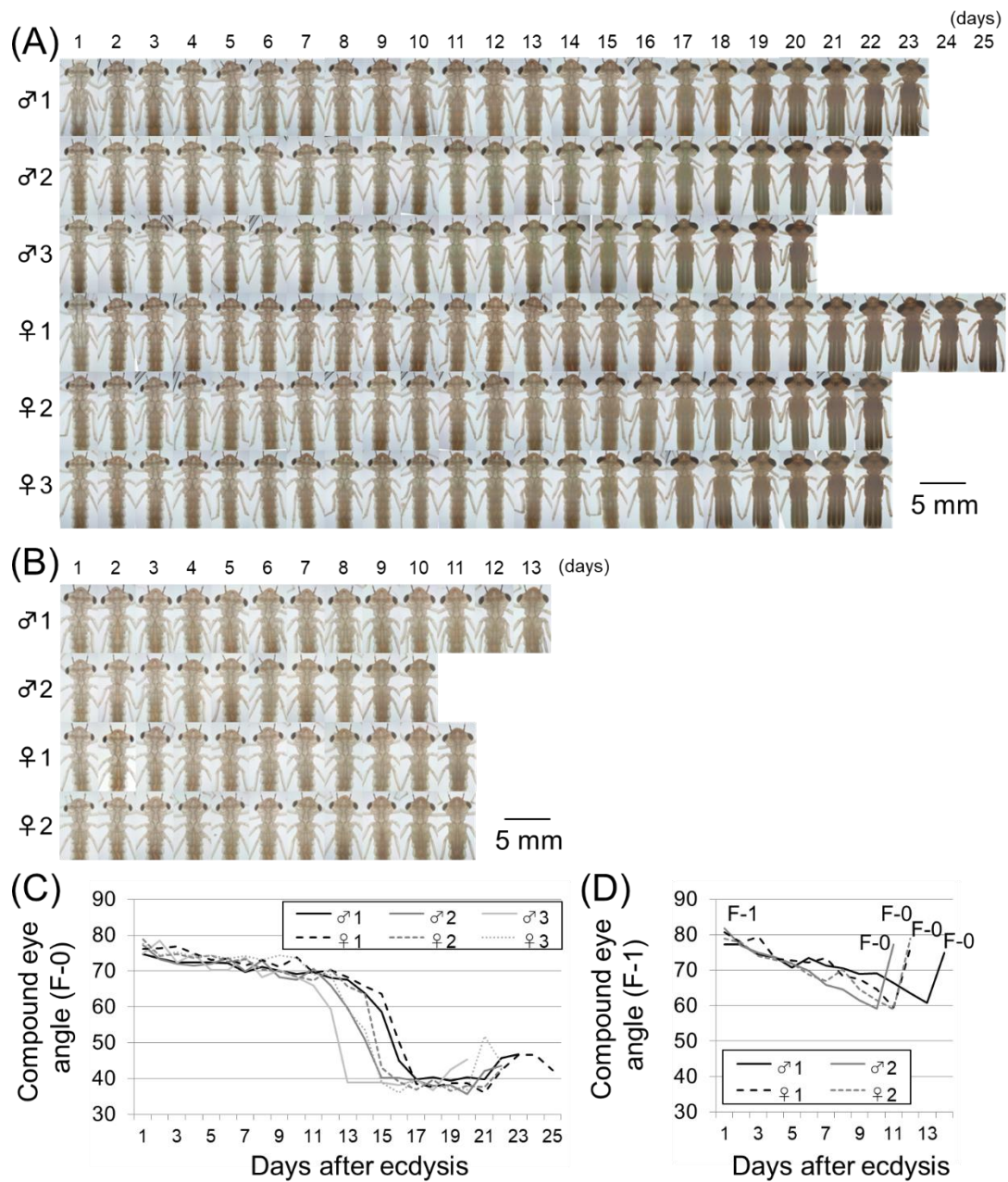


Figure 7-7.

Analyses of morphological changes in the larval development of hybrids. (A) Photos of six final instar (F-0) larvae used for analyses. (B) Photos of four penultimate instar (F-1) larvae used for analyses. (C) Compound eye angles of final instar (F-0) larvae. (D) Compound eye angles of penultimate instar (F-1) larvae.

Figure 7-8.

...(5年以内に雑誌等で刊行予定のため、非公開。)

Figure 7-9.

...(5年以内に雑誌等で刊行予定のため、非公開。)

Figure 7-10.

...(5年以内に雑誌等で刊行予定のため、非公開。)

Figure 7-11.

...(5年以内に雑誌等で刊行予定のため、非公開。)

Table 7-1.

Time series of obtaining and rearing hybrids in this study.

Aug. 20th, 2017	Morning	Four teneral gynochrome (form <i>infuscans-obsolata</i>) females of <i>Ischnura elegans</i> were captured in Ikeda town, Hokkaido.
Aug. 25th, 2017	Morning	Three mature males of <i>I. senegalensis</i> were captured in Tsukuba city, Ibaraki.
	Afternoon	Three <i>I. senegalensis</i> males and four <i>I. elegans</i> females were put together in the adult-rearing cage.
Aug. 28th, 2017	AM9:30-10:30	One copulation was observed (Fig. 7-1).
	PM0:30	Copulated female was moved into a petri dish with a wet filter paper after we observed oviposition-like behavior.
Aug. 29th, 2017	Morning	297 eggs were laid into the filter paper.
Sep. 7th, 2017	Morning	243 1st instar larvae were hatched (Three individuals died immediately after hatching.).
	Afternoon	240 1st instar larvae were moved to each well of 48-well plastic plates individually.
Nov. 30th, 2017 - Jan. 13th, 2018		61 adults (30 males and 31 females) were emerged.

General Conclusion and Discussion

(5年以内に雑誌等で刊行予定の部分の記述については非公開。)

Throughout this doctoral thesis, I focused on the metamorphosis and color formation in Odonata (dragonflies and damselflies). In order to provide the basic information and the experimental systems required for these purposes, I first described morphological changes of 158 individuals, representing 49 species and 14 families of Odonata, to determine appropriate criteria for metamorphic staging of final larval instar (Chapter 1) and then established electroporation-mediated RNAi methods applicable to diverse Odonata species (Chapter 2). Using these information and techniques, I successfully obtained a number of new findings on the molecular mechanisms underlying metamorphosis and color formation in Odonata (Chapter 3 to Chapter 7). A schematic overview of the achievements in this study is presented as Fig. 8-1.

Odonata species change body color dramatically through metamorphosis from brown dull-colored aquatic larvae to colorful terrestrial adults. Therefore, it is very important to elucidate the molecular mechanisms underlying body color formation in understanding metamorphosis. On the ground that the effects of electroporation-mediated RNAi on gene function were most pronounced in epidermis (not wings or genital organs) in this study, changes in body color patterns were utilized as important indicators of metamorphosis in Odonata.

... (5年以内に雑誌等で刊行予定のため、非公開。)

In Chapter 7, I report a successful interspecific hybridation between a female of *I. elegans* and a male of *I. senegalensis* in the laboratory. Notably, these two species show different dominant-recessive patterns of female color polymorphism, and females have different

light blue patterns on the abdomen between species. If the F2 generation can be obtained in the future, linkage analysis may enable identification of the gene responsible for the female color polymorphism and species-specific light blue abdominal patterns. . . . (5年以内に雑誌等で刊行予定のため、非公開。)

In conclusion, based on the comparative gene expression analysis by RNA-sequencing using more than 200 samples (Supplementary Table 1) and RNAi experiments targeting more than 200 genes (Supplementary Table 2), I successfully identified genes that regulate metamorphosis and color formation in Odonata. Many of them are novel findings with no similar reports in other insects. This study sheds light on the molecular mechanisms underlying the evolution of metamorphosis and the diversity of color patterns not only in Odonata but also in diverse insects in general.

References

. . . (5年以内に雑誌等で刊行予定のため、非公開。)

Figure 8-1.

... (5年以内に雑誌等で刊行予定のため、非公開。)

Figure 8-2.

... (5年以内に雑誌等で刊行予定のため、非公開。)

Figure 8-3.

... (5年以内に雑誌等で刊行予定のため、非公開。)

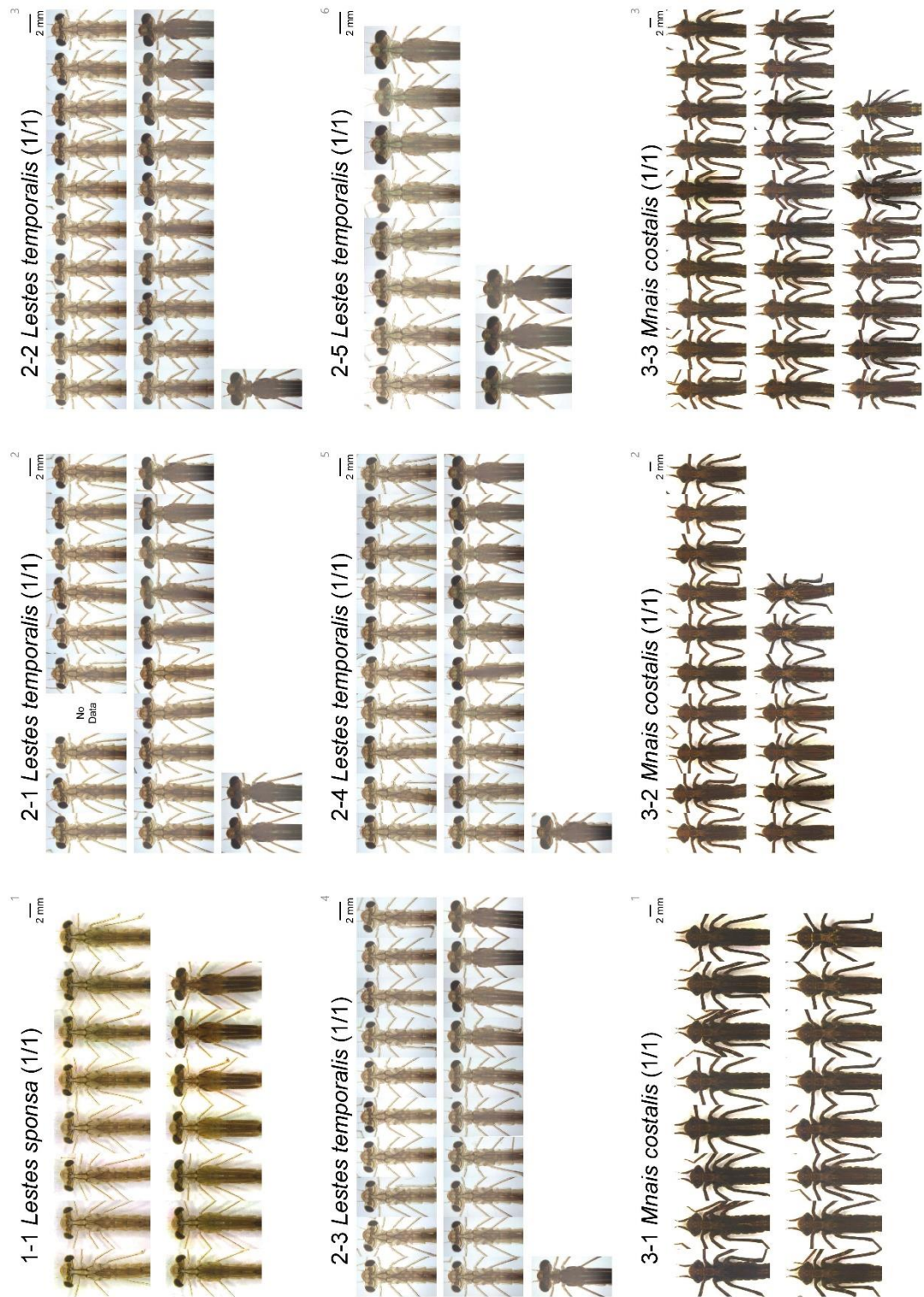
Acknowledgements

I would like to express the most profound appreciation to my supervisor Prof. Takema Fukatsu for his kind support, encouragement, and advise throughout my PhD course. I would also like to extend my deepest gratitude to Dr. Ryo Futahashi for his supervision. My success and great experience would not have been possible without their support and mentoring.

I also thank Dr. Minoru Moriyama for his support during my PhD course including pigment analysis by LC-MS and RNA-sequencing data analysis. I thank Drs. Mayako Kutsukake, Ryuichi Koga, Akiko Koto, Kohei Oguchi, and other members of the Fukatsu laboratory for the helpful discussion and assistance.

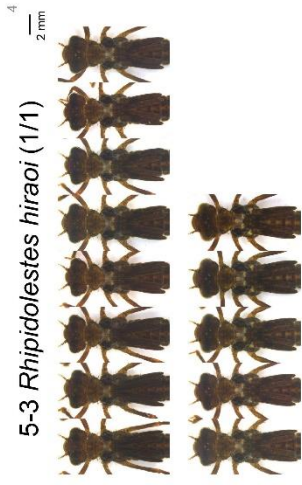
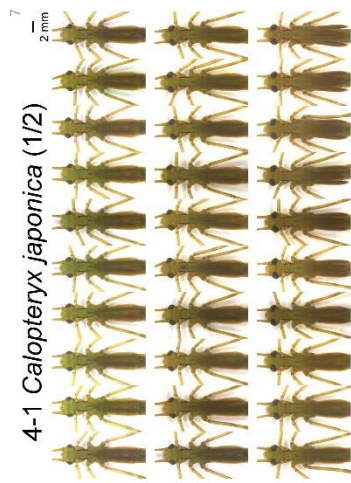
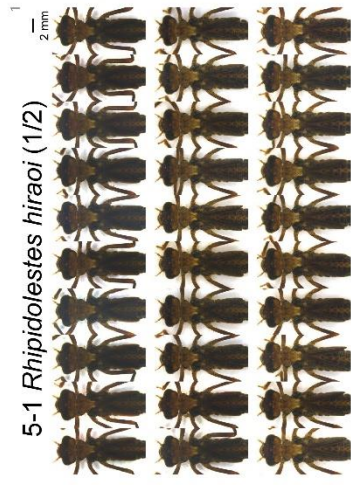
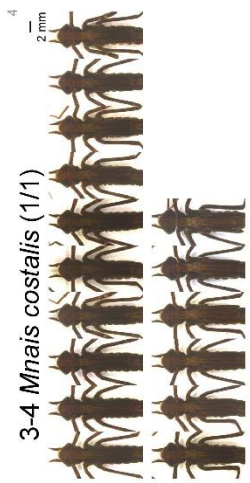
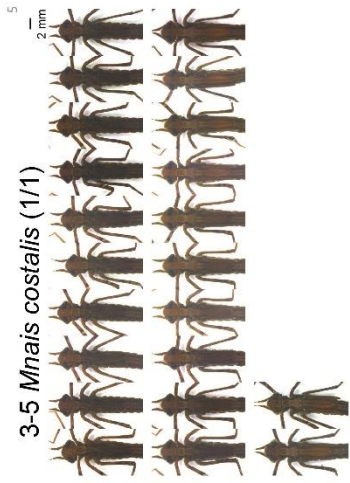
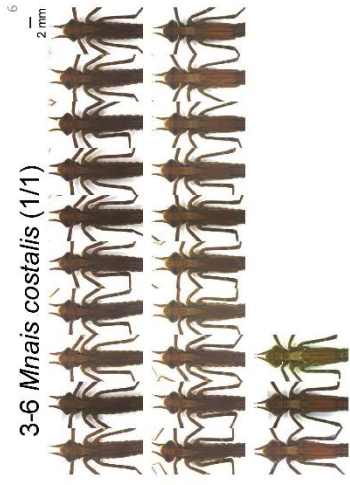
I thank Dr. Mizuko Osanai-Futahashi for providing the chemical structure diagrams used in this study, and Drs. Ryouka Kawahara-Miki, Shunsuke Yajima, and Kazutoshi Yoshitake for analysis of RNA-sequencing data. I also thank Sayumi Oishi, Mutsumi Sakurai and Naoto Motoyama for feeding damselfly larvae when I had to be away of lab, Misa Shinya for helpful assistance, and Motoharu Fukui, Hiroyuki Futahashi, Naoki Futahashi, Bin Hirota, Hiroyuki Koga, Akira Kotabe, Sae Nomura, Jun Okude, Akira Ozono, Mika Sugimura, Mitsutoshi Sugimura and Ryutaro Suzuki for collecting Odonata larvae and providing Odonata photos.

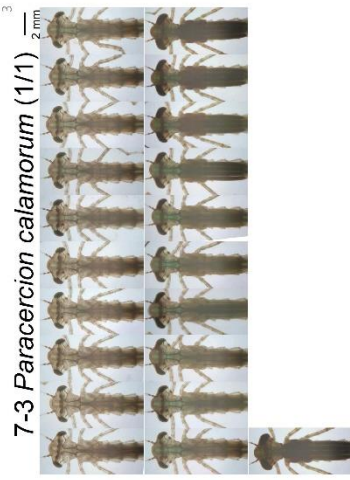
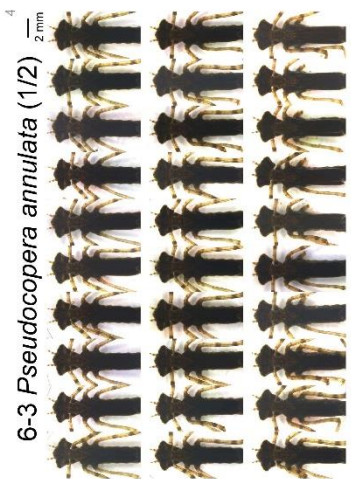
Finally, I am deeply indebted to my parents who allowed me to study further in graduate school with their support and encouragement throughout my graduate course.

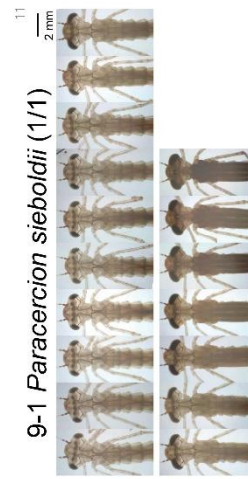
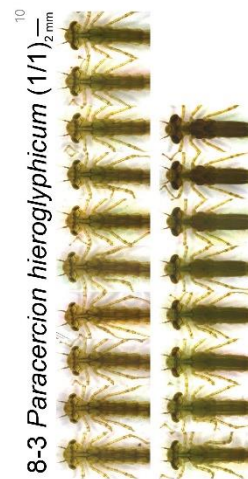
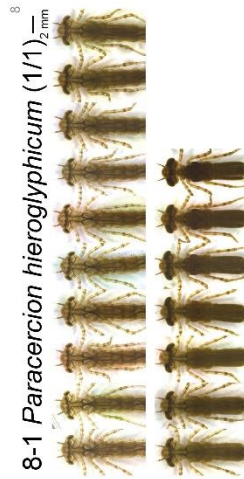
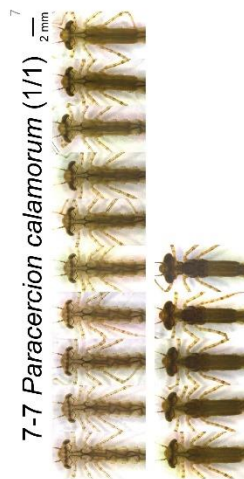
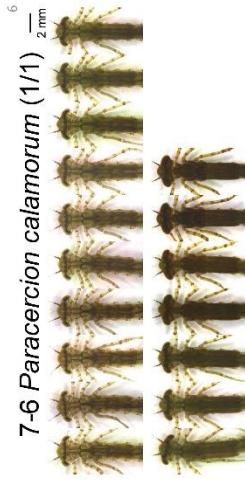
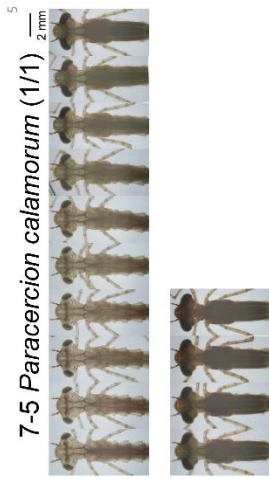
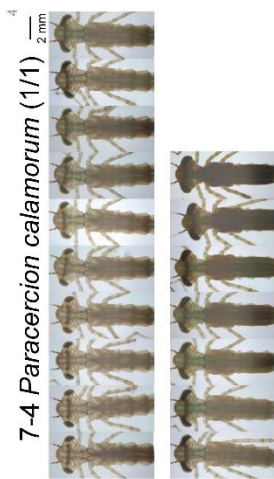


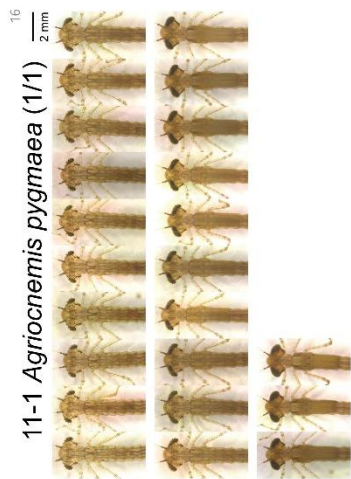
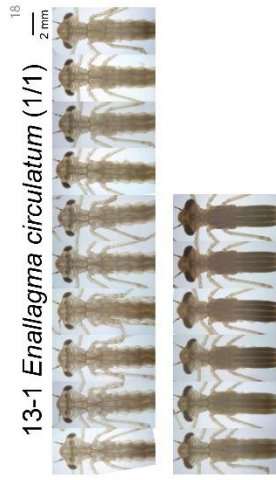
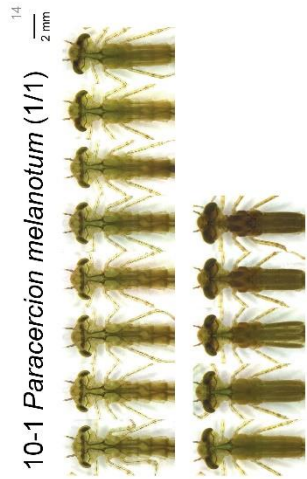
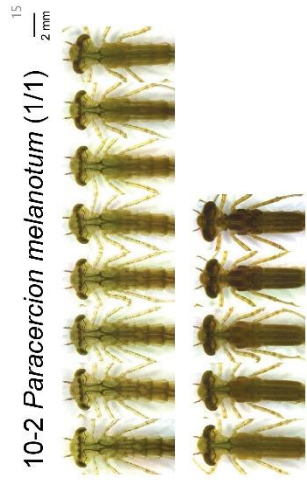
Supplementary Figure S1.

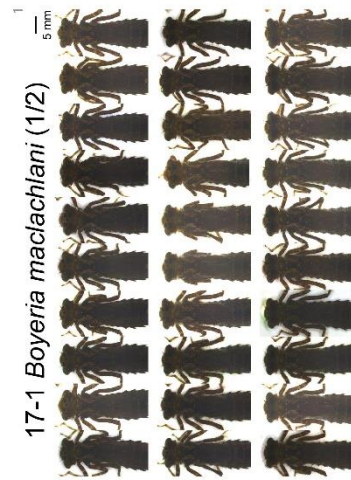
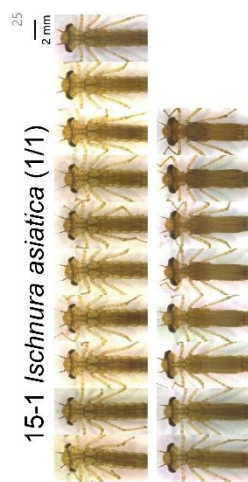
All the adjusted photos of F-0 instar larvae taken in this study. Individual data are shown in Table S1.

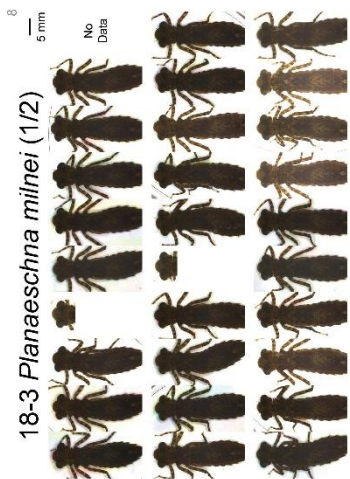
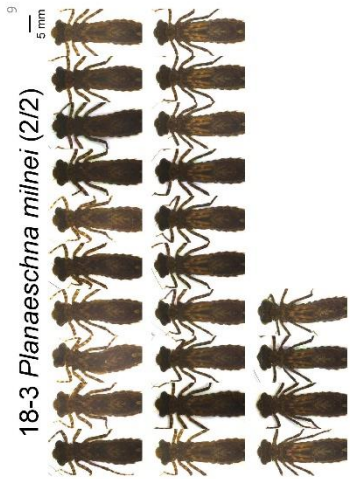
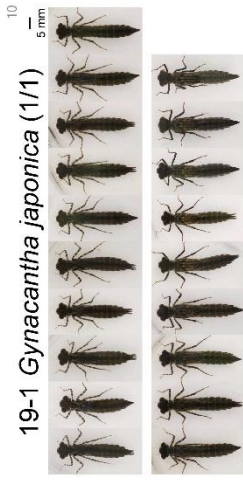
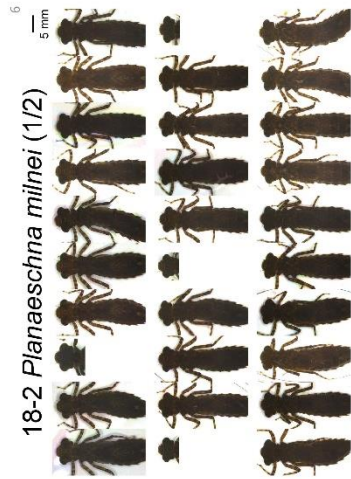


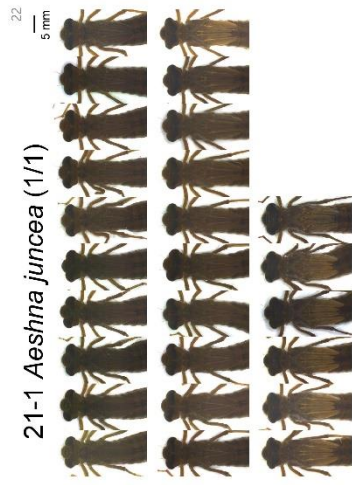


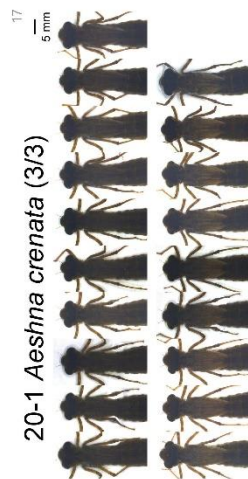


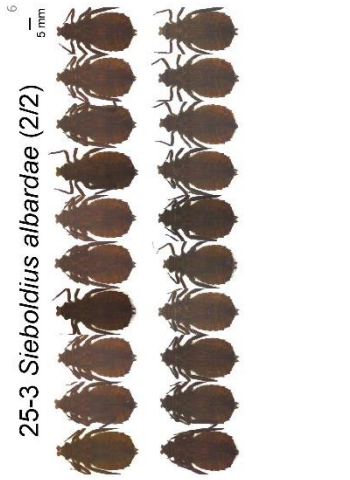
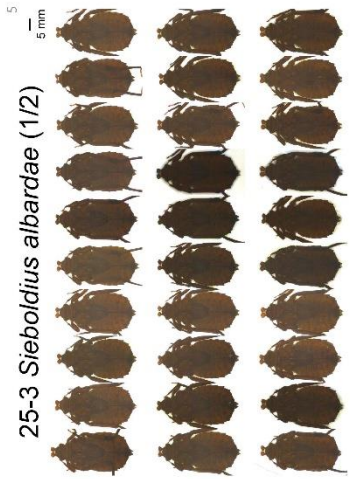
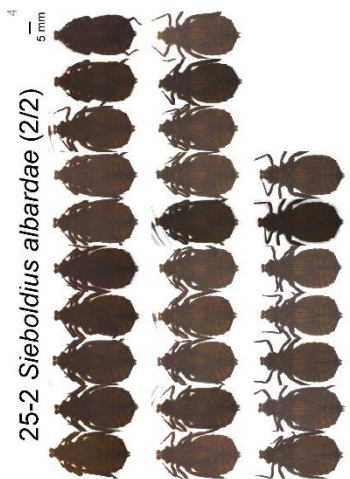
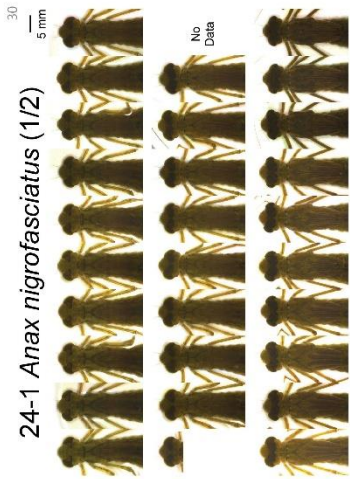


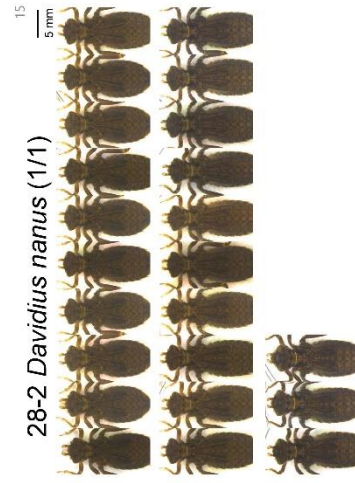
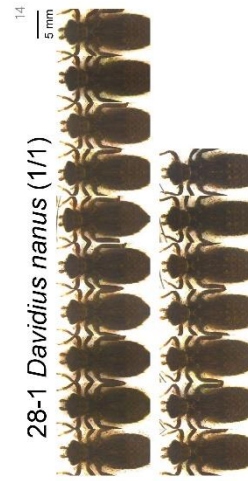
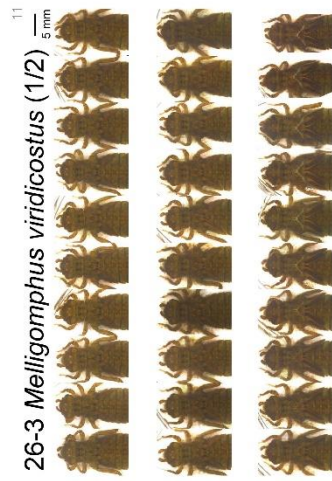
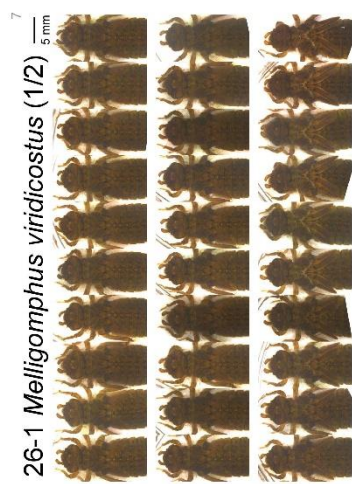


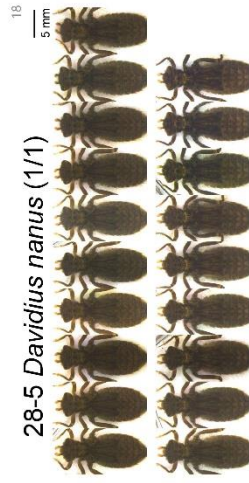
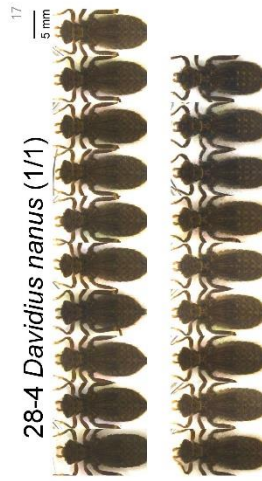


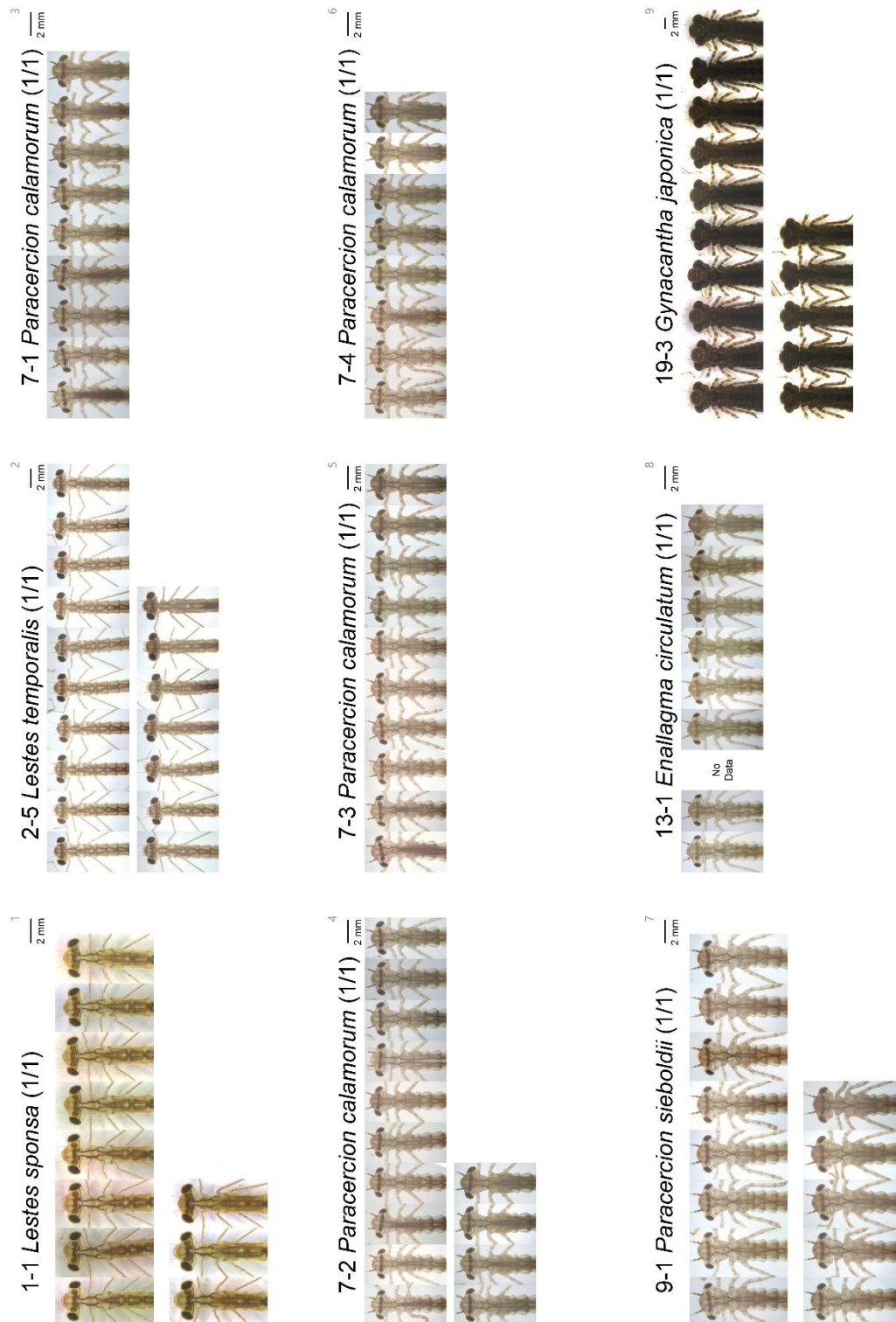






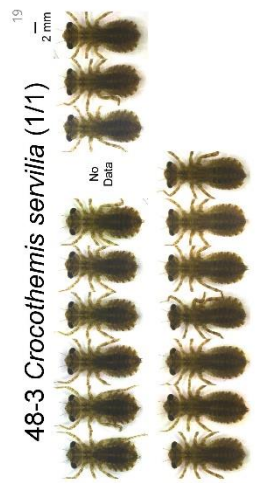


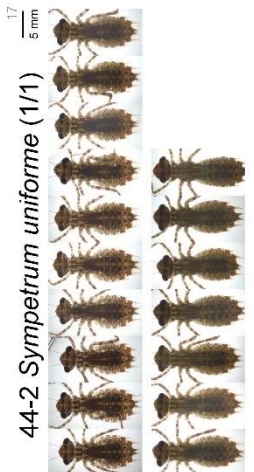
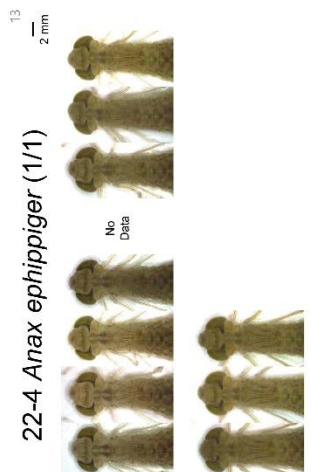
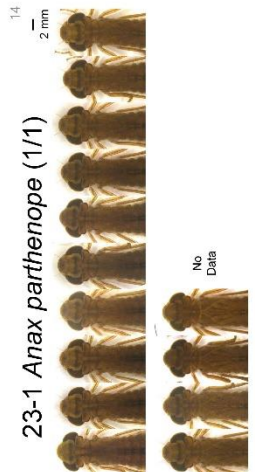
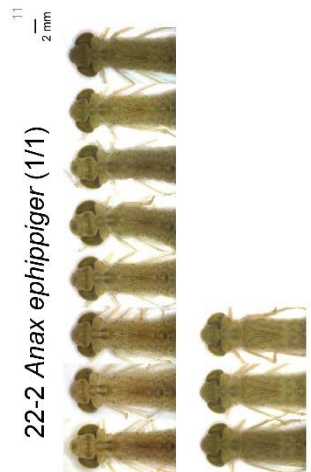




Supplementary Figure S2.

All the adjusted photos of F-1 instar larvae taken in this study. Individual data are shown in Table S1.

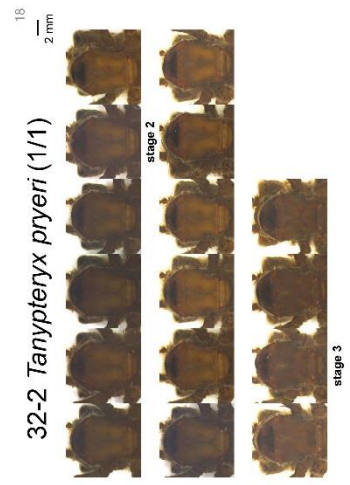
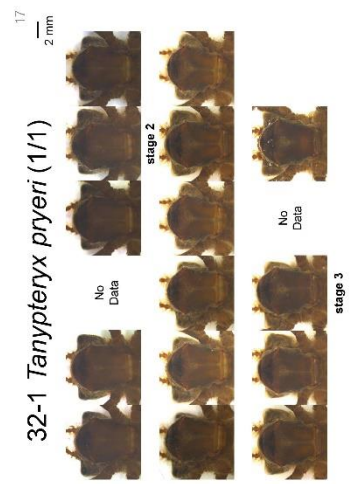
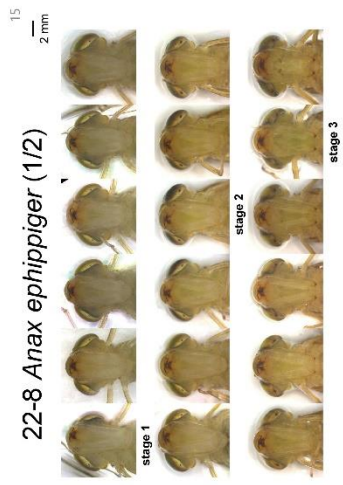
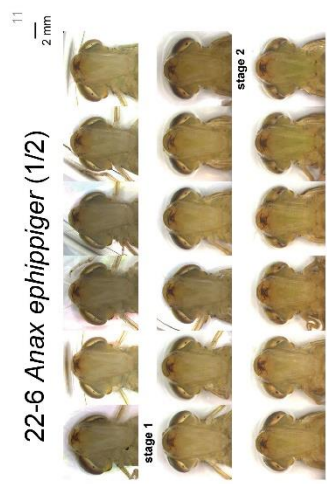


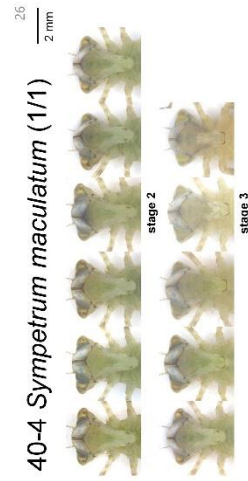
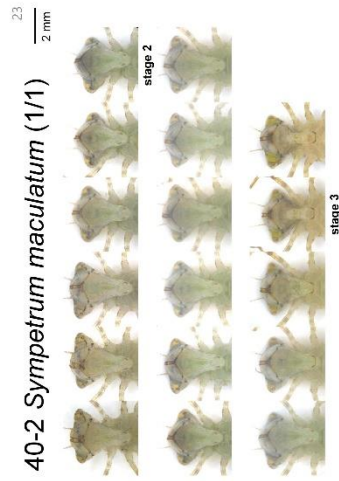
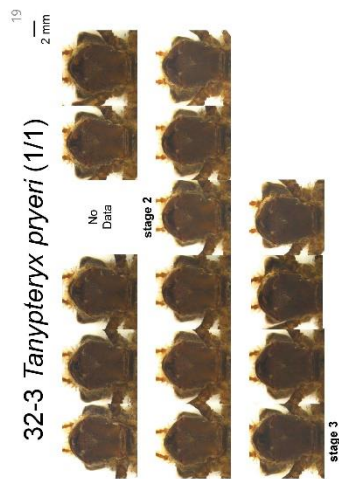
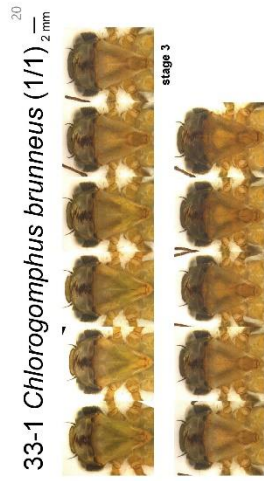
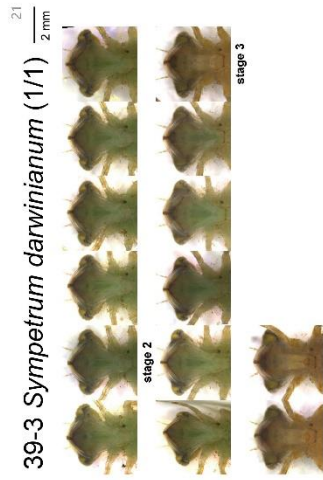




Supplementary Figure S3.

All the adjusted photos of the ventral heads focusing on the shrinking larval labium.





Supplementary Table 1. Sample and RNA-sequencing data used in this study.

... (5年以内に雑誌等で刊行予定のため、非公開。)

Supplementary Table 2. Primers used for dsRNA synthesis in this study.

... (5年以内に雑誌等で刊行予定のため、非公開。)